PhD Thesis

Complexation on the Surface of Quantum Dots for Ion and Molecular Sensing

Submitted by

Mihir Manna

Under the Supervision of

Prof. Arun Chattopadhyay

Department of Chemistry
Indian Institute of Technology Guwahati
Guwahati-781039, Assam, India

February, 2022

Complexation on the Surface of Quantum Dots for Ion and Molecular Sensing

A thesis submitted by

Mihir Manna

(Roll No. 166122014)

to

Indian Institute of Technology Guwahati

for the award of the degree of

Doctor of Philosophy

Department of Chemistry
Indian Institute of Technology Guwahati
Guwahati-781039, Assam, India

February, 2022

Abstract

In the field of ion and molecule sensing, quantum dots and their modified forms have demonstrated their utility with many advantages. Among different types of optical sensors, ratiometric sensors have more advantages like self-calibration, visual color change, and independence of intensity fluctuation. Due to these properties, the ratiometric sensors are comparatively more reliable and efficient. Quantum dot complex (QDC) – that is made up of inorganic complex functionalized on the surface of a quantum dot - is a perfect nano-system that can be utilized as a ratiometric sensor due to its multiple independent emissions, high thermal, and photostability, high quantum yield, etc. The present thesis focuses on the fabrication of different QDC-based ratiometric optical nanoprobes for (i) toxic and heavy metal ion (like Hg^{2+} and Cu^{2+}) sensing, (ii) phosphate ion sensing, and (iii) selective recognition and sensing of long-chain unsaturated fatty acids (LCUFAs).

The present thesis is divided into five chapters. A brief discussion of each chapter is given below.

Chapter 1 describes the literature survey of quantum dots, their surface modification technics, and sensing applications.

Chapter 2 presents a ratiometric optical nanoprobe for Hg^{2+} and Cu^{2+} sensing. A dual emitting QDC formed by N-methyl salicylaldimine (MSA) and Mn^{2+}-doped ZnS Qdots has been used to fabricate the sensor, which changed its color from purple to blue to detect Hg^{2+} and Cu^{2+} with a limit of detection (LOD) of 85.5 nM for Hg^{2+} and 34.9 nM for Cu^{2+}.

Chapter 3 demonstrates a QDC-based ratiometric phosphate sensor consisting of $Zn(QS)_2$ (QS = 8-hydroxyquinoline-5-sulfonate) complex on the surface of Mn^{2+}-doped ZnS Qdots. The change in color of the QDC from white to orange helped to detect phosphate ions with a detection limit of 5.9 nM. Quantitative measurement of phosphate concentration in environmental water and commercial fertilizer was also made possible using the presented nanoprobe.

Chapter 4 presents a QDC-based nanoprobe for selective recognition and ratiometric sensing of long-chain unsaturated fatty acids (LCUFAs). The nanoprobe has been

designed by the formation of ZnQ_2 complex (Q = 8-hydroxyquinoline) on the surface of Mn^{2+}-doped ZnS Qdots. A color change from white to cyan was observed during the detection of LCUFAs. The LOD was calculated for three different LCUFAs and found to be 0.127 μM for oleic acid, 0.126 μM for linoleic acid, and 0.103 μM for erucic acid. The nanoprobe successfully detected LCUFAs in commercial vegetable oils with high accuracy.

Chapter 5 contains an overview and future prospects of the present thesis.

Statement

This thesis entitled **"*Complexation on the Surface of Quantum Dots for Ion and Molecular Sensing*"** is a work of research and investigation carried out by me under the supervision of Prof. Arun Chattopadhyay, Professor, Department of Chemistry, Indian Institute of Technology Guwahati. This thesis has been submitted by me to the Department of Chemistry, Indian Institute of Technology Guwahati for the award of the degree of Doctor of Philosophy. I further declare that this work has not been submitted anywhere else for any degree, diploma, associateship or membership etc. of any Institute or University to the best of my knowledge.

Mihir Manna

Mihir Manna

Department of Chemistry,
IIT Guwahati,
Guwahati-781039, Assam, India

Date: 29.01.2022

Place: Guwahati, Assam

Certificate

It is certified that the thesis entitled **"*Complexation on the Surface of Quantum Dots for Ion and Molecular Sensing*"** being submitted to the Indian Institute of Technology Guwahati by Mihir Manna (Roll. No. 166122014) for the award of the degree of Doctor of Philosophy in Chemistry, is a bonafide record of research work carried out by him. The information and data reported by him are solely the results of his original findings. He has meticulously carried out the investigations and followed the guidelines of the laboratory. This work has not been submitted elsewhere for any degree or diploma.

Prof. Arun Chattopadhyay

Thesis Supervisor

Professor,

Department of Chemistry, IIT Guwahati,

Guwahati-781039, Assam, India.

Date: 30.01.2022

Place: Guwahati, Assam

Dedicated to my

Parents and Elder Brother

Acknowledgment

" गुरुर्ब्रह्मा ग्रुरुर्विष्णुः गुरुर्देवो महेश्वरः ।
(Gurur Brahma Gurur Vishnu Gurur Devo Maheshwarah)

गुरुः साक्षात् परब्रह्मा तस्मै श्री गुरवे नमः ॥ "
(Gurur Sakshat Para Brahma Tasmai Shri Gurave Namaha)

It's very difficult to express my gratitude to the person who taught me that ethics and honesty are more important than publishing a paper. He helped me to be emotionally attached to the beautiful world of science. Without his guidance and freedom, it was impossible to survive in this long journey of research. He taught me how to keep patience and stay calm in any difficult situation, how to utilize each and every minute of my life to improve myself, how to work by proper planning to be more productive, and many more. He is none other than my guru, my PhD supervisor Prof. Arun Chattopadhyay. The word "grateful" is nothing to express my gratitude to my guru for his contribution to my life.

I would like to acknowledge my doctoral committee members for their valuable suggestions and advice regarding my research work.

I am thankful to my lab members for providing a friendly and helpful environment. I am also thankful to my collaborators for their help and healthy professional relationships.

I would like to thank Department of Chemistry, Centre for Nanotechnology, and CIF for providing me research facilities.

Next, I want to thank my family members and friends for their unconditional love and support.

I am grateful to each and everybody connected to my life and helped me to be what I am now.

Thank you so much.

Mihir Manna

Table of Contents

Chapter 1

Introduction

Nanosized materials are intriguing because they can connect the two levels of materials i.e., bulk and molecular, opening up new application possibilities, particularly in optoelectronics, chemistry, and biology. Depending upon the size and shape, nanostructured materials can be categorized as (i) zero dimensional (e.g. quantum dots), (ii) one dimensional (e.g. quantum wires), and (iii) two dimensional (e.g. nanosheets). During the past three decades, zero dimensional nanomaterials (especially quantum dots: Qdots) have been getting special attention due to their size-dependent optoelectronic properties in the field of biology, sensing, catalysis, drug delivery, light-emitting devices, and solar cells. The utility of the Qdots has been expanded from the advancement of fundamental research to the diverse field of technological applications. In this context, the surface of Qdots has played a significant role in expanding their scope of technological as well as daily-life applications. Hence, surface modified Qdots have a bright future in the field of chemical research and technology.

1.1 Quantum Dots:

1.1.1 A Brief Idea:

Quantum dots (Qdots) are zero-dimensional colloidal semiconductor nanocrystals (NCs) ranging in size from 1 to 10 nm.[1] Qdots are said to be 100 times more stable and 20 times brighter than organic dye molecules.[2-3] Due to their small size, they confine the motion of the charge carriers i.e., electrons of the conduction band and holes of the valence band. These properties differentiate Qdots from bulk form of materials of the same composition. These characteristics allow them to be used in a variety of disciplines, from optoelectronic devices to biological applications.[4-7]

1.1.2 Discovery:

The discovery of semiconductor nanocrystal took place in 1981 by Russian scientist Alexey I. Ekimov et al. in a glass matrix.[5] After that, in 1985, Louis E. Brus reported for the first time the synthesis of colloidal cadmium sulfide (CdS) nanocrystals.[6] But this newly discovered zero-dimension colloidal semiconductor nanocrystals got the

well-known name "Quantum Dots" in the year 1988 by Mark Reed.[7] That name was given by observing the size (i.e., dimension) and quantum mechanical behavior of the electronic states of Qdots.

1.1.3 Types:

Depending upon composition, Qdots can be categorized as binary, ternary and quaternary types. Binary Qdots are basically composed of the elements from the II-VI (for example, ZnS, ZnSe, CdS, CdSe, etc.), III-V (for example, InP, InAs, etc.), and IV-VI (for example, PbS, PbSe, PbTe, etc.) group of the periodic table. Ternary Qdots are usually composed of the elements from the I-III-VI group of the periodic table (for example, $CuInS_2$, $AgInS_2$, $CuInSe_2$, $GaInP_2$, etc.). In the recent past, quaternary Qdots like $CuZnInS_3$ and Zn−Ag−In−Se have also been reported, which are composed of the I-II-III-VI group of the periodic table.[8-23]

Qdots can also be categorized - based on the value of the wave vector (k) during the electronic transition from the valence band to conduction band - into two categories of (i) direct and (ii) indirect bandgap Qdots.[1]

$k = 2\pi/\lambda$, where λ is the wavelength of the electron.

If the Schrodinger equation (one dimensional) is solved by using the above equation the following energy equation can be obtained.

$E = h^2k^2/8\pi^2m$, where E, h, k, and m represent the energy of the electron, Planck's constant, wave vector, and mass of electron respectively.[1]

If it is observed that during the electronic transition of a Qdot, the wave vector remains unchanged then that Qdotot can be called a direct bandgap Qdot. On the other hand, if the wave vector i.e., the value of "k" changes during electronic transition then that Qdot can be called as indirect bandgap Qdot (Fig 1.1).[1] II-VI and III-V Qdots are examples of direct bandgap and hence show high fluorescence quantum yield, whereas Si and Ge are the examples of indirect bandgap Qdots.[1]

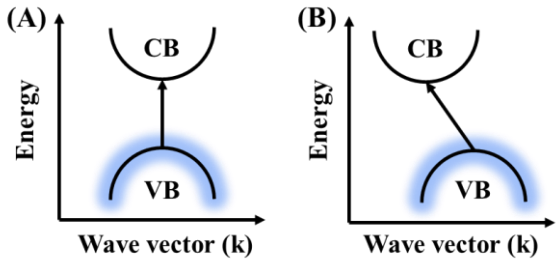

Fig 1.1 Illustrative re-presentation of (A) direct and (B) indirect band gap in the electronic structure of semiconductor. VB and CB stand for valence band and conduction band, respectively.

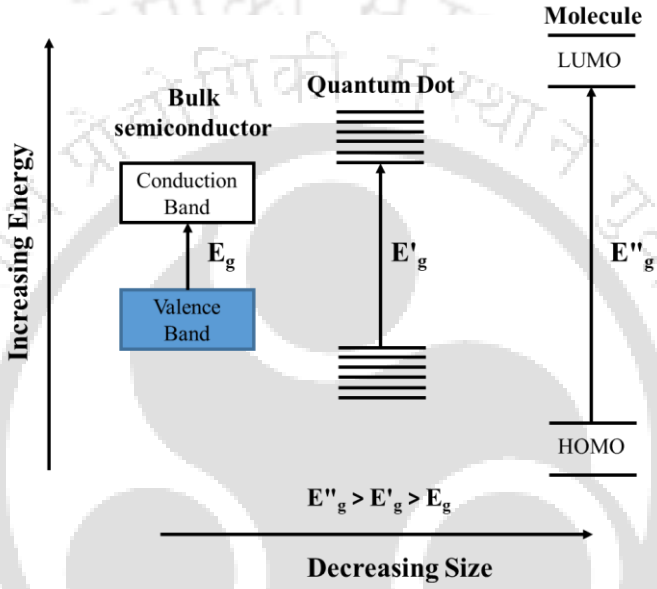

Fig 1.2 Illustrative representation to understand the comparison among the electronic structure of bulk semiconductor, quantum dot and single molecule. Transition energy gap increases with decrease in size.

1.1.4 Optoelectronic properties and their tuning parameters:

1.1.4.1 The Origin: Quantum Confinement Effect

The unique size-dependent optoelectronic properties of Qdots arise due to quantum confinement effect. From the name "Quantum Confinement" it can be understood that matter is confined in a quantum dimension (i.e. comparable to the wavelength of an electron). If exciton (the pair of the electron in conduction band and hole in valence band, generated upon excitation) of a semiconductor material is confined in a dimension comparable or less than the excitonic Bohr radius (which is comparable to the wavelength of an electron) of that material then that exciton behaves like a particle

in a 1-D box. As a result, some quantum mechanical properties like discretization of electronic energy levels are observed. This situation arises when the semiconductor materials form nano-dimensioned Qdots. Smaller the size of the Qdots stronger the confinement effect is observed. That means as the size of the Qdot decreases the quantum confinement effect and hence band gap (the gap between valence band and conduction band) increases (Fig 1.2). The reverse is also true. It can be said that the electronic structure of Qdot is intermediate between the band (observed in bulk material) and bond (observed in the molecule). Due to these unique properties, Qdots are sometimes called "artificial atoms". The quantum confinement effect of Qdots, which is based on their size, causes them to have amazing optical properties. Based upon the above-mentioned quality of Qdot, optical properties can be tuned by tuning the size of the Qdot according to the requirement of the application.[4, 24-27]

The unique optical properties of Qdot not only depend on size but also depend on incorporated impurities and the nature of the surface of the Qdot. Therefore optoelectronic properties of Qdot can be tuned according to the requirement of the application by controlling (i) size, (ii) incorporated impurity, and (iii) surface of the Qdot.

1.1.4.2 Size

As mentioned above due to the quantum confinement effect electronic bandgap and optical property of Qdot can be tuned by tuning its size keeping composition unaltered. The change of bandgap with the size is not a qualitative analogy. They are correlated quantitatively by "Brus equation";

$$E_g(Qdot) = E_g(bulk) + \left(\frac{h^2}{8R^2}\right)\left(\frac{1}{m_e} + \frac{1}{m_h}\right) - \frac{1.8e^2}{4\pi\varepsilon\varepsilon_0 R}$$

Where, E_g, h, R, m_e, m_h, e and ε represent bandgap, Planck constant, the radius of Qdot, effective mass of the electron, effective mass of hole, and dielectric constant of the material, respectively. From the above equation, it's clear that the bandgap of Qdot changes inversely with the size of the Qdot.[1] For example, CdSe/ZnS Qdots have displayed a wide range of emission color depending upon particle size (Fig 1.3).[28]

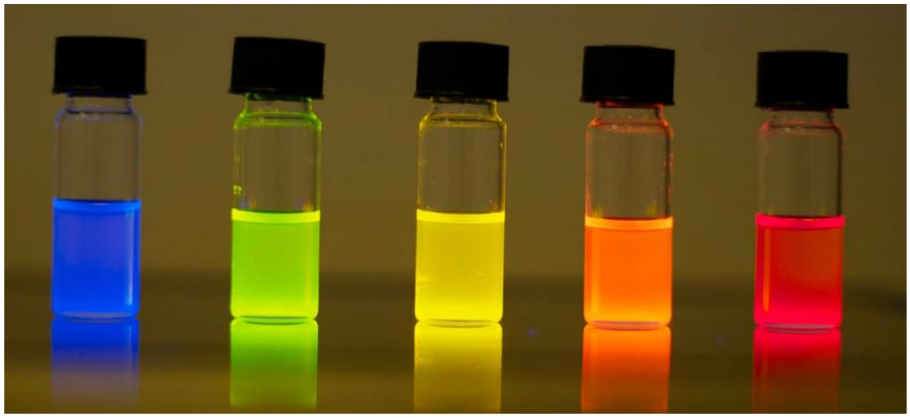

Fig 1.3 Wide range of emission color from CdSe/ZnS Qdots of different size. (Reprinted with permission from Reference [28]. Copyright *ACS Nano* 2014 American Chemical Society.)

1.1.4.3 Doping

Another way to tune the optical property of Qdot keeping the morphology unchanged is the incorporation of some impurities, in short by doping. The dopant generates new trap states in between the valence band and conduction band. Now recombination of exciton takes place from these newly generated trap states, which results in a red-shift in emission. In addition to this property, doped Qdots have another important property and that is a longer photoluminescence lifetime. These unique properties make doped Qdots more useful in the field of device fabrication and bioimaging. From early reports, it was observed that if transition metals (like Cu, Mn) or lanthanides are used as dopants then that doped Qdot emits in the visible region.[29-36] For instance, when Mn^{2+} was used as a dopant in II-VI Qdots, a wide range of emission colors ranging from blue to orange was observed (**Fig 4**).[31] The Stokes shifted emission from doped Qdots originated from the electronic transition in dopant ion. For instance, the orange emission from the Mn^{2+} doped ZnS Qdot generated due to the $^4T_1$-$^6A_1$ transition.[30,32]

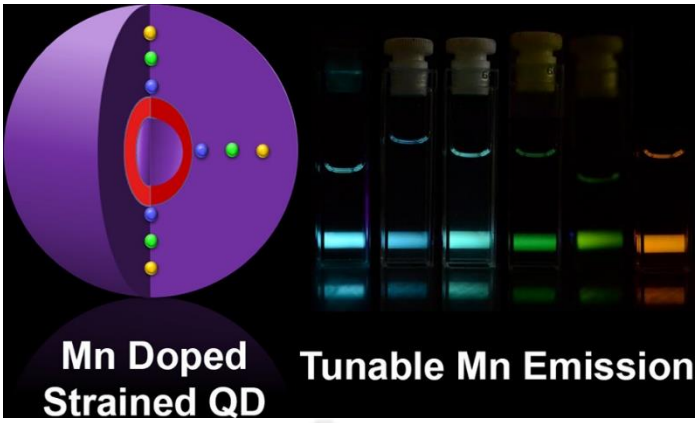

Fig 1.4 Tunable emission from Mn^{2+}-doped ZnSe/CdSe/ZnSe core/shell Qdots depending upon the position of Mn^{2+} in the epitaxial shell. (Reprinted with permission from Reference [31]. Copyright *J. Phys. Chem. Lett.* 2014 American Chemical Society.)

1.1.4.4 Surface

Similar to other nanocrystals, Qdot has a high surface-to-volume ratio due to its nanoscale dimension. That's why the surface of Qdot is a major dictator of its chemical as well as optical properties. Modification of the surface is the easiest way to tune the optical and chemical properties of Qdot without altering its morphology even after synthesis.[37-44] As the crystal structure is terminated at the surface of Qdot the outer coordination side of the surface atoms are unsaturated (called "dangling bond").[41] This structural property makes surface atoms different from core atoms. This unsaturation in coordination makes surface atoms chemically reactive. Interestingly, the number of atoms present on the surface of Qdot having dangling bonds is higher than the atoms present in the core due to the high surface-to-volume ratio. That's why the reactivity of Qdot is usually much higher than that of bulk form. When these reactive dangling bonds participate in any chemical process to be coordinated with different inorganic, organic, or bio-molecules and become saturated then that process is called "surface passivation". Surface passivation leads to non-radiative recombination of exciton, which results in a decrease in quantum yield.[39,40] The most popular strategies to passivate the surface are the generation of an inorganic layer (called "shell") on the surface and coordination with external molecules via the dangling bond. So, the surface of Qdot is a very crucial part that determines chemical reactivity, optical property, and quantum yield of Qdot.[37-44]

1.1.5 Surface Modification:

The surface modification of Qdots is vital for controlling their optical properties and applications. Modification of the surface is the easiest way to alter the outer layer of the Qdots after synthesis without altering the core structure and dimension. Not only does the simplicity but also the cost-effectiveness of the post-synthetic surface modulation process make Qdot a superior option for device construction and biological applications. In the surface modulation process, mainly, dangling bonds present on the surface are passivated to get greater stability, better optical properties, and increased applicability in the different fields. The surface passivation of Qdots is a popular key by which one can manage several optical properties such as excited-state lifetime, emission maxima, photoluminescence quantum yield, etc. So it's very important to understand the nature of the surface of Qdots and its modification techniques.[37,38] There are several surface modulation techniques such as core/shell formation, chemical reaction on the surface, ligand exchange, etc. that have been well-studied.

1.1.5.1 Formation of shell on the surface

A well-known strategy for modification of the surface of Qdot is to generate a coating of inorganic shell over the surface. The inorganic shell is usually made of some semiconductor material different from the material of the core. The size of Qdot usually increases by 1-3 nm after the formation of the shell. Not only is the single-layered shell but also multi-layered shell formation also possible where lattice mismatch plays an important role. This process of shell formation gives Qdots some excellent improvement in their optical properties like enhancement of quantum yield and photoluminescence lifetime up to 20-30 times.[45,46] The shell enhances the optical properties due to mainly two reasons, first, it passivates the dangling bonds on the surface, and second, it creates an energy barrier of high potential, which prevents the charge carriers from leaking out. The passivation of dangling bonds reduces the surface trap states while prevention of leakage of charge carriers increases excitons in Qdots. Both the above-mentioned factors increase the probability of exciton recombination via a radiative pathway, which leads to the enhancement of quantum yield and photoluminescence lifetime. For instance, the quantum yield of CdSe Qdots can be increased up to 20 times by coating with a ZnS shell.[45] The shell formation over the Qdots allows more capping ligands to bind to the surface of the shell, which makes Qdots more stable in their colloidal form.

1.1.5.2 Ligand Exchange

The most common surface functionalization technique for Qdots is ligand exchange, allowing a wider range of characteristics and applications. In this technique, a comparatively stronger capping ligand having a greater affinity towards surface metal ions replaces the existing comparatively weaker capping ligand and forms coordination with surface metal ions.[47-50] In general, Qdots synthesized in the organic phase include long-chain organic molecules as capping ligands, limiting their biological uses due to their very poor aqueous phase stability. If the hydrophobic ligands coordinated on the surface of Qdots are replaced with hydrophilic ligands using the ligand exchange technique then the stability of Qdots in an aqueous medium, as well as applicability in the biological field, will increase.

Many studies have been done to observe the effect of ligand exchange such as Kamat et al. reported that the emission color of CdSe Qdots can be tuned by exchanging capping ligands.[49] In their study, they replaced dodecylamine ligands with 3-mercaptopropionic acid on the surface of Qdots, which results in the color change from blue to red (Fig 1.5).[49] In another study, Brown et al. reported that by coordinating with a small ligand on the surface of PbS Qdot the bandgap could be tuned.[50] So the simple ligand exchange strategy can increase the applicability of synthetically hydrophobic Qdots in the aqueous medium. With the help of the ligand exchange technique, Qdots can be used as a probe for targeted drug delivery, bio-sensing, bio-imaging, targeted drug delivery, pH sensing, and sensing of water pollutants. For example, Erogbogbo et al. used phospholipid and polyethylene glycol coated Si Qdot for bioimaging.[51] Medintz et al. used CdSe/ZnS core/shell Qdot to sense intracellular pH.[52] Zhao et al. successfully used hydrophobic $CuInS_2$/ZnS core/shell Qdot in bioimaging application with the help of ligand exchange with short-chain polar ligands like 3-mercaptopropionic acid and glutathione.[53]

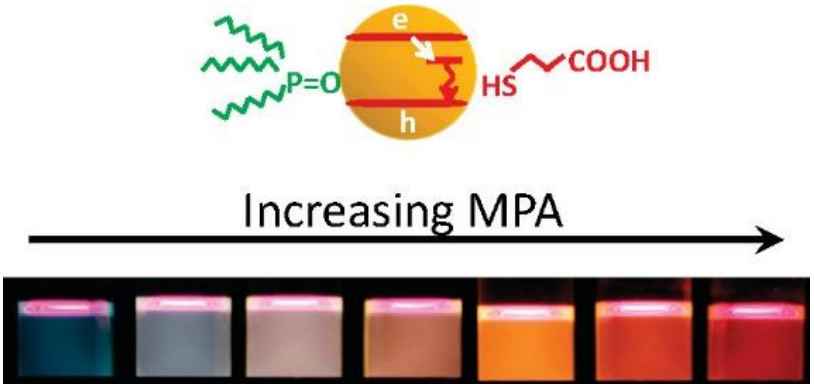

Fig 1.5 Change in emission color of CdSe Qdots depending upon the concentration of MPA attached on the surface via ligand exchange. (Reprinted with permission from Reference [49]. Copyright *Langmuir* 2010 American Chemical Society.)

1.1.5.3 Complexed Quantum Dots: Complexation Reaction on the Surface

Another surface modification technique is complex formation on the Qdot surface with the help of complexation reaction with an external organic molecule to achieve better optical and thermal properties. In comparison to typical ligand exchange, the surface complexation process is a fundamentally new and unique method for surface modification. Although inorganic complexation reactions between a metal ion and organic molecule have been well studied for a long time, the same reaction on the surface of nanomaterials is a challenging task as the behavior and reactivity of material in nanoscale is very different from the bulk.[54-63]

Recently, our group has reported that coordination complex formation is possible on the surface of Qdot after synthesis, and using this surface modification emission color could be tuned over the full visible region. Not only that, that newly formed quantum dot complex (QDC) was used in sensing, bio-imaging, and light-emitting devices. It was found that QDC showed better optical (like a longer excited-state lifetime and higher quantum yield) and thermal (like thermal stability) properties than individual free Qdot and inorganic complex. The extent to which the complex forms is determined by the concentration and capacity of the external ligands to bind. For example, a good chelating ligand 8-hydroxyquinoline forms a green luminescent zinc quinolate (ZnQ_2) complex by coordinating with the surface Zn^{2+} ions of ZnS Qdot. This ZnQ_2 attached ZnS Qdot showed almost 10 times greater photoluminescence quantum yield and higher thermal stability (stable up to 300 °C) (Fig 1.6).[54] Using this surface modification technique one can get different emission colors simultaneously by attaching different ligands on the surface of Qdot. This advantage makes QDC much more useful in different fields of

application like light-emitting devices, bio-imaging, etc. The surface complexation technique can be used to transfer hydrophobic Qdots into an aqueous phase from the organic medium without lowering the quantum yield and keeping the size unchanged (Fig 1.7A).[57] In another study, Fe_3O_4-ZnS nanocomposite bonded with ZnQ_2 complex was used as a probe in cancerous cell imaging. Two important properties helped the above-mentioned nanoprobe to be suitable for targeted bioimaging.[59] One is the superparamagnetic nature of Fe_3O_4 and the second is the high photoluminescence quantum yield of ZnQ_2-ZnS QDC.

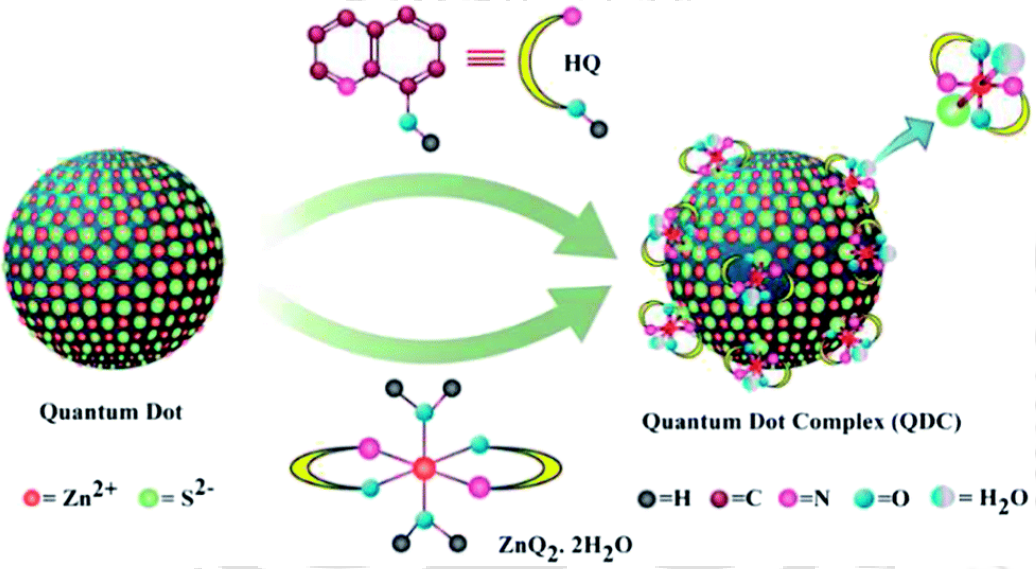

Fig 1.6 Formation of ZnQ_2 complex on the surface of ZnS QDOT through complexation reaction with 8-hydroxyquinoline. (Reprinted with permission from Reference [54]. Copyright *RSC Adv.* 2014 Royal Society of Chemistry.)

As mentioned earlier, different emission colors can be generated by attaching different inorganic complexes with different ligands on the Qdot surface. Controlling the relative emission intensity ratio of different colors, which can be achieved by controlling the relative concentration ratio of used ligands, one can generate white light-emitting nanomaterials having high quantum yield and photostability. For example, orange color emitting Mn^{2+}-doped ZnS Qdots has been converted to the white light emitter in both liquid and solid state when green- and blue-emitting inorganic complexes became attached on the surface (Fig 1.7B).[60] Similarly, greenish-blue emitter inorganic complex converted red-emitting $CuInS_2$/ZnS core/shell Qdots to a white light emitter after

complexation on its surface.[61] In another study white light-emitting material was generated from ZnO Qdots having yellow emission and blue-emitting complex through complexation reaction.[62] Thus, QDC's interesting unique optical properties in both solution and solid phase have a promising future in bioimaging, display technology, photocatalysis, sensing, and light-emitting devices.

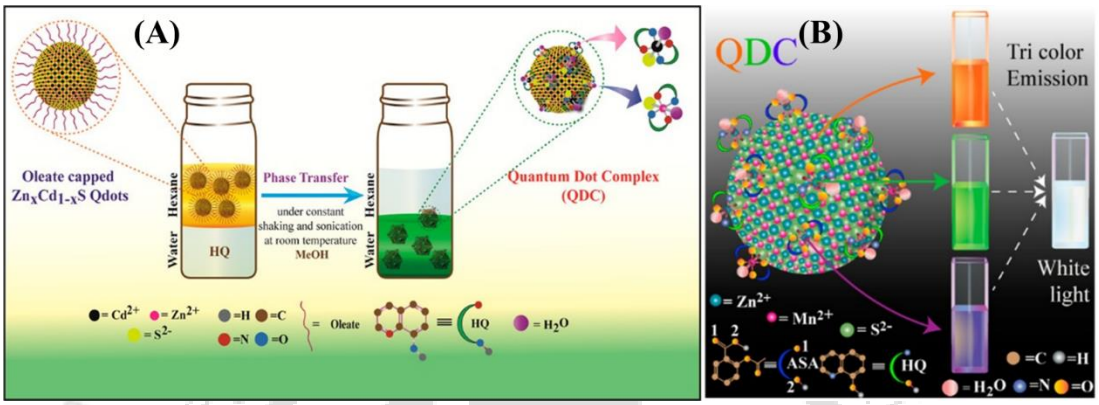

Fig 1.7 (A) Phase transfer of oleate-capped $Zn_xCd_{1-x}S$ Qdots from organic phase to aqueous phase by comlexation reaction with 8-hydroxyquinoline. (Reprinted with permission from Reference [57]. Copyright *Langmuir* 2014 American Chemical Society.) (B) Generation of white light by using dual complexation strategy on the surface of Mn^{2+}-doped ZnS Qdot. (Reprinted with permission from Reference [60]. Copyright *J. Phys. Chem. Lett.* 2015 American Chemical Society.)

1.2 Sensing Applications:

A chemical sensor works through two processes, one is recognition and another is transduction. The analyte (element to be determined) interacts with the recognition site of the sensor and the extent of interaction depends on the concentration of the analyte. By measuring the change in physical or chemical properties of the sensor element the concentration of the analyte can be determined. Signal transduction is the process of converting concentration changes into usable data. The sensing element and signal transducer are included together in a single chemical sensor. The employment of a photo luminescent-based optical sensor is always favorable since it allows for quick, sensitive, and accurate detection of an analyte molecule in a simple and cost-effective way.[64]

Depending upon the effect of analyte on the emission spectra optical sensors can detect any analyte in three different ways: first, by quenching of photoluminescence intensity

with respect to a particular emission maximum; second, by enhancing the photoluminescence intensity with respect to a particular emission maximum (called turn-on optical sensing); and third, by ratiometric change of emission intensities.[65] In the first and second methods, sensor detects analyte concentration depending upon only signal "on" or signal "off". These two methods have some major limitations like fluctuation of emission intensity due to other reasons (such as instrumental setup, the effect of local concentration, and non-homogeneous distribution of analyte), no possibility of visual color change during sensing, and no scope of change in chromaticity. On the other hand, in ratiometric optical sensors, the presence of two or more emission maxima can solve the above mentioned issues. Among those emission maxima one act as a reference, which takes care of unwanted intensity fluctuation. That's why the ratiometric sensing technique is a more reliable method for accurate quantitative detection of an analyte.[65] Qdots have some special unique characteristic features like size, capping ligand, surface functionalization controlled photoluminescence, and integrated recognition site and transducer, which make them popular optical chemical sensors. Qdots' optical characteristics are substantially determined by the nature of the surface and chemical characteristics of the capping ligands, making them unique nanoprobes for detecting ions, pesticides, explosives, pH, and essential biomolecules.[64-77]

1.2.1 Ion Sensing:

Qdot-based optical chemical sensors can be used for ion sensing if any ion interacts with or adsorb by surface ions or ligands. Upon photo-excitation, accept or donate electrons from the appropriate donor or acceptor, respectively. To get better sensitivity and limit of detection (LOD) surface-complexed Qdots are used instead of only Qdots.[66-77] Some reported Qdot-based ion sensors are discussed separately for (1) cations and (2) anions.

1.2.1.1 Cation Sensing

Each metal ion has a permitted threshold limit of concentration in drinking water or a living body. If the concentration of any metal ion crosses the limit then it becomes toxic. So, making a simple, efficient and cost-effective cation sensor is important. Generally, the Qdots having thiol or carboxylate or a nucleic acid group-containing surface ligand are reported as cation sensors. Some of the surface ligands used are mercaptopropionic acid, mercaptoacetic acid, mercaptosuccinic acid, glutathione,

thioglycolic acid, dihydrolipoic acid, and L-cysteine.[66-68]

Among cations, heavy metal ions are more toxic for living beings. For example, excess amount of Hg^{2+} in the human body causes various severe diseases like Minamata, Pink diseases, and neurological disorders. In the case of Cu^{2+} also excess concentration in the human body produces some serious illnesses like Alzheimer's, Parkinson's, and Wilson's diseases.[78-88] Therefore, heavy metal ion sensing with high accuracy and selectivity is very important and challenging for researchers.

For instance, with the help of calixarene capped CdSe/ZnS Qdots and L-carnitine capped CdSe/ZnS Qdots as nanoprobe, Hg^{2+} has been detected with a LOD of $1.5 \times 10^{-10}\ M$ and $1.8 \times 10^{-7}\ M$, respectively.[89,90] A nanohybrid composed of reduced glutathione capped CdTe Qdots and mercaptopropionic acid capped CdTe Qdots have been used for Hg^{2+} detection.[91] To avoid toxicity issue of cadmium containing Qdots, a cetyltrimethylammonium bromide (CTAB) capped Mn^{2+}-doped ZnS Qdots modified by thymine-rich aptamer has been used to detect Hg^{2+} with a LOD of $1.5 \times 10^{-10}\ M$ (Fig 1.8).[92]

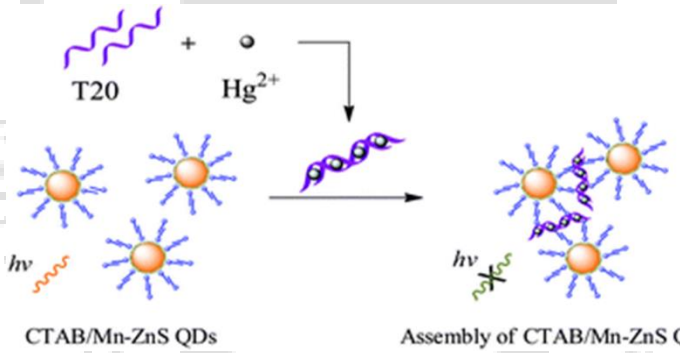

Fig 1.8 Room-temperature phosphorescence based Hg^{2+} sensor made of cetyltrimethylammonium bromide (CTAB) capped Mn^{2+}-doped ZnS Qdots and label-free thymine-rich aptamer. (Reprinted with permission from Reference [92]. Copyright *Analyst* 2012 Royal Society of Chemistry.)

Chen et al. have developed two different sensors for Zn^{2+} and Cu^{2+} ions using two different ligands (thioglycerol and L-cysteine) capped CdS Qdots.[93] L-cysteine capped CdS Qdots detected Zn^{2+} by enhancing photoluminescence intensity with a LOD of $0.8 \times 10^{-6}\ M$ while thioglycerol capped CdS Qdots detected Cu^{2+} ions by quenching photoluminescence intensity with a LOD of $0.1 \times 10^{-6}\ M$.

Singh et al. have developed a single chemical sensor by CdSe/ZnS Qdots functionalized

with chromogenic Schiff-base to simultaneously detect Cu^{2+} and Fe^{3+}.[94] Activity and selectivity of Schiff-base receptors towards Cu^{2+} and Fe^{3+} ions increase by attaching with CdSe/ZnS Qdots.

1.2.1.2 Anion Sensing:

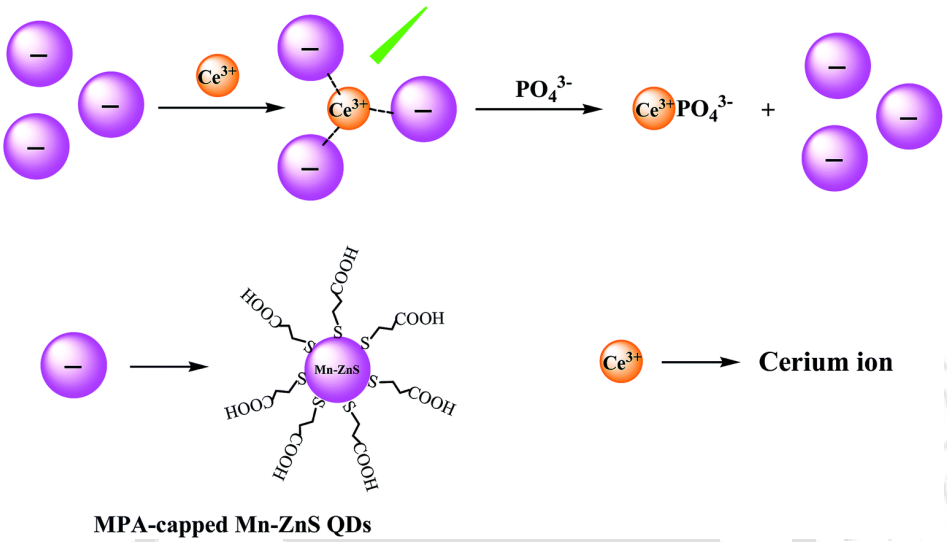

Fig 1.9 Illustrative representation of phosphate sensing using Mn-ZnS-Qdots/Ce^{3+} nanohybrids. (Reprinted with permission from Reference [108]. Copyright *RSC Adv.* 2017 Royal Society of Chemistry.)

Monitoring the concentration of anions like cyanide, phosphate, fluoride, sulfide, etc is a very important factor for human health, medical diagnosis, and environmental pollution.[95] Various Qdots or their surface modified forms have demonstrated their ability to detect above mentioned anions. For example, tert-butyl-N-(2-mercaptoethyl) carbamate capped CdSe Qdots successfully detected highly toxic CN^- anion up to $0.11 \times 10^{-6}\ M$.[96] Fluoride (F^-) ion, which has an important role in dental health has been detected by turn-on fluorescence mechanism using surface modified CdSe/ZnS Qdots. Here a surfactant $[C_{12}H_{25}N^+(CH_3)_2(CH_2)_4(CH_3)_2{-}N^+C_{12}H_{25}]{-}2Br^-$ and cetyltrimethylammonium bromide (CTAB) were used for surface modification of CdSe/ZnS Qdots.[97] MPA capped Mn-doped ZnS Qdots alone demonstrated its ability to detect sulfide (S^{2-}) ions up to $0.15 \times 10^{-6}\ M$.[98] Phosphate is one of the most important physiological process-controlling minerals in the human body. To maintain the ratio of $H_2PO_4^-/HPO_4^{2-}$ in the human body equal to 1:4 is important to avoid diseases like skeletal dysplasia, hyperparathyroidism, Fanconi syndrome, etc. In environmental water,

phosphate helps to grow many microorganisms that consume dissolved oxygen in the water. That's why the excess amount of phosphate decreases the quality of environmental water and acts as a pollutant.[99-107] So, the development of an efficient and highly sensitive phosphate detector is necessary, which can work in the aqueous medium. For example, MPA capped Mn-doped ZnS Qdots modulated by Ce^{3+} was found to be a turn-on sensor for phosphate ion detection with a LOD of $2.71 \times 10^{-6}\ M$. Here the affinity of phosphate to lanthanides takes a vital role in the detection mechanism (Fig 1.9).[108]

1.2.2 pH sensing:

pH is one of the most important parameters for any living system. Maintaining an appropriate pH in every biological system is essential for functioning all biological processes well. That's why the development of pH sensors is so important. The best way to develop a QDot-based chemical sensor is the functionalization of the surface of QDOTs with pH-sensitive molecules. For example, CdTe QDots capped with mercaptosuccinic acid were reported to sense pH from 3 to 11 due to protonation and deprotonation of capping ligands.[109] Medintz et al. used dopamine and peptide conjugated CdSe/ZnS core/shell QDot to detect intracellular pH.[52]

1.2.3 Fatty acid sensing:

Fatty acids (FAs) in mammalian cells are necessary to synthesize phospholipids and generate energy. Besides they help in several biological processes like activity of cell membranes and hypothalamus, gene expressions, metabolic regulation, etc. FAs are a major ingredient of dietary food products like vegetable oils, cosmetics, etc. However, excess amounts of FAs in the human body is harmful and causes several issues like coronary heart disease, multiple sclerosis, and chronic pain.[110-128] In cell FAs undergo two processes to prevent their excess accumulation: one, they inhibit the further synthesis of FAs, and second, excess FAs are incorporated in triglycerides (TGs). But these above-mentioned processes are not possible in the case of saturated FAs. That's why saturated FAs are considered not good for health.[129-134] Thus, recognition of unsaturated FAs from saturated FAs is very important to verify the quality of FAs containing foods. A Qdot-based nanoprobe has been developed for visual detection of oleic acid where 3-mercaptopropionic acid (MPA) capped CdSe/ZnS Qdots is self-assembled with rhodamine B-labeled bovine serum albumin (BSA) protein (Fig 1.10).[121] This nanoprobe works using the FRET mechanism to detect oleic acid with the detection limit of 10-1000

nM.

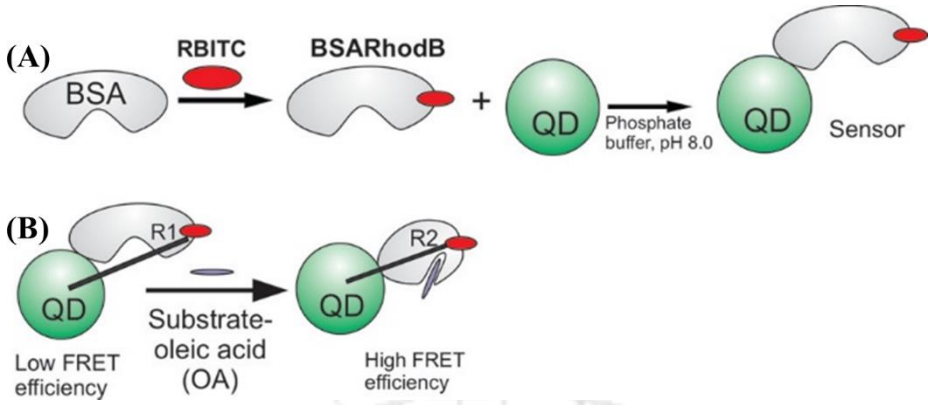

Fig 1.10 Schematic representation of (A) the formation of the oleic acid sensor by complexation between mercaptopropionic acid (MPA) capped CdSe/ZnS Qdots and with rhodamine B-labeled BSA protein, (B) the conformational changes of the sensor during the sensing of oleic acid. (Reprinted with permission from Reference [121]. Copyright Bioconjugate Chem. 2011 American Chemical Society.)

1.3 Ratiometric Sensing:

Change in visual color during detection of an analyte is always a preferable method in sensing application as it allows humans to understand the presence of that analyte through "naked-eyes". Therefore the development of a visual detection technique is always at first priority.[135] Here a ratiometric optical sensor serves this purpose. Ratiometric nanoprobes have taken an important role to detect environmental pollutants, biologically important molecules, pH, molecules related to human disease, etc. The main advantage of the ratiometric optical sensor is, unlike the single emission-dependent nanoprobe, that it takes care of the fluctuation of response intensity due to excitation source or detector, self-calibration, and visual color change.[66, 136-141]

Ratiometric optical sensors can follow two strategies to estimate the analyte: one is a reversible change in two optical signals simultaneously and the second one is the change in only one optical signal keeping the other one unhampered. Surface-modified Qdot is perfectly suitable to be a ratiometric optical sensor as more than one optical signal can be obtained by suitable surface complexation.

A very sensitive ratiometric Hg^{2+} sensor has been designed by combining red-emitting silica NPs-embedded CdTe/CdS Qdots and green-emitting glutathione (GSH)-capped CdTe/CdS Qdots. Here CdTe/CdS Qdots of two different sizes have been used to get two different emission colors. The inner part of the probe i.e., red-emitting silica

NP-embedded CdTe/CdS Qdots are insensitive towards Hg^{2+} whereas the outer part i.e., green-emitting CdTe/CdS Qdots capped by GSH are sensitive towards Hg^{2+}. In contact with Hg^{2+}, the green emission has been quenched, which leads to the color of the probe turning red. The sensitivity of this nanoprobe is up to 3.1 nM (Fig 1.11).[142]

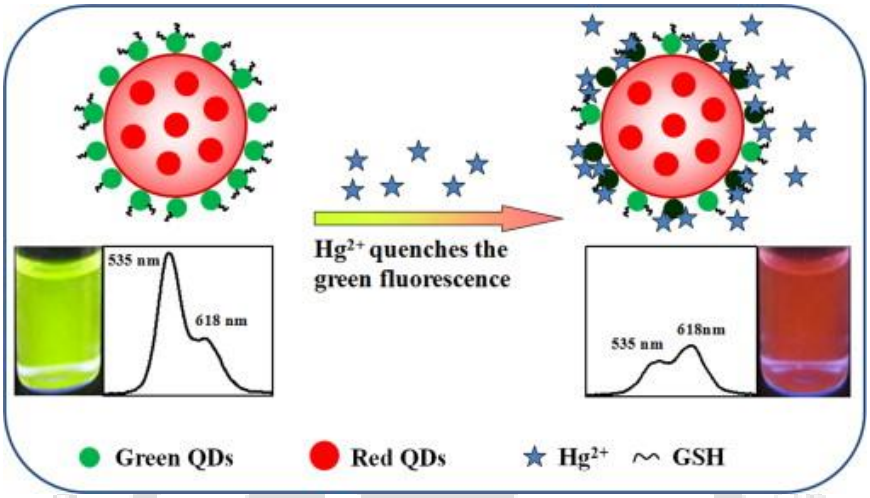

Fig 1.11 Schematic representation of dual emitting Qdot-based nanoprobe for the visual detection of Hg^{2+}. (Reprinted with permission from Reference [142]. Copyright *Talanta* 2014 Science Direct.)

A ratiometric, toxic material-free nanoprobe has been designed as a pH sensor by using surface-modified Mn-doped ZnS Qdots. 8-hydroxyquinoline-5-sulfonic acid has been used to form a greenish-blue emitting complex on the surface of Mn-doped ZnS Qdots. As the host Qdot itself has orange-red emission so the nanoprobe combined with the surface complex emitted white light at 320 nm excitation. During sensing of pH, the emission color has been changed from white to orange with the increase of pH and reversed back to white upon a decrease of pH within the range from 6.5 to 10.3 (Fig 1.12).[137]

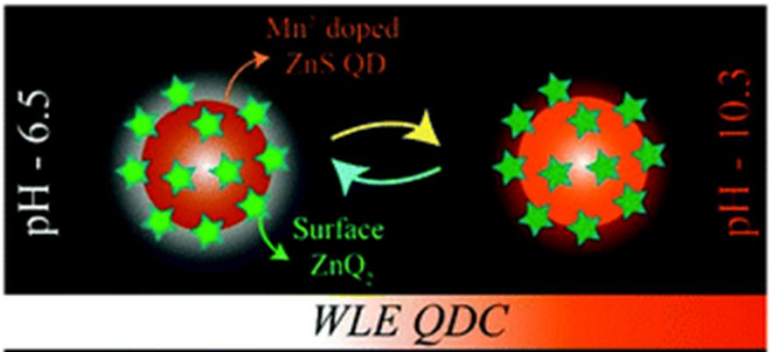

Fig 1.12 Reversible ratiometric pH sensor composed of surface-complexed white light emitting quantum dot complex (QDC). (Reprinted with permission from Reference [137]. Copyright *Chem. Commun.* 2019 Royal Society of Chemistry.)

A ratiometric sensor has been developed to detect dopamine, a redox-active neurotransmitter, using white light-emitting surface-modified ZnO Qdots. The surface of the yellow-emitting ZnO Qdot has been functionalized with a blue-emitting $Zn(MSA)_2$ complex, where MSA stands for N-methyl salicylaldimine. This white light-emitting nanoprobe successfully detected dopamine with a LOD of by changing its color to blue (Fig 1.13).[143]

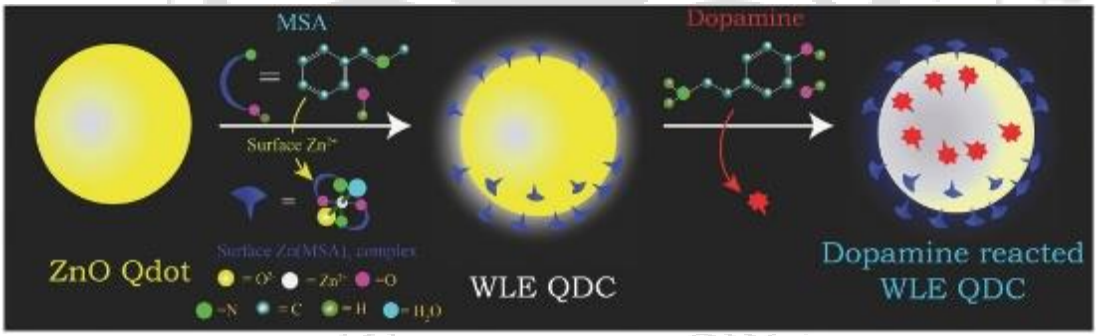

Fig 1.13 Scematic representation of dopamine sensing using white light emitting surface-complexed ZnO Qdots. (Reprinted with permission from Reference [143]. Copyright Small 2018 Wiley Online Library.)

1.4. Thesis Overview:

There are three independent ratiometric nanosensors that have been described in this thesis. A brief description of those nanosensors is given below.

Chapter 1 consists of the literature review of quantum dots, their surface modification strategies and sensing applications.

Chapter 2 presents a ratiometric optical nanosensor fabricated using a dual emitting quantum dot complex (QDC) for simultaneous detection of Hg^{2+} and Cu^{2+}. N-methyl salicylaldimine (MSA) has been used to form a blue-emitting complex (λ_{em} = 430 nm) on the surface of orange emitting Mn^{2+}-doped ZnS Qdots (λ_{em} = 600 nm) to fabricate the dual emitting nanosensor. When Hg^{2+} or Cu^{2+} was added to the dual emitting QDC, the orange emission was quenched and blue emission got enhanced resulting in a visual color change from purple to blue. The nanosensor showed high selectivity towards Hg^{2+} and Cu^{2+} among other interfering metal ions and a low detection limit of 85.5 nM for Hg^{2+} and 34.9 nM for Cu^{2+}, respectively.

In **chapter 3**, a ratiometric phosphate sensor has been developed using a white light-emitting (WLE) QDC that was composed of greenish blue-emitting $Zn(QS)_2$ (QS = 8-hydroxyquinoline-5-sulfonate) complex (λ_{em} = 480 nm) on the surface of orange emitting Mn^{2+}-doped ZnS Qdots (λ_{em} = 585 nm). In presence of phosphate, the emission corresponding to $Zn(QS)_2$ complex (i.e., at 480 nm) was quenched keeping the other emission (i.e., at 585 nm) unhampered. As a result, a visual color change from white to orange has been observed. The nanosensor selectively detected phosphate with a LOD of 5.9 nM. The newly fabricated nanoprobe successfully demonstrated its ability to detect phosphate in environmental water also.

Chapter 4 describes a QDC-based nanoprobe for recognition and ratiometric sensing of long-chain unsaturated fatty acids (LCUFAs). A WLE QDC has been fabricated by the formation of green-emitting ZnQ_2 complex (Q = 8-hydroxyquinoline, λ_{em} = 512 nm) on the surface of orange emitting Mn^{2+}-doped ZnS Qdots (λ_{em} = 590 nm), which acted as a ratiometric sensor to detect LCUFAs. Among some common unsaturated fatty acids, saturated fatty acids, amino acids, and cations, the nanoprobe selectively responded towards only LCUFAs. In this study, sodium salt of oleic acid, linoleic acid and erucic acid have been used as LCUFAs, and LODs were found to be 0.127, 0.126, and 0.103 μM, respectively. This nanosensor successfully detected the concentration of spiked LCUFAs in saponified daily-used vegetable oils such as sunflower, edible, and soybean oils.

The summarization of the thesis and plausible future prospects of the presented thesis works are described in **Chapter 5**.

1.5. Bibliography:

1. (a) C. J. Murphy and J. L. Coffer, *Applied Spectroscopy*, 2002, **56**, 16A-27A. (b) K. Dohnalová, A. N. Poddubny, A. A. Prokofiev, W. D. A. M. de Boer, C. P. Umesh, J. M. J. Paulusse, H. Zuilhof and T. Gregorkiewicz, *Light: Science & Applications*, 2013, **2**, e47-e47. (c) J.-W. Luo, A. Franceschetti and A. Zunger, *Physical Review B*, 2008, **78**, 035306. (d) A. N. Poddubny and K. Dohnalová, *Physical Review B*, 2014, **90**, 245439. (e) J. Rautert, T. S. Shamirzaev, S. V. Nekrasov, D. R. Yakovlev, P. Klenovský, Y. G. Kusrayev and M. Bayer, *Physical Review B*, 2019, **99**, 195411. (f) T. S. Shamirzaev, A. V. Shumilin, D. S. Smirnov, J. Rautert, D. R. Yakovlev and M. Bayer, *Physical Review B*, 2021, **104**, 115405. (g) H. Fu and A. Zunger, *Physical Review Letters*, 1998, **80**, 5397-5400.
2. M. A. Walling, J. A. Novak and J. R. E. Shepard, *Int J Mol Sci*, 2009, **10**, 441-491.
3. C. W. Chan Warren and S. Nie, *Science*, 1998, **281**, 2016-2018.
4. A. P. Alivisatos, *Science*, 1996, **271**, 933-937.
5. A. I. Ekimov and A. A. Onushchenko, *JETP Lett.* 1981, **6**, 345–349.
6. R. Rossetti, S. Nakahara and L. E. Brus, *J. Chem. Phys.*, 1983, **79**, 1086-1088.
7. M. A. Reed, J. N. Randall, R. J. Aggarwal, R. J. Matyi, T. M. Moore and A. E. Wetsel, *Phys. Rev. Lett.*, 1988, **60**, 535-537.
8. M. A. Hines and P. Guyot-Sionnest, *J. Phys. Chem. B*, 1998, **102**, 3655-3657.
9. H.-S. Chen, B. Lo, J.-Y. Hwang, G.-Y. Chang, C.-M. Chen, S.-J. Tasi and S.-J. J. Wang, *J. Phys. Chem. B*, 2004, **108**, 17119-17123.
10. Z. A. Peng and X. Peng, *J. Am. Chem. Soc.*, 2001, **123**, 183-184.
11. D. W. Lucey, D. J. MacRae, M. Furis, Y. Sahoo, A. N. Cartwright and P. N. Prasad, *Chem. Mater.*, 2005, **17**, 3754-3762.
12. O. Micic, J. Sprague, C. Curtis, K. Jones, J. Machol, A. Nozik, H. Giessen, B. Fluegel, G. Mohs and N. Peyghambarian, *J. Phys. Chem.*, 1995, **99**, 7754-7759.
13. I. Moreels, Y. Justo, B. De Geyter, K. Haustraete, J. C. Martins and Z. Hens, *ACS Nano*, 2011, **5**, 2004-2012.
14. H. Zhong, Z. Bai and B. Zou, *J. Phys. Chem. Lett.*, 2012, **3**, 3167-3175.
15. O. Yarema, D. Bozyigit, I. Rousseau, L. Nowack, M. Yarema, W. Heiss and V. Wood, *Chem. Mater.*, 2013, **25**, 3753-3757.

16. R. Xie, M. Rutherford and X. Peng, *J. Am. Chem. Soc.*, 2009, **131**, 5691-5697.
17. D. Pan, L. An, Z. Sun, W. Hou, Y. Yang, Z. Yang and Y. Lu, *J. Am. Chem. Soc.*, 2008, **130**, 5620-5621.
18. B. Mao, C.-H. Chuang, J. Wang and C. Burda, *J. Phys. Chem. C*, 2011, **115**, 8945-8954.
19. S.-W. Kim, J. P. Zimmer, S. Ohnishi, J. B. Tracy, J. V. Frangioni and M. G. Bawendi, *J. Am. Chem. Soc.*, 2005, **127**, 10526-10532.
20. Y. Chen, S. Li, L. Huang and D. Pan, *Inorg. Chem.*, 2013, **52**, 7819-7821.
21. H. Zhang, J. S. Son, J. Jang, J.-S. Lee, W.-L. Ong, J. A. Malen and D. V. Talapin, *ACS Nano*, 2013, **7**, 10296-10306.
22. J. Zhang, R. Xie and W. Yang, *Chem. Mater.*, 2011, **23**, 3357-3361.
23. D. Deng, L. Qu, J. Zhang, Y. Ma and Y. Gu, *ACS Appl. Mater. Interfaces*, 2013, **5**, 10858-10865.
24. D. A. Hines and P. V. Kamat, *University of Notre Dame PhD Thesis*, 2015, 5-6.
25. T. Kippeny, L. A. Swafford and S. J. Rosenthal, *J. Chem. Educ.*, 2002, **79**, 1094.
26. P. Kambhampati, Book chapter in *Handbook of Photoluminescent Semiconductor Materials – Taylor & Francis*, 2011**.**
27. P. Kambhampati, *Acc. Chem. Res.*, 2011, **44**, 1-13.
28. A. Rogach, *ACS Nano*, 2014, **8**, 6511-6512.
29. A. Nag, R. Cherian, P. Mahadevan, A. V. Gopal, A. Hazarika, A. Mohan, A. S. Vengurlekar and D. D. Sarma, *J. Phys. Chem. C*, 2010, **114**, 18323-18329.
30. N. Pradhan, S. Das Adhikari, A. Nag and D. D. Sarma, *Angew. Chem. Int. Ed.*, 2017, **56**, 7038-7054.
31. A. Hazarika, A. Pandey and D. D. Sarma, *J. Phys. Chem. Lett.*, 2014, **5**, 2208-2213.
32. P. V. Kamat, *J. Phys. Chem. Lett.*, 2011, **2**, 2832-2833.
33. G. K. Grandhi and R. Viswanatha, *J. Phys. Chem. Lett.*, 2013, **4**, 409-415.
34. W. Zhang, X. Zhou and X. Zhong, *Inorg. Chem.*, 2012, **51**, 3579-3587.
35. D. Mocatta, G. Cohen, J. Schattner, O. Millo, E. Rabani and U. Banin, *Science*, 2011, **332**, 77-81.
36. M. D. Regulacio and M.-Y. Han, *Acc. Chem. Res.*, 2010, **43**, 621-630.
37. D. A. Hines and P. V. Kamat, *ACS Appl. Mater. Interfaces*, 2014, **6**, 3041-3057.
38. M. A. Boles, D. Ling, T. Hyeon and D. V. Talapin, *Nat. Mater.*, 2016, **15**, 141-153.

39. C. Giansante, *Acc. Chem. Res.*, 2020, **53**, 1458-1467.
40. D. A. Hines and P. V. Kamat, *J. Phys. Chem. C*, 2013, **117**, 14418-14426.
41. J. Owen, *Science*, 2015, **347**, 615-616.
42. C. Giansante and I. Infante, *J. Phys. Chem. Lett.*, 2017, **8**, 5209-5215.
43. R. Grisorio, D. Quarta, A. Fiore, L. Carbone, G. P. Suranna and C. Giansante, *Nanoscale Adv.*, 2019, **1**, 3639-3646.
44. C. Giansante, *J. Phys. Chem. C*, 2018, **122**, 18110-18116.
45. J. McBride, J. Treadway, L. C. Feldman, S. J. Pennycook and S. J. Rosenthal, *Nano Lett.*, 2006, **6**, 1496-1501.
46. D. Vasudevan, R. R. Gaddam, A. Trinchi and I. Cole, *J. Alloys Compd.*, 2015, **636**, 395-404.
47. A. Nag, M. V. Kovalenko, J.-S. Lee, W. Liu, B. Spokoyny and D. V. Talapin, *J. Am. Chem. Soc.*, 2011, **133**, 10612-10620.
48. C. Giansante, *Nanoscale*, 2019, **11**, 9478-9487.
49. D. R. Baker and P. V. Kamat, *Langmuir*, 2010, **26**, 11272-11276.
50. P. R. Brown, D. Kim, R. R. Lunt, N. Zhao, M. G. Bawendi, J. C. Grossman and V. Bulović, *ACS Nano*, 2014, **8**, 5863-5872.
51. F. Erogbogbo, K.-T. Yong, I. Roy, R. Hu, W.-C. Law, W. Zhao, H. Ding, F. Wu, R. Kumar, M. T. Swihart and P. N. Prasad, *ACS Nano*, 2011, **5**, 413-423.
52. I. L. Medintz, M. H. Stewart, S. A. Trammell, K. Susumu, J. B. Delehanty, B. C. Mei, J. S. Melinger, J. B. Blanco-Canosa, P. E. Dawson and H. Mattoussi, *Nat. Mater.*, 2010, **9**, 676-684.
53. C. Zhao, Z. Bai, X. Liu, Y. Zhang, B. Zou and H. Zhong, *ACS Appl. Mater. Interfaces*, 2015, **7**, 17623-17629.
54. S. Bhandari, S. Roy and A. Chattopadhyay, *RSC Advances*, 2014, **4**, 24217-24221.
55. S. Roy, S. Bhandari and A. Chattopadhyay, *J. Phys. Chem. C*, 2015, **119**, 21191-21197.
56. S. Bhandari, S. Roy, S. Pramanik and A. Chattopadhyay, *Langmuir*, 2015, **31**, 551-561.
57. S. Bhandari, S. Roy, S. Pramanik and A. Chattopadhyay, *Langmuir*, 2014, **30**, 10760-10765.
58. S. Roy, S. Bhandari, M. Manna, S. De and A. Chattopadhyay, *Phys. Chem. Chem. Phys.*, 2019, **21**, 589-596.

59. S. Bhandari, R. Khandelia, U. N. Pan and A. Chattopadhyay, *ACS Appl. Mater. Interfaces*, 2015, **7**, 17552-17557.
60. S. Pramanik, S. Bhandari, S. Roy and A. Chattopadhyay, *J. Phys. Chem. Lett.*, 2015, **6**, 1270-1274.
61. S. Pramanik, S. Bhandari and A. Chattopadhyay, *J. Mater. Chem. C*, 2017, **5**, 7291-7296.
62. S. Roy, S. Pramanik, S. Bhandari and A. Chattopadhyay, *Langmuir*, 2017, **33**, 14627-14633.
63. S. Bhandari, S. Roy, S. Pramanik and A. Chattopadhyay, *Langmuir*, 2019, **35**, 14399-14413.
64. F. G. Banica, Chemical Sensors and Biosensors Fundamentals and Applications, first ed., Wiley, 2012, ISBN 9780470710661.
65. X. Huang, J. Song, B. C. Yung, X. Huang, Y. Xiong and X. Chen, *Chem. Soc. Rev.*, 2018, **47**, 2873-2920.
66. S. Silvi and A. Credi, *Chem. Soc. Rev.*, 2015, **44**, 4275-4289.
67. P. Wu and X.-P. Yan, *Chem. Soc. Rev.*, 2013, **42**, 5489-5521.
68. J. Patel, B. Jain, A. K. Singh, M. A. B. H. Susan and L. Jean-Paul, *Microchem. J.*, 2020, **155**, 104755.
69. Y. Wang, R. Hu, G. Lin, I. Roy and K.-T. Yong, *ACS Appl. Mater. Interfaces*, 2013, **5**, 2786-2799.
70. X. Chen, Y. Liu and Q. Ma, *J. Mater. Chem. C*, 2018, **6**, 942-959.
71. M. A. Farzin and H. Abdoos, *Talanta*, 2021, **224**, 121828.
72. U. Badıllı, F. Mollarasouli, N. K. Bakirhan, Y. Ozkan and S. A. Ozkan, *TrAC Trends in Anal. Chem.*, 2020, **131**, 116013.
73. N. Hildebrandt, C. M. Spillmann, W. R. Algar, T. Pons, M. H. Stewart, E. Oh, K. Susumu, S. A. Díaz, J. B. Delehanty and I. L. Medintz, *Chem. Rev.*, 2017, **117**, 536-711.
74. M. Stanisavljevic, S. Krizkova, M. Vaculovicova, R. Kizek and V. Adam, *Biosens. Bioelectron.*, 2015, **74**, 562-574.
75. J. Zhou, Y. Yang and C.-y. Zhang, *Chem. Rev.*, 2015, **115**, 11669-11717.
76. J. Zhang, F. Cheng, J. Li, J.-J. Zhu and Y. Lu, *Nano Today*, 2016, **11**, 309-329.
77. H. Yin, A. Truskewycz and I. S. Cole, *Microchimica Acta*, 2020, **187**, 1-25.
78. P. Wu, X. Hou, J.-J. Xu and H.-Y. Chen, *Nanoscale*, 2016, **8**, 8427-8442.
79. X. Sun, P. Liu, L. Wu and B. Liu, *Analyst*, 2015, **140**, 6742-6747.

80. E. S. Childress, C. A. Roberts, D. Y. Sherwood, C. L. M. LeGuyader and E. J. Harbron, *Anal. Chem.*, 2012, **84**, 1235-1239.
81. X. Liu, L. Wang, N. Zhang and D. Shangguan, *Anal. Methods*, 2015, **7**, 8019-8024.
82. F. Yarur, J.-R. Macairan and R. Naccache, *Environ. Sci.: Nano*, 2019, **6**, 1121-1130.
83. S.-L. Pan, K. Li, L.-L. Li, M.-Y. Li, L. Shi, Y.-H. Liu and X.-Q. Yu, *Chem. Commun.*, 2018, **54**, 4955-4958.
84. E. Babaee, A. Barati, M. B. Gholivand, A. Taherpour, N. Zolfaghar and M. Shamsipur, *J. Hazard. Mater.* , 2019, **367**, 437-446.
85. Y. Gao, C. Zhang, S. Peng and H. Chen, *Sensors and Actuators B*, 2017, **238**, 455-461.
86. R. Gui, H. Jin, Y. Wang and J. Sun, *Sensors and Actuators B*, 2017, **245**, 386-394.
87. H. Li, X. Wang, Z. Cai, L. Lu, J. Tao, B. Sun, Y. Yang, Q. Xu, Z. Yu and P. Zhao, *Anal Bioanal Chem*, 2017, **409**, 6655-6662.
88. M. Lan, J. Zhang, Y.-S. Chui, P. Wang, X. Chen, C.-S. Lee, H.-L. Kwong and W. Zhang, *ACS Appl. Mater. Interfaces*, 2014, **6**, 21270-21278.
89. H. Li, Y. Zhang, X. Wang, D. Xiong and Y. Bai, *Materials Letters*, 2007, **61**, 1474-1477.
90. H. Li, Y. Zhang and X. Wang, *Sensors and Actuators B*, 2007, **127**, 593-597.
91. D. S. M. Ribeiro, R. C. Castro, R. N. M. J. Páscoa, J. X. Soares, S. S. M. Rodrigues and J. L. M. Santos, *J. Lumin.*, 2019, **207**, 386-396.
92. W. Y. Xie, W. T. Huang, H. Q. Luo and N. B. Li, *Analyst*, 2012, **137**, 4651-4653.
93. Y. Chen and Z. Rosenzweig, *Anal. Chem.*, 2002, **74**, 5132-5138.
94. N. Singh, R. C. Mulrooney, N. Kaur and J. F. Callan, *Chem. Commun.*, 2008, 4900-4902.
95. Y. Lou, Y. Zhao and J.-J. Zhu, *Nanoscale Horizons*, 2016, **1**, 125-134.
96. W. J. Jin, J. M. Costa-Fernández, R. Pereiro and A. Sanz-Medel, *Analytica Chimica Acta*, 2004, **522**, 1-8.
97. H. Li and X. Wang, *Sensors and Actuators B*, 2008, **134**, 238-244.
98. B.-H. Zhang, F.-Y. Wu, Y.-M. Wu and X.-S. Zhan, *J. Fluoresc.*, 2010, **20**, 243-250.
99. L. Han, S. G. Liu, Y. Z. Yang, Y. Z. Fan, J. Zhou, X. Y. Zhang, N. B. Li and H.

Q. Luo, *J. Mater. Chem. C*, 2020, **8**, 13063-13071.

100. X. Li, P. Liu, X. Niu, K. Ye, L. Ni, D. Du, J. Pan and Y. Lin, *Nanoscale*, 2020, **12**, 19383-19389.
101. Y. Ma, Y. Zhang, X. Li, P. Yang, J.-Y. Yue, Y. Jiang and B. Tang, *Anal. Chem.*, 2020, **92**, 3722-3727.
102. X. Li, X. Niu, P. Liu, X. Xu, D. Du and Y. Lin, *Sensors and Actuators B*, 2020, **321**, 128546.
103. G. Li and C. Tong, *Analytica Chimica Acta*, 2020, **1133**, 11-19.
104. N. Gao, J. Huang, L. Wang, J. Feng, P. Huang and F. Wu, *Appl. Surf. Sci.*, 2018, **459**, 686-692.
105. C. Dai, C.-X. Yang and X.-P. Yan, *Anal. Chem.*, 2015, **87**, 11455-11459.
106. D. Yan, Y. He, Y. Ge and G. Song, *J. Fluoresc.*, 2017, **27**, 227-233.
107. Z. Zhang, J. Feng, P. Huang, S. Li and F.-Y. Wu, *Sensors and Actuators B*, 2019, **298**, 126891.
108. J. Qin, D. Li, Y. Miao and G. Yan, *RSC Advances*, 2017, **7**, 46657-46664.
109. T. K. Nideep, M. Ramya, U. Sony and M. Kailasnath, *Mater. Res. Express*, 2019, **6**, 105002.
110. K. Niki, T. Tsutsui, M. Yamashina, M. Akita and M. Yoshizawa, *Angew. Chem. Int. Ed.*, 2020, **59**, 10489-10492.
111. S. Mosca, D. Ajami and J. Rebek, *Proc. Natl. Acad. Sci.*, 2015, **112**, 11181.
112. K. Schierbaum, T. Weiss, E. T. Van Veizen, J. Engbersen, D. Reinhoudt and W. Göpel, *Science*, 1994, **265**, 1413-1415.
113. K. Wang, J. H. Jordan and B. C. Gibb, *Chem. Commun.*, 2019, **55**, 11695-11698.
114. K. Yazaki, Y. Sei, M. Akita and M. Yoshizawa, *Nat. Commun.*, 2014, **5**, 5179.
115. J. N. Lee, H. Kim, H. Yao, Y. Chen, K. Weng and J. Ye, *Proc. Natl. Acad. Sci.*, 2010, **107**, 21424.
116. Y.-S. Cho, D. H. Ma and K. H. Ahn, *J. Mater. Chem. C*, 2016, **4**, 2871-2876.
117. F. Zhang, X. Wang, H. Tang, X. Jie, X. Jiang and W. Wei, *Nanotechnology*, 2018, **30**, 065502.
118. B. J. Shorthill, C. T. Avetta and T. E. Glass, *J. Am. Chem. Soc.*, 2004, **126**, 12732-12733.
119. A. Bartolome, C. Bardliving, G. Rao and L. Tolosa, *Anal. Biochem.*, 2005, **345**, 133-139.
120. K. Fujimoto, S. Yamada and M. Inouye, *Chem. Commun.*, 2009, 7164-7166.

121. S. V. Dezhurov, I. Y. Volkova and M. S. Wakstein, *Bioconjugate Chem.*, 2011, **22**, 338-345.
122. A. R. Saltiel and C. R. Kahn, *Nature*, 2001, **414**, 799-806.
123. E. Honoré, J. Barhanin, B. Attali, F. Lesage and M. Lazdunski, *Proc. Natl. Acad. Sci.*, 1994, **91**, 1937.
124. X. Chen, K.-M. Lee and J.-Y. Yoon, *Bull. Korean Chem. Soc.*, 2011, **32**, 3775-3778.
125. S. C. Smolinske, Handbook of Food, Drug, and Cosmetic Excipients, 1992, pp. 1–448.
126. D. Funk Colin, *Science*, 2001, **294**, 1871-1875.
127. D. Mozaffarian, M. B. Katan, A. Ascherio, M. J. Stampfer and W. C. Willett, *N. Engl. J. Med.*, 2006, **354**, 1601-1613.
128. L. Zhang, P. Li, X. Sun, X. Wang, B. Xu, X. Wang, F. Ma, Q. Zhang and X. Ding, *J. Agric. Food Chem.*, 2014, **62**, 8745-8751.
129. J. Ntambi, *J. Biol. Chem.*, 1992, **267**, 10925-10930.
130. J. Ou, H. Tu, B. Shan, A. Luk, R. A. DeBose-Boyd, Y. Bashmakov, J. L. Goldstein and M. S. Brown, *Proc. Natl. Acad. Sci.*, 2001, **98**, 6027-6032.
131. V. C. Hannah, J. Ou, A. Luong, J. L. Goldstein and M. S. Brown, *J. Biol. Chem.*, 2001, **276**, 4365-4372.
132. R. V. Farese Jr and T. C. Walther, *Cell*, 2009, **139**, 855-860.
133. J. N. Lee, X. Zhang, J. D. Feramisco, Y. Gong and J. Ye, *J. Biol. Chem.*, 2008, **283**, 33772-33783.
134. T. Coll, E. Eyre, R. Rodríguez-Calvo, X. Palomer, R. M. Sánchez, M. Merlos, J. C. Laguna and M. Vázquez-Carrera, *J. Biol. Chem.*, 2008, **283**, 11107-11116.
135. S. Paterson and R. De La Rica, *Analyst*, 2015, **140**, 3308-3317.
136. A. Bonanno, I. Pérez-Herráez, E. Zaballos-García and J. Pérez-Prieto, *Chem. Commun.*, 2020, **56**, 587-590.
137. S. Pramanik, S. Roy, A. Mondal and S. Bhandari, *Chem. Commun.*, 2019, **55**, 4331-4334.
138. L. He, W. Lin, Q. Xu and H. Wei, *Chem. Commun.*, 2015, **51**, 1510-1513.
139. Y.-N. Chen, P.-C. Chen, C.-W. Wang, Y.-S. Lin, C.-M. Ou, L.-C. Ho and H.-T. Chang, *Chem. Commun.*, 2014, **50**, 8571-8574.
140. K. Paek, S. Chung, C.-H. Cho and B. J. Kim, *Chem. Commun.*, 2011, **47**, 10272-10274.

141. T. Jin, A. Sasaki, M. Kinjo and J. Miyazaki, *Chem. Commun.*, 2010, **46**, 2408-2410.

142. Q. Mu, Y. Li, H. Xu, Y. Ma, W. Zhu and X. Zhong, *Talanta*, 2014, **119**, 564-571.

143. S. Pramanik, S. Bhandari, U. N. Pan, S. Roy and A. Chattopadhyay, *Small*, 2018, **14**, 1800323.

Chapter 2

A Dual-emitting Quantum Dot Complex Nanoprobe for Ratiometric and Visual Detection of Hg^{2+} and Cu^{2+} ions

2.1 Abstract:

In this chapter, we report the use of a dual emitting quantum dot complex (QDC; composed of blue emitting metal-methylsalicylaldimine complex being on the surface of orange emitting Mn^{2+}-doped ZnS quantum dot) for ratiometric and visual detection of Hg^{2+} and Cu^{2+} ions - following the alterations in luminescence color, intensity ratio, chromaticity and hue of the QDC.

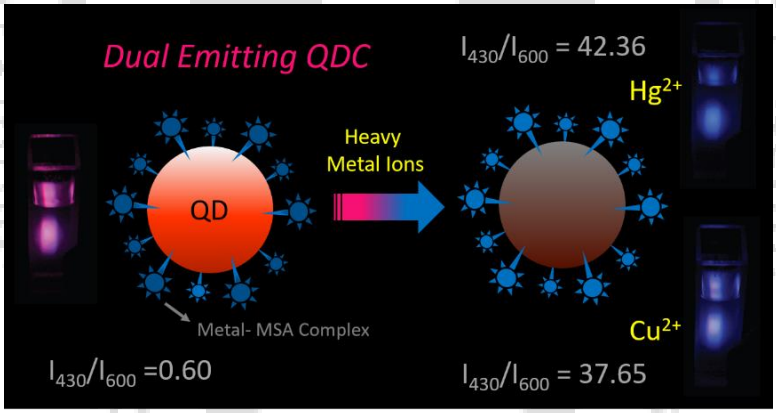

* [Manna et al. *J. Mater. Chem. C*, 2020, **8**, 6972--6976] - Reproduced by permission from the Royal Society of Chemistry.

2.2 Introduction:

Ratiometric nanoprobe stands out as an important optical sensor for the rapid and sensitive detection of human disease related molecules and environmental pollutants, especially when compared with single-wavelength intensity dependent nanoprobes.[1-7] Notably, the disadvantages related to fluctuation in intensity depending on light source and detector, local concentration of analytes limit the real life sensing application of single-wavelength intensity dependent nanoprobes.[1-7] On the other hand, the advantages of self-calibration and precise quantification, visual colour change and in addition to overcome the issues of background and instrumentation limitations make the ratiometric nanoprobe as the potential candidate.[1-7]

Heavy metals (such as Hg^{2+} and Cu^{2+} ions) are known to be responsible human diseases and hazardous for the environment.[8-9] For example, the accumulation of toxic Hg^{2+} ions causes muscle weakness, neurological disorder, Minamata and Pinks diseases in the human body while the abnormal content of Cu^{2+} ions leads to human diseases such as Parkinson's, Alzheimer's, and Wilson's diseases.[8-9] Thus, the rapid, sensitive, selective and visual detection of trace amounts of Hg^{2+} and Cu^{2+} ions is highly desirable in environmental monitoring applications. Numerous optical nanoprobes (such as quantum dots (Qdots), carbon Qdots, atomic nanoclusters and organic dyes), based on the changes to the signal intensity at a particular wavelength, have been demonstrated to be useful for quantifying Hg^{2+} and Cu^{2+} ions.[8-9] Among them, Qdots-based nanoprobes are advantageous due to their unique optical features such as high quantum yield and photostablity.[3, 10] However, the application potential of these nanoprobes is generally limited due to the problems linked to the fluctuation in the luminescence intensity, as stated above. This creates an opportunity for ratiometric sensors not only to address the issues arising out of single-wavelength intensity dependent nanoprobe but also to make easier visual detection of heavy metal ions. Incidentally, a few ratiometric optical nanoprobes are already available for the detection of Hg^{2+} and Cu^{2+} ions.[8-9] For example, (i) a dual emitting nanocomposite – comprised of carbon Qdots and rhodamine – sense Hg^{2+} ions, with a limit of detection (LOD) of 42 nM in a wide pH range, (ii) C- Qdots mixed with CdTe/CdS Qdots have been used to detect Cu^{2+} ions with a LOD of 38 nM and (iii) the nanocomposite, composed of the combination of two different C- Qdots, has been used to sense Hg^{2+} (LOD-0.08 μM) and Cu^{2+} (LOD-0.05 μM) ions.[9] However, the carbon based ratiometric nanoprobes require multiple synthesis and critical purification

steps – which restrict their large-scale application potential. Thus it would be important to fabricate a new, cost-effective and biocompatible metal Qdot-based ratiometric nanoprobe for the visual, sensitive and selective detection of Hg^{2+} and Cu^{2+} ions.

Surface modification of metal chalcogenide Qdot, especially with inorganic complex, is of central importance for fabricating newer nanocomposites with superior optical features and advanced applications such as white light generation, targeted bioimaging, optical sensing of neurotransmitter molecule (dopamine) and measuring of physiological pH.[3,10] For example, white light emitting inorganic complex coupled metal chalcogenide Qdot (also known as quantum dot complex (QDC)) were used in ratiometric and visual detection of dopamine molecule and physiological pH in the range of 6.5-10.6 based on the color changes from white to blue and white to orange, respectively.[3,10c] However, the application of QDC is not yet explored towards visual, ratiometric and sensitive detection of heavy metal ions (Hg^{2+} and Cu^{2+} ions). Hence, the development and use of a dual emitting QDC, consisting of metal chalcogenide Qdot and luminescent inorganic complex, towards ratiometric and visual detection Hg^{2+} and Cu^{2+} ions can be considered as an important target with advantages over competing sensors as mentioned above.

Herein we report the fabrication of a ratiometric optical nanoprobe, based on the formation of blue emitting $M(MSA)_2$ complex (with λ_{em}-430 nm; N-methylsalicylaldimine (MSA) is the complexing agent and M stands for Zn and Mn) on the surface of a nontoxic orange emitting Mn^{2+}-doped ZnS Qdots (with λ_{em}-600 nm). The purple coloured luminescent $M(MSA)_2$ complex coupled Mn^{2+} doped ZnS Qdot is termed herein as dual-emitting QDC. Notably, the photostable dual-emitting QDC showed the visual changes in the luminescence color (with change in chromaticity and hue) from purple to blue in the presence of Hg^{2+} and Cu^{2+} ions. The luminescence intensity ratio (I_{430}/I_{600}) of QDC changed from 0.60 to 42.36 and 37.65 in the presence of 16.67 μM of Hg^{2+} and 13.33 μM Cu^{2+} ions, respectively. The QDC showed LOD of 85.5 and 34.9 nM for Hg^{2+} and Cu^{2+} ions, respectively and also displayed high selectivity in the presence of interfering metal ions. This is the first report involving the utilisation of QDC (thus both the complex and the Qdot simultaneously) towards visual luminescent based sensing of trace amount of heavy metal ions following the changes in luminescence color, intensity ratio, chromaticity and hue.

2.3 Experimental Section:

2.3.1 Materials: Manganese acetate tetrahydrate (Merck), zinc acetate dihydrate (Merck), sodium sulphide (Merck), 1 M methylamine in methanol (Sigma-Aldrich), salicylaldehyde (Sigma-Aldrich), mercury acetate (Merck), copper acetate (Merck), lead acetate (Merck), cobalt acetate (Merck), nickel acetate (Merck), cadmium acetate (Merck), sodium acetate (Merck), methanol (Merck) were purchased and used directly without any purification.

2.3.2 Synthesis of Mn^{2+}-doped ZnS Qdots: The synthesis of Mn^{2+}-doped ZnS Qdots was performed using a reported protocol.[3, 10d] Concisely, 5.0 mM of sodium sulphide was added into a 50 mL aqueous solution containing of the mixture of 5.0 mM of zinc acetate dihydrate and 0.75 mM of manganese acetate tetrahydrate. The subsequent mixture was refluxed for 4 h under continuous stirring at 100 °C. The so-obtained white colloidal particles were centrifuged with a speed of 12,000 rpm for 10 min. The centrifuged pellet was thoroughly washed and redispersed into the same amount of water and centrifuged again with same experimental conditions. The washing cycle was repeated (in the presence of methanol) and finally the pellet was dispersed in 200.0 mL of methanol. The so obtained colloidal dispersion was used for further experiments. The Qdots were characterized by using fluorescence, UV-vis, TEM and XRD analyses.

2.3.3 Preparation of MSA Solution: The synthesis of MSA Ligand was carried out following a reported procedure.[10c, 10f] Briefly, the addition of 4.0 mmol of methylamine into a solution of 2.0 mmol of salicylaldehyde (in 20.0 mL methanol) resulted in yellow color mixture, which was kept for 6 h under stirring condition at 25 °C. Then, the resulting MSA ligand was purified by column chromatographic technique.

2.3.4 Synthesis of Dual-Emitting QDC: The dual-emitting QDC was synthesized by addition of 150.0 µL of 5.0 mM of MSA (methanol) to the 10.0 mL methanolic dispersion of Mn^{2+} doped ZnS Qdots (with absorbance of 0.03 at 355 nm). The resulting mixture was centrifuged at a speed of 12000 rpm and the pellet was further redispersed in the equal amount of solvent. The optimum amount of the MSA ligand was found to be 75.0 µM for the fabrication of purple colored dual-emitting QDC. The dual-emitting QDC was characterized by using fluorescence, UV-vis, TEM and XRD analyses.

2.3.5 Heavy Metal Ion Sensing: The heavy metal ion sensing of QDC was performed following individual sequential addition of the solutions of 1.0 mM Hg^{2+} and Cu^{2+} ions (as their acetate salts) to 3.0 mL dispersion of QDC (having absorbance of 0.03 at 355 nm). The limit of detection (LOD) was calculated by using 3σ/k plot. The changes in the luminescence properties (such as color, intensity ratio, chromaticity and hue) of the QDC were monitored to detect the mentioned heavy metal ions.

2.3.6 Selectivity Experiment: The selectivity experiment was carried out by using higher concentration (83.33 μM) of interfering metal ions compared to Hg^{2+} (16.67 μM) and Cu^{2+} ions (13.33 μM). The 5.0 mM acetate salts of Pb, Ni, Co, Cd, Mn, Na were added to 3.0 mL of QDC (having absorbance of 0.03 at 355 nm) separately so that the final concentration of interfering ions were to be 83.33 μM while 16.67 μM of Hg^{2+} ions and 13.33 μM of Cu^{2+} ions were used for the selectivity experiment. Emission spectra and corresponding intensity ratio were monitored to describe selectivity of the QDC.

2.3.7 Instruments: Transmission electron microscopy (TEM; JEOL JEM 2100F, maximum accelerating voltage: 200 kV) was used to analyze the size and lattice fringe of the materials. TEM and inverse fast Fourier transform analyses were done by using Gatan Digital Micrograph software. Brucker D2 Advance X-ray diffractometer was used to record the diffraction patterns of the materials. HORIBA Jobin Yvon FluoroMax-4 spectrofluorimeter and Perkin Elmer LAMBDA 750 UV–vis spectrophotometer were used to record the luminescence and absorption spectra of the materials, respectively. OSRAM color calculator (CIE-1931) was used to calculate the chromaticity of the samples. Hue analysis was performed by using Image-J software following earlier protocols.[3]

2.4 Results and Discussion:

The as-synthesized Mn^{2+}-doped ZnS Qdots showed emission maximum at 600 nm (Fig. 2.1B) with an absorption edge at 325 nm (Fig. A.2.1, Appendix). It is to be noted that the Mn^{2+}-doped ZnS Qdots were synthesized following our earlier reported protocol (where the mol% of dopant Mn^{2+} had been measured as 2.84%).[10d] The orange emitting Qdots also showed average particle size of 5.0 $\pm$ 0.2 nm and 0.3 nm lattice fringe (due to the (111) lattice plane of cubic ZnS) in the transmission electron microscopic (TEM) analysis (Fig. A.2.2, Appendix).[10d,e] The characteristics peaks of (111), (220) and (311) lattice planes of cubic ZnS were observed at 28.8º, 47.8º, and 56.7º, respectively,

in the powder X-ray diffraction analysis of Mn^{2+} doped ZnS Qdots (Fig. A.2.2, Appendix).[10d,e] These clearly indicated the successful synthesis of Mn^{2+}-doped ZnS Qdots. Digital photographs (captured using a spectrofluorimeter at an excitation of 355 nm light) showed the changes of luminescence color from orange to purple when Mn^{2+}-doped ZnS Qdots were complexed with MSA ligands (Fig. 2.1A).

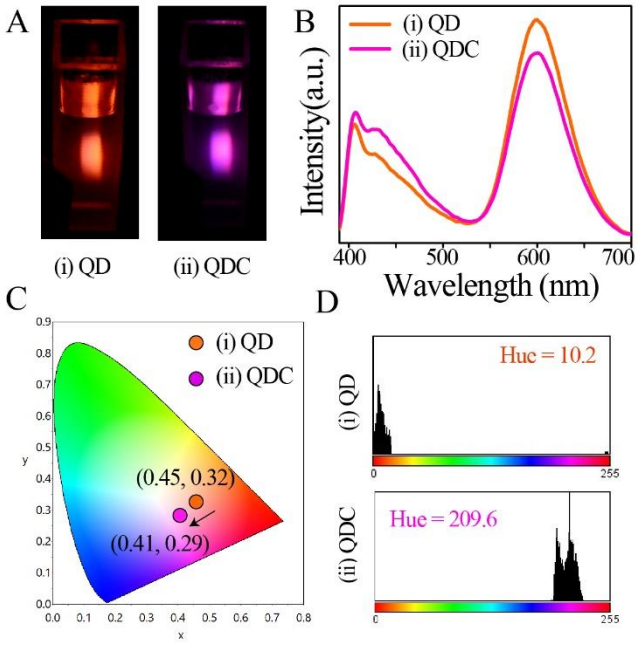

Fig. 2.1 (A) Digital photographs (captured using 355 nm light from a spectrofluorimeter), **(B)** emission spectra (λ_{ex} = 355 nm), **(C)** corresponding chromaticity color coordinates in CIE diagram and **(D)** hue histograms of (i) Mn^{2+} doped ZnS Qdots and (ii) dual-emitting QDC. Hue histograms were obtained by analysing the digital photographs as depicted in (A) using Image-J software.

The MSA complexed Mn^{2+}-doped ZnS Qdots – termed herein as dual-emitting QDC – showed two emission peaks at 600 nm and 430 nm (Fig. 2.1B).[10c] It is to be noted that the emission of QDC at 600 nm is originated from the $^4T_1$-$^6A_1$ electronic transition of Mn^{2+} dopants of Mn^{2+}-doped ZnS Qdots present in the QDC.[10c,d] According to literature reports, the emission of QDC at 430 nm is due to the electronic transition between the lowest unoccupied molecular orbital (LUMO) and the highest occupied molecular orbital (HOMO) of the formed $M(MSA)_2$ surface inorganic complex.[10f,g] The dual-emitting QDC showed color chromaticity of (0.41, 0.29) and hue mean value of 209.6, while (0.45, 0.32) color chromaticity and 10.2 hue value were observed for the Mn^{2+}-doped ZnS QDots (Fig. 2.1C and D). It is to be mentioned here that chromaticity and hue are the analytical parameters for ascertaining the luminescence colors in the CIE-

1931 and HSV (Hue, saturation and value) color spaces, respectively.[10h] The results clearly indicated the formation of dual-emitting QDC with contributions from blue emitting metal-MSA complex and orange emitting Mn^{2+}-doped ZnS Qdot. The optimum amount of MSA for the synthesis of dual-emitting QDC was found to be 75.0 μM for 3.0 mL of Mn^{2+}-doped ZnS QDs, with absorbance of 0.03 at 355 nm. Also, no significant change in the absorption edge of Qdot – following complexation – was noticed (Fig. A.2.1, Appendix). Furthermore, no morphological alterations in terms of size, lattice fringe and X-ray diffraction pattern were observed when Mn^{2+}-doped ZnS Qdots were complexed with MSA (Fig. A.2.3, Appendix). Hence, the obtained results clearly supported the successful formation of dual emitting QDC. Furthermore, the dual emitting QDC was found to be photostable with regard to their emission peaks (at 600 and 430 nm) in the presence of continuous irradiation of 355 nm light for half an hour (Fig. A.2.4, Appendix). This indicated the usefulness of photostable dual emitting QDC towards futuristic sensing applications.

Interestingly, the digital photographs (captured with an excitation of 355 nm light using a spectrofluorimeter) of the QDC in the presence of heavy metal ions (such as Hg^{2+} and Cu^{2+} ions) showed the changes in the visual luminescence color from purple to blue (Fig. 2.2A). The sequential addition of Hg^{2+} ions (in the range of 0.67 – 16.67 μM) led to the monotonous decrease of emission intensity at 600 nm of the QDC (with an absorbance of 0.03 at 355 nm), while the emission intensity at 430 nm gradually increases (Fig. 2.2Bi). A Similar observation was made in terms of emission intensity of dual emitting QDC upon treatment with Cu^{2+} ions (in the range of 0.67 – 13.33 μM; Fig. 2.2Bii). Accordingly, the luminescence intensity ratio of (I_{430}/I_{600}) of dual emitting QDC changed with the increasing concentration of either of Hg^{2+} or Cu^{2+} ions (Fig. 2.2C). For example, when the dual emitting QDC was treated with 16.67 μM of Hg^{2+} ions, the intensity ratio of I_{430}/I_{600} changes from 0.60 to 42.36, while the intensity ratio I_{430}/I_{600} changes from 0.60 to 37.65 of dual emitting QDC upon treatment with 13.33 μM of Cu^{2+} ions. No significant changes in the absorption edge was noticed when dual emitting QDC treated with Hg^{2+} or Cu^{2+} ions (Fig. A.2.5, Appendix). Additionally, the linear relationship between intensity ratio (I_{430}/I_{600}) and concentration of heavy metal ions (Hg^{2+}: 0.67 to 3.33 μM and Cu^{2+}: in the range of 0.67 to 5.33 μM) was observed. The limits of detection (LOD) of Hg^{2+} and Cu^{2+} ions were found to be of 85.5 and 34.9 nM, respectively – which are more sensitive and quite suitable for the detection of Hg^{2+} and

Cu^{2+} ions, as compared to those of the earlier reported ratiometric optical nanoprobes (Table A.2.1, Appendix).[8,9] It is to be noted here that the application of other ratiometric nanoprobes have drawbacks such as toxicity issue, complicated and costly fabrication strategy and sensitivity (Table A.2.1, Appendix).[8,9] Furthermore, the sequential changes in the color chromaticity coordinates from (0.41, 0.29) to (0.16, 0.08) and (0.16, 0.09) of the QDC, following addition of Hg^{2+} and Cu^{2+} ions, respectively, clearly supported the visual color changes from purple to blue (Fig. 2.2D). Additionally, the shifts in the hue mean value from 209.6 to 168.3 and 164.0 of the QDC following addition of Hg^{2+} and Cu^{2+} ions, respectively, were observed (Fig. 2.2E). The results also supported the visual color changes from purple to blue of dual emitting QDC in presence of Hg^{2+} and Cu^{2+} ions. Hence, the current dual-emitting QDC has the required ability to sense trace amount of Hg^{2+} and Cu^{2+} ions and thus could be useful for futuristic sensing applications.

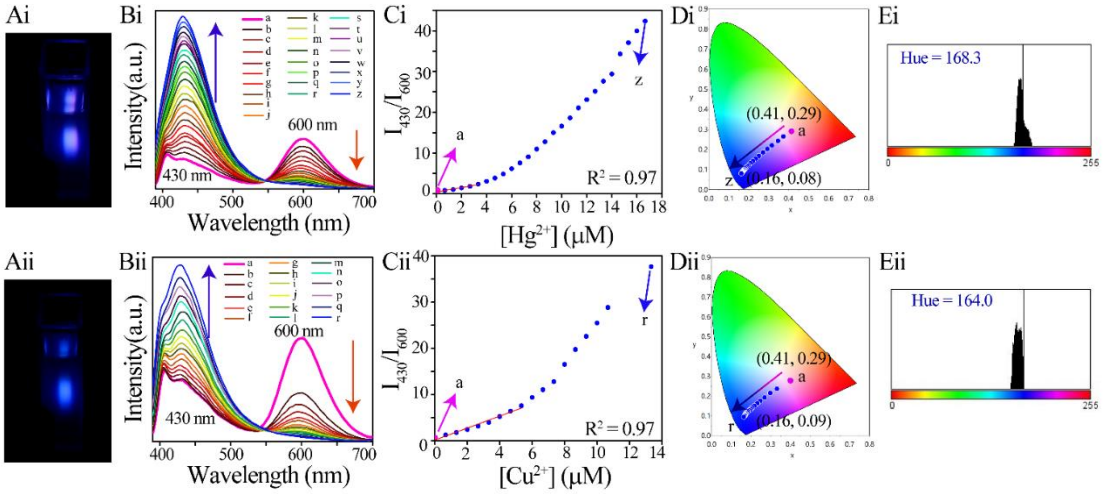

Fig. 2.2 (A) Digital photographs (captured using 355 nm light from a spectrofluorimeter) of the dual-emitting QDC following addition of (i) Hg^{2+} and (ii) Cu^{2+} ions. **(B)** Emission spectra (λ_{ex} = 355 nm), **(C)** changes in luminescence intensity ratio (I_{430}/I_{600}) and **(D)** corresponding chromaticity color coordinates in CIE diagram of the dual-emitting QDC following sequential addition of different concentrations of (i) Hg^{2+} ((a)0.0, (b) 0.67, (c) 1.33, (d) 2.0, (e) 2.67, (f) 3.33, (g) 4.0, (h) 4.67, (i) 5.33, (j) 6.0, (k) 6.67, (l) 7.33, (m) 8.0, (n) 8.67, (o) 9.33, (p) 10.0, (q) 10.67, (r) 11.33, (s) 12.0, (t) 12.67, (u) 13.33, (v) 14.0, (w) 14.67, (x) 15.33, (y) 16.0, and (z) 16.67 μM), and (ii) Cu^{2+} ions ((a)0.0, (b) 0.67, (c) 1.33, (d) 2.0, (e) 2.67, (f) 3.33, (g) 4.0, (h) 4.67, (i) 5.33, (j) 6.0, (k) 6.67, (l) 7.33, (m) 8.0, (n) 8.67, (o) 9.33, (p) 10.0, (q) 10.67, and (r) 13.33 μM). **(E)** Hue histograms of the dual-emitting QDC following addition of (i) Hg^{2+} and (ii) Cu^{2+} ions (obtained by analysing the digital photographs as depicted in (A) using Image-J software).

Importantly, the selectivity of the dual emitting QDC towards the detection of Hg^{2+} and Cu^{2+} ions was tested in the presence of interfering metal ions (such as Na^{+}, Cd^{2+}, Ni^{2+}, Mn^{2+}, Co^{2+} and Pb^{2+} ions) with higher concentrations (83.33 μM) as compared to Hg^{2+} and Cu^{2+} ions. Notably, no significant changes in the visual color and luminescence intensity ratio (I_{430}/I_{600}) of QDC, following addition of interfering metal ions, were noticed (Fig. 2.3A and B). The results indicated the high selectivity of the presented nanoprobe towards detection of Hg^{2+} and Cu^{2+} ions in the presence of the mentioned interfering metal ions. The change in the luminescence color and intensity ratio (I_{430}/I_{600}) can be accounted for based on the strong binding affinity of the quencher heavy metal ions (such as Hg^{2+} and Cu^{2+} ions) on the surface of Mn^{2+}-doped ZnS Qdots, being present in the dual emitting QDC. It is to be noted that the solubility products of HgS (K_{SP}= 2 x 10^{-53}) and CuS (K_{SP}= 8 x 10^{-37}) are much low compared to ZnS (K_{SP}= 2 x 10^{-25}).[12] The low solubility product of the mentioned heavy metal ions might have favoured the displacement of surface Zn^{2+} ions and consequently helped form HgS and CuS on the surface of the Qdot when dual emitting QDC was treated with Hg^{2+} and Cu^{2+} ions, respectively. The formed HgS and CuS might have been responsible for quenching the emission intensity (at 600 nm) of Qdot (present in the dual emitting QDC) owing to non-radiative energy transfers, as supported by earlier reports.[12] The solubility products of the sulphide forms of the mentioned interfering metal ions (such as Na^{+}, Cd^{2+}, Ni^{2+}, Mn^{2+}, Co^{2+} and Pb^{2+} ions) are either similar to or higher than that of the solubility product of ZnS.[12e] This clearly indicated that there may be less chance of the formation of metal sulphides when QDC reacted with the above-mentioned interfering metal ions. Thus, interfering metal ions did not have significant effect on the intensity ratio and visual color change of QDC and consequently demonstrated the solubility-driven selectivity of QDC towards Hg^{2+} and Cu^{2+} ions in the presence of mentioned metal ions. It is also plausible that the formation of HgS and CuS on the surface might have reduced the absorption and emission due to surface defect states of the Qdots. The enhancement in the emission intensity of $Zn(MSA)_2$ complex could be due to enhancement in the absorption in the absence of strong absorption due to the Qdots (i.e., lowering of inner filter effect).[13] When the dispersions of Hg^{2+} and Cu^{2+} ion treated QDC were centrifuged separately and redispersed into the same amount of solvent, the pellet showed weak luminescence while the strong luminescence at 430 nm was observed for supernatant (Fig. A.2.6, Appendix). As we have proposed earlier, $Zn(MSA)_2$ complex might be bonded to the surface through the dangling sulphide ions.[10] In other words, the fifth and sixth coordinates of $Zn(MSA)_2$

were occupied by dangling sulphide (of the Qdots) and solvent molecule. When Hg^{2+} or Cu^{2+} ions were added to the medium, the facile formation of HgS or CuS could replace the $Zn(MSA)_2$ complex (even partially at low concentrations of the added ions), which might have come out from the surface to the medium. The attached HgS or CuS reduced the emission intensity of the Qdots and thus the redispersion of the pellet had weak luminescence. On the other hand, the detached $Zn(MSA)_2$ complex present in the medium contributed to the luminescence of the supernatant and thus the supernatant had the enhanced luminescence (Fig. A.2.6, Appendix). It may be plausible that $Zn(MSA)_2$ present in the supernatant had sulphide ions occupying the fifth coordinate thus enhancing the intensity of the luminescence. Furthermore, the possibility of the enhanced luminescence behaviour due to free $Zn(MSA)_2$ complex formation is supported by the observation of enhancement in luminescence when only MSA was treated with Zn^{2+} ions (Fig. A.2.7, Appendix). Thus, the combined effect of the solubility product-driven formation of heavy metal sulphides (HgS and CuS), lowering the inner filter effect of Qdots and detachment of $Zn(MSA)_2$ complex resulted the change in the luminescence properties (such as color, intensity ratio, chromaticity and hue) of dual emitting QDC that helped to detect the presence of Hg^{2+} and Cu^{2+} ions.

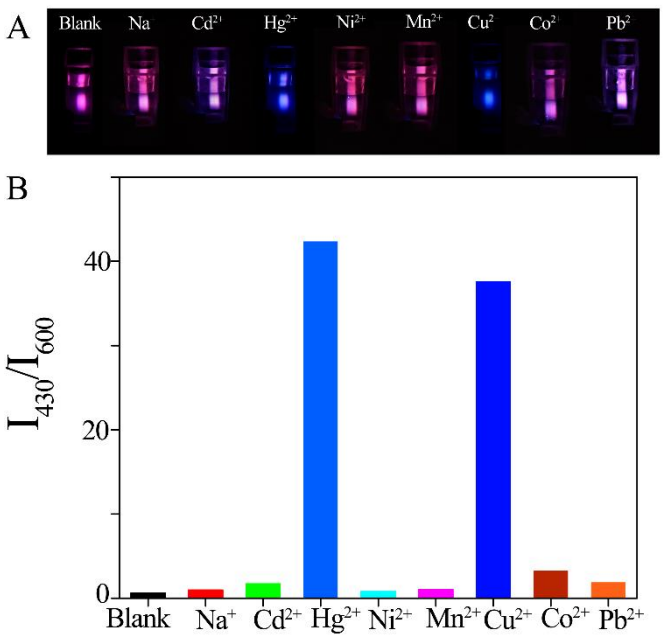

Fig. 2.3 (A) Digital photographs (using 355 nm light from a spectrofluorimeter) and **(B)** bar diagram of the comparison of the luminescence intensity ratio (I_{430}/I_{600}) of the dual-emitting QDC following addition of one of Na^+, Cd^{2+}, Hg^{2+}, Ni^{2+}, Mn^{2+}, Cu^{2+}, Co^{2+} and Pb^{2+} ions, as in the

legends. The concentrations of Hg^{2+} and Cu^{2+} ions were 16.67 and 13.33 μM, respectively, while the concentration of other metal ions was 83.33 μM.

According to earlier observations, the detection of Hg^{2+} and Cu^{2+} ions using Mn^{2+}-doped ZnS Qdots is possible.[14] This could be achieved by observing the quenching in emission intensity at a particular wavelength, however, without altering their visual luminescence color, chromaticity and hue.[14] This opens up the utility of the presented dual emitting QDC, having luminescent $M(MSA)_2$ complex on the surface of Mn^{2+}-doped ZnS Qdot, towards visual and ratiometric detection of Hg^{2+} and Cu^{2+} ions. In the present case, the synergistic effect of both the emitting species (i.e., Mn^{2+}-doped ZnS Qdot and $M(MSA)_2$ complex) present in the QDC play pivotal roles towards visual and ratiometric detection of Hg^{2+} and Cu^{2+} ions, which could not be attained by using either of the emitting species.

2.5 Conclusion:

In conclusion, the purple color dual emitting QDC, comprised of the blue emitting $M(MSA)_2$ complex and orange emitting Mn^{2+} doped ZnS Qdot, demonstrated their use as ratiometric and visual detection of Hg^{2+} and Cu^{2+} ions. The changes in the luminescence color from purple to blue, intensity ratio (I_{430}/I_{600}), chromaticity and hue of dual-emitting QDC helped to detect Hg^{2+} and Cu^{2+} ions, with LOD of 85.5 and 34.9 nM, respectively. The current ratiometric nanoprobe displayed high selectivity towards Hg^{2+} and Cu^{2+} ions in the presence of the above-mentioned interfering metal ions. The visual, ratiometric, sensitive and selective sensing ability of the dual-emitting QDC made them apt candidates for the detection of heavy metal ions such as Hg^{2+} and Cu^{2+} ions.

2.6 Bibliography:

1. S. Silvi, and A. Credi, *Chem. Soc. Rev*., 2015, **44**, 4275-4289.
2. A. Bonanno, I. Perez-Herraez, E. Zaballos-Garcia and J. Perez-Prieto, *Chem. Commun*., 2020, **56**, 587-590.
3. S. Pramanik, S. Roy, A. Mondal and S. Bhandari, *Chem. Commun*., 2019, **55**, 4331-4334.
4. L. He, W. Lin, Q. Xu and H. Wei, *Chem. Commun*., 2015, **51**, 1510-1513.
5. Y. Chen, P. Chen, C. Wang, Y. Lin, C. Ou, L. Ho and H. Chang, *Chem. Commun*., 2014, **50**, 8571-8574.
6. K. Paek, S. Chung, C. Cho and B. J. Kim, *Chem. Commun*., 2011, **47**, 10272-10274.
7. T. Jin, A. Sasaki, M. Kinjo and J. Miyazaki, *Chem. Commun*., 2010, **46**, 2408–2410.
8. (a) P. Wu, X.D. Hou, J.J. Xu and H.Y. Chen, *Nanoscale* 2016, **8**, 8427–8442. (b) X.Y. Sun, P.C. Liu, L.L. Wu and B. Liu, *Analyst* 2015, **140**, 6742–6747. (c) E.S. Childress, C.A. Roberts, D.Y. Sherwood, C.L. LeGuyader and E.J. Harbron, *Anal. Chem*., 2012, **84**, 1235–1239. (d) X. Liu, L. Wang, N. Zhang and D. Shangguan, *Anal. Methods*, 2015, **7**, 8019–8024.
9. (a) F. Yarur, J. Macairan and R. Naccache, *Environ. Sci.: Nano*, 2019, **6**, 1121-1130. (b) S. Pan, K. Li, L. Li, M. Li, L. Shi, Y. Liu and X. Yu, *Chem. Commun*., 2018, **54**, 4955-4958. (c) E. Babaee, A. Barati, M. B. Gholivand, A. Taherpour, N. Zolfaghar and M. Shamsipur, *J. Hazard. Mater*. 2019, **367**, 437–446. (d) Y. Gao, C. Zhang, S. Peng and H. Chen, *Sens. and Actuators B Chem.*, 2017, **238**, 455–461. (e) R. Gui, H. Jin, Y. Wang and J. Sun, *Sens. Actuators B Chem*., 2017, **245**, 386-394. (f) H.M. Li, X.F. Wang, Z.Cai, L. Lu, J. Tao, B. Sun, Y.Y. Yang, Q. Xu, Z.Q. Yu and P. Zhao, *Anal. Bioanal. Chem.*, 2017, **409**, 6655–6662. (g) M. Lan, J. Zhang, Y.-S. Chui, P. Wang, X. Chen, C.-S. Lee, H.-L. Kwong and W. Zhang, *ACS Appl. Mater. & Interfaces*, 2014, **6**, 21270. **(h)** S. Pan, K. Li, L. Li, M. Li, L. Shi, Y. Liu and X. Yu, *Chem. Commun*., 2018, **54**, 4955.
10. (a) S. Bhandari, S. Roy, S. Pramanik and A. Chattopadhyay, *Langmuir*, 2019, 35, **45**, 14399-14413. (b) S. Bhandari, R. Khandelia, U. Pan and A. Chattopadhyay, *ACS Appl. Mater. Interfaces*, 2015, **7**, 17552–17557S. (c) S. Pramanik, S. Bhandari, U. N.

Pan, S. Roy and A. Chattopadhyay, *Small*, 2018, **14**, 1800323. (d) S. Pramanik, S. Bhandari, S. Roy and A. Chattopadhyay, *J. Phys. Chem. Lett.*, 2015, **6**, 1270. (e) S. Bhandari, S. Roy, S. Pramanik and A. Chattopadhyay, *Langmuir* 2015, **31**, 551–561. (f) S. Roy, S. Pramanik, S. Bhandari and A. Chattopadhyay, *Langmuir*, 2017, **33**, 14627. (g) N. Komiya, M. Okada, K. Fukumoto, D. Jomori and T. Naota, *J. Am. Chem. Soc*., 2011, **133**, 6493. (h) S. Roy, S. Pramanik and S. Bhandari, *Chem. Asian. J*., 2019, **6**, 1270.

11. (a) J. Liu, X. Ren, X. Meng, Z. Fang and F. Tang, *Nanoscale*, 2013, **5**, 10022–10028. (b) N. Zhang, Y. Si, Z. Sun, L. Chen, R. Li, Y. Qiao and H. Wang, *Anal. Chem*., 2014, **86**, 11714–11721.

12. (a) A. Jaiswal, S. S. Ghosh and A. Chattopadhyay, *Langmuir* 2012, **28**, 15687-15696. (b) S. Parani, N. Tsolekile, B. M.M. May, K. Pandian and O. S. Oluwafemi, Vasilios N. Stavrou, IntechOpen, DOI: 10.5772/intechopen.70669. (c) L. He, Z. Bao, K. Zhang, D. Yang, B. Sheng, R. Huang, T. Zhao, X. Liang, X. Yang, A. Yang, C. Zhang, P. Cui, J. A. Zapien and H. Zhou, *Microchimica Acta*., 2018, **185**, 511. (d) B. Dong, L. Cao, G. Su, W. Liu, H. Qu and D. Jiang, *J. Colloid. Inter. Sci.*, 2009, **339**, 78-82. (e) https://www.periodni.com/solubility_product_constants.html.

13. (a) P. Li, Y. Hong, H. Feng and S. F.Y. Li, *J. Mater. Chem. B*, 2017, **5**, 2979. (b) H. C. Chang, J. A. Ho, *Anal. Chem*., 2015, **87**, 10362. (c) Y. Zhai, L. Jin, P. Wang, and S. Dong, *Chem. Commun*., 2011, **47**, 8268. (d) Q. Zhang, Y. Sun, M. Liu and Y. Liu, *Nanoscale*, 2020, **12**, 1826. (e) N. Gonzalez, S. P. L. Corral, G. Zanini, H. Montejano and C. C. Acebal, *Analyst*, 2020, **145**, 2279.

14. (a) W. Y. Xie, W. T. Huang, H. Q. Luo and N. Li, *Analyst*, 2012, **137**, 4651–4653. (b) W. S. Zou, M. Y. Deng, Y. Q. Wang, X. Zhao, W. H. Li and X. H. Huang, *Microchim Acta*, 2019, **186**, 41. (c) P. Wu, T. Zhao, S. Wang and X. Hou, *Nanoscale*, 2014, **6**, 43-64.

Chapter 3

A Ratiometric and Visual Sensing of Phosphate by White Light Emitting Quantum Dot Complex

3.1 Abstract:

Ratiometric and visual sensing of phosphate by using a white light emitting quantum dot complex (WLE QDC) is reported herein. The WLE QDC comprised of Mn^{2+}-doped ZnS quantum dot (with λ_{em}=585 nm) and surface zinc quinolate ($ZnQS_2$) complex (with λ_{em}= 480 nm). The limit of detection was estimated to be of 5.9 nM in the linear range of 16.6 - 82.6 nM. This was accomplished by monitoring the variations in the photoluminescence color, intensity ratio (I_{480}/I_{585}), chromaticity and hue of the WLE QDC in the presence of phosphate. The high selectivity and sensitivity of WLE QDC toward phosphate was observed. The chemical interaction of $ZnQS_2$ (present in WLE QDC) with phosphate might have led to the observed specificity in photoluminescence changes. The presented WLE QDC was successfully employed for the quantification of phosphate in samples prepared using environmental water and commercial fertilizer.

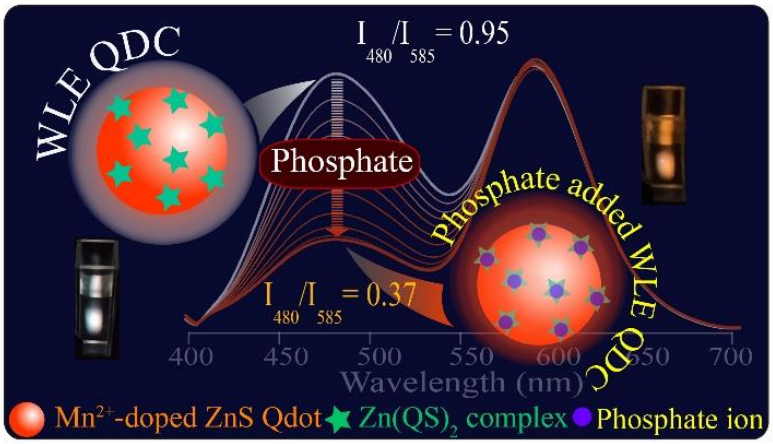

* [Manna et al. *Langmuir*, 2021, **37**, 5506-5512.] - Reproduced by permission from American Chemical Society.

3.2 Introduction:

Ratiometric photoluminescence sensing provides an accurate, and reliable optical detection of disease diagnostics and environmental pollutants.[1-7] The reduction of the influence from the fluctuations related to environmental factors, self-calibration and precise quantification make ratiometric luminescent probe as an advanced option for on-site detection and practical utilization compared to single emitting luminescent probe.[1-7] Additionally, the ratiometric luminescent probe has the ability to ensure the detection of analyte via the visual color changes, which has not been reported for single emitting luminescent probes.[1-7] Thus, development of such probes especially for chemical interaction specific changes are of great value.

Inorganic phosphate, the second most abundant mineral existing in the human body,[8-16] plays a vital role in physiological processes such as preservation of the body's phosphate balance and homeostasis, energy metabolism, cell signaling and bone mineralization.[8-16] Particularly, the amount of phosphate in body fluids (with a the normal ratio of $H_2PO_4^-/HPO_4^{2-}$ being 1:4 at physiological pH) is used to monitor the health conditions of individual humans. The abnormal content of the phosphate may lead to diseases such as muscle weakness, skeletal dysplasia, cardiovascular complications, hyperparathyroidism, vitamin D deficiency, and Fanconi syndrome.[8-16] On the other hand, it has been reported that phosphate pollution in the ground and surface water is a cause for concern in eutrophication.[8-16] Importantly, the presence of excess phosphate in the ground and surface water causing rapid reproduction of microorganisms (algae) with depletion in dissolved oxygen, and thus reducing the quality of water and hampering the local ecosystem.[8-16] The normal limit of dissolved phosphate in water for good environmental quality is 0.02 mg/L (despite of eutrophication).[8-16] The above two requirements themselves make a case for developing rapid and easy detection methods for phosphate.

The currently reported methods for the detection of phosphate are based on electrochemistry, opto-fluidic chip, ion chromatography, colorimetry and fluorimetry.[8-16] Luminescence based methods are popular because of high sensitivity, ease and fastness of measurements.[8-16] While there are a few methods that are based on the application of ratiometric fluorescence probes toward the detection of phosphate, the majority are still based on single emitting luminescent probes.[8-16] For example, (i) lanthanide coordination polymers -based ratiometric probe senses phosphate with a

limit of detection (LOD) of 0.13 μM, (ii) dual-functional lanthanide metal organic frameworks (MOFs) has been utilized with a LOD of 4.4 nM, (iii) rhodamine B (RhB), incorporated Zr–based MOF(UiO-66-NH2) showed LOD of 2.0 μM and (iv) the composite of 8-hydroxyquinoline-5-sulfonate and Mg^{2+} ions with positively charged gold nanoclusters (AuNCs) has been used to sense phosphate with LOD of 0.14 μM.[8, 12, 13, 16] However, the complicated and laborious syntheses, sensitivity (in terms of detection limit), structural instability and cost-effectiveness limit their practical application potential (Table A.3.1, Appendix). On the other hand, most of the ratiometric sensors for phosphate is based on the combination of metal organic frameworks (MOFs) and luminescent dyes/nanoclusters.[9-15] The mentioned MOF based ratiometric sensors have drawbacks similar to the mentioned above.[9-15] Therefore, there is still room for developing new ratiometric luminescent nanoprobes that are more effective.

Among others, colloidal quantum dot (Qdot) based ratiometric luminescent nanoprobes are easy to develop and work efficiently for ratiometric and visual detection environmental pollutants and molecular disease marker.[5-7] For instance, single peak emission based nanocomposite of Mn^{2+}-doped ZnS Qdot - Ce^{3+} ions detect phosphate in the linear range of 8-320 μM with LOD of 2.71 μM whereas graphene Qdot-Ce^{3+} senses phosphate with LOD of 0.1 μM in the linear range of 0.5–190 μM.[17-18] However, as mentioned before, multiple emission based detection is superior to single emission based techniques.[5-6] In other words, ratiometric sensor with emissions at a minimum of two different wavelengths would be able to sense analyte (visually and spectroscopically) by selectively quenching or enhancing one emission. Such clear distinction may not be possible with change in emission characteristics based on probes having single wavelength emission.[5-6] Recent results suggest that single particle composites of Qdot and inorganic luminescence complex on its surface – defined as quantum dot complex (QDC) – provide new opportunities in visual and ratiometric sensing of neurotransmitter dopamine, reversibly assessing physiological pH in the range of 6.5 to 10.6 and sensing of heavy metals (like Hg^{2+} and Cu^{2+} ions).[5-7] Thus, it may be possible to use water soluble and biofriendly QDC – that emits white light –for ratiometric and visual detection of phosphate. Importantly, QDC has been a preferred important white light emitting (WLE) material for optoelectronic and ratiometric sensing applications, in comparison to other multicomponent based WLE materials due

to their ease of aqueous based synthesis, biocompatibity, relatively low toxicity, cost-effectiveness, single component nature and for possible specific chemical interaction with the analyte.[19-22]

Herein we report the development of a ratiometric WLE nanoprobe, which was comprised of greenish blue emitting surface $Zn(QS)_2$ complex (λ_{em}-480 nm; QS stands for 8-hydroxyquinoline-5-sulfonate) and orange emitting Mn^{2+}-doped ZnS Qdot (λ_{em}-585 nm). The $Zn(QS)_2$ attached Qdot – emitted white light – is called herein as WLE QDC. Interestingly, in the presence of phosphate, white light emission from QDC was diminished along with concurrent appearance of orange emission. The changes in the photoluminescence intensity ratio (I_{480}/I_{585}) of WLE QDC from 0.95 to 0.37, chromaticity from (0.33, 0.35) to (0.43, 0.39) and hue from 99.47 to 17.5 were observed in the presence of phosphate. The LOD of phosphate by WLE QDC was estimated to be 5.9 nM in the linear range of 16.6-82.6 nM. It is to be mentioned here that the presented WLE QDC nanoprobe is highly sensitive and is thus suitable for selective sensing of phosphate, as compared to previously reported ratiometric nanoprobes, which have drawbacks related to cost-effectiveness, complicated fabrication method, structural instability, toxicity and sensitivity (the details of which are given in Table A.3.1, Appendix).[8-16] High selectivity of WLE QDC toward detecting phosphate ion was noticed even in the presence of interfering chemical species. Notably, a reliable analysis of phosphate in real environmental water and commercial fertilizer was performed by using WLE QDC. Overall, the presented WLE QDC offers a model ratiometric spectroscopic nanoprobe and provides facile option for visual sensing of phosphate in environmental water and commercial fertilizer and by overcoming important drawbacks of traditional chemical sensors.

3.3 Experimental Section:

3.3.1 Materials: Sodium dihydrogen phosphate (Merck, assay = 98.0–100.5 %), trisodium phosphate dodecahydrate (Merck, assay = 98.0–102.0 %), zinc acetate dihydrate (Merck, assay = 99.5 – 101.0 %), sodium sulfide flakes purified (Merck, assay > 50.0 %), manganese acetate tetrahydrate (Merck, assay ≥ 99.0 %), 8-hydroxyquinoline-5-sulfonic acid hydrate (HQS: Sigma-Aldrich, assay = 98.0 %),

sodium acetate (Merck, assay ≥ 99.0 %), sodium fluoride (Merck, assay ≥ 99.5 %), sodium bromide (Merck, assay ≥ 99.995 %), sodium chloride (Merck, assay ≥ 99.5 %), sodium iodide (Merck, assay ≥ 99.5%), sodium nitrite (Merck, assay ≥ 99.0 %), sodium nitrate (Merck, assay ≥ 99.5 %), sodium sulfate (Merck, assay ≥ 99.0 %), sodium sulfite (Merck, assay = 97.0 – 100.5 %), disodium oxalate (Merck, assay ≥ 99.8 %), calcium chloride (Merck, assay ≥ 98.0 %), magnesium chloride (Merck, assay ≥ 98.0 %), potassium chloride (Merck, assay ≥ 99.5 %), quinine sulfate (Sigma-Aldrich, assay = 99.0 – 101.0 %) and methanol (Merck, assay ≥ 99.9 %) were purchased and used directly without further purification. Milli-Q grade water was used for experiments.

3.3.2 Fabrication of Mn^{2+}-doped ZnS Qdots: Mn^{2+}-doped ZnS Qdots were fabricated using a reported method.[5, 7] Briefly, to an aqueous mixture of 5.0 mM of zinc acetate dihydrate and 1.0 mM manganese acetate tetrahydrate, 5.0 mM of sodium sulfide was added and the resulting mixture was refluxed for 4 h under constant stirring at 100 °C. The milky white colloidal mixture was centrifuged with a speed of 20000 rpm for 15 min. The pellet (obtained after centrifugation) was thoroughly washed and redispersed into the same amount of solvent and centrifuged further with same experimental conditions. The washing cycle was repeated again and last the pellet was dispersed in 200.0 mL of water under sonication and the colloidal dispersion was used for further experiments.

3.3.3 Preparation of HQS Solution: 5.0 mM of HQS solution was prepared by dissolving 11.3 mg of solid HQS in 10.0 mL of methanol-water mixture (methanol:water = 6:4) under sonication at room temperature. The molecular structure of the HQS is given in the Fig A.3.1, Appendix.

3.3.4 Synthesis of WLE QDC: The WLE QDC was prepared by addition of 15.0 µL of 5.0 mM of HQS (methanol-water) to the 3.0 mL water dispersion of Qdots (with absorbance of 0.07 at 335 nm). The resulting mixture of HQS added Qdots was centrifuged at a speed of 20000 rpm for 15 min and the so obtained pellet was further redispersed in the equal amount of water. The optimum amount of the HQS ligand was calculated to be 25 µM for the synthesis and characterization of WLE QDC.

3.3.5 Phosphate Sensing: The phosphate sensing of WLE QDC was executed following sequential addition of the solutions of 0.01 mM sodium dihydrogen phosphate to 3.0 mL dispersion of WLE QDC (having absorbance of 0.18 at 335 nm). The limit of detection (LOD) was estimated by using 3σ/k plot. The experiment was

performed in triplicate. The variations in the luminescence characteristics (such as color, intensity ratio (I_{480}/I_{585}), chromaticity and hue) of WLE QDC were monitored to sense phosphate in water.

3.3.6 Selectivity Experiment: The selectivity experiment was performed by using 10 times higher concentration (26.0 μM) of interfering anions and cations compared to phosphate (2.6 μM). One of the 15.6 μL 5.0 mM anions such as F^-, Br^-, Cl^-, I^-, NO^{2-}, NO_3^-, SO_4^{2-}, $S_2O_3^{2-}$, CH_3COO^- and $C_2O_4^{2-}$ or the cations such as Na^+, K^+, Ca^{2+} and Mg^{2+} (which are usually present in water) was added to 3.0 mL of WLE QDC (having absorbance of 0.18 at 335 nm) separately to confirm the selectivity of WLE QDC toward phosphate in the presence of the mentioned anions and cations. Emission spectra and corresponding intensity ratio ($I_{480/585}$) were monitored to define selectivity of the WLE QDC.

3.3.7 Environmental and Model Sample Analyses. For the analysis of phosphate content in environmental sample, water samples were collected from the Brahmaputra River (Guwahati, Assam, India) and then were filtered with a 0.2 μm syringe filter. The filtered and phosphate - spiked water samples were analyzed by the above-mentioned spectrofluorometric procedure and using WLE QDC. Similar method was used for the determination of phosphate in tap water (as available in our research laboratory) and drinking mineral water (Silver Drop company; purchased from local market). Furthermore, the determination of phosphate by WLE QDC was also tested in commercial fertilizer (company: Unitedlys; as-purchased from the local market). To prepare fertilizer containing stock solution, 5.0 g of solid fertilizer was dissolved in 40.0 mL Milli-Q water. Then the mixture was sonicated for 15 min and the resulting solution was filtered twice through Whatman-42 filter paper and 0.2 μm filter, respectively. The filtrate was used as a stock solution for experiment.

3.3.8 Instruments: HORIBA Jobin Yvon FluoroMax-4 spectrofluorimeter was used to record the luminescence quantum yield and photostability of the samples. Digital photographs were taken using Samsung Mobile (A20) under spectrofluorimeter illumination. OSRAM color calculator (CIE-1931) and Image-J were used to calculate the chromaticity and hue of the samples. UV–vis spectrophotometer (PerkinElmer Lambda 35) was used to record the absorption spectra of the samples. Transmission

electron microscopy (TEM; JEOL JEM 2100F, maximum accelerating voltage: 200 kV) was used to analyze the dimension and lattice distance of the samples. High resolution TEM and inverse fast Fourier transform analyses were performed by using Gatan Digital Micrograph software. X-ray diffraction patterns of the samples were recorded by using Rigaku TTRAX-III X-ray diffractometer.

3.4 Results and Discussion:

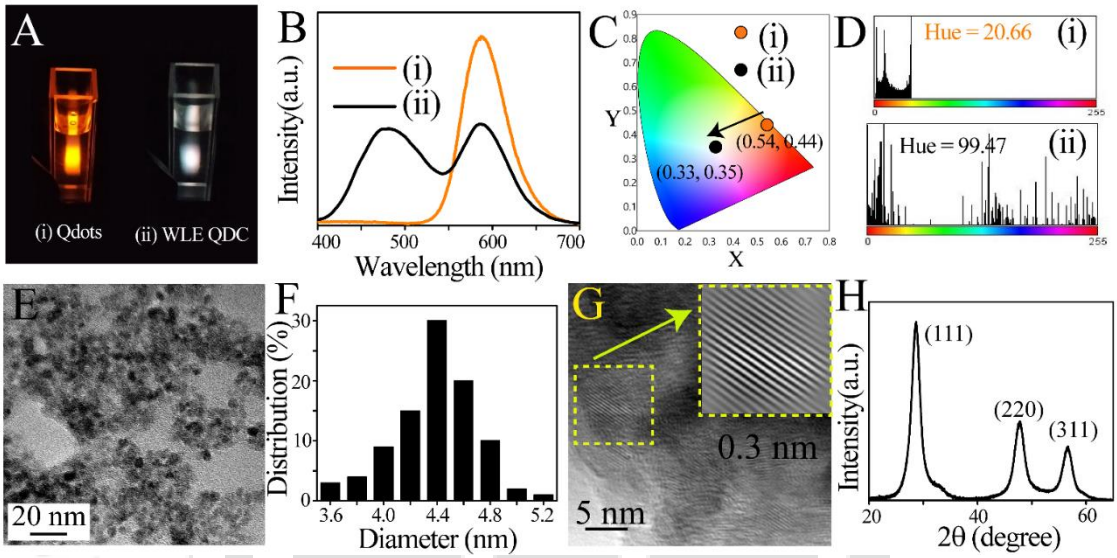

Fig 3.1 (A) Photographs (λ_{ex}= 335 nm), **(B)** emission spectra (λ_{ex} = 335 nm), **(C)** corresponding chromaticity color coordinates in CIE diagram and **(D)** hue histograms of (i) Qdots and (ii) WLE QDC. **(E)** Transmission electron microscopic (TEM) image (scale bar = 20 nm), **(F)** corresponding particle size distribution,**(G)** high resolution TEM image (scale bar = 5 nm) and corresponding inverse fast Fourier transformed (IFFT) analysis (inset), and **(H)** powder X-ray diffraction diagram of WLE QDC.

The QDC was fabricated via the formation of $Zn(QS)_2$ complex on the surface of a presynthesized Qdot (having absorbance of 0.07 at 335 nm) with 25.0 μM of external organic ligand HQS. The details of the synthesis and characterization of Qdots and QDC are mentioned in the Experimental Section. Notably, a new peak at 365 nm in the absorption spectra of Qdots appeared when Qdots reacted with HQS (Fig A.3.2, Appendix).[7] Upon 335 nm light excitation, the QDC displayed white light while only Qdots showed orange color emission (Fig 3.1A). The $Zn(QS)_2$ attached Qdot – that emitted white light –is called hereafter as WLE QDC. The Qdots displayed emission at

585 nm while WLE QDC showed dual emissions at 585 and 480 nm (Fig 3.1B). Notably, the orange emission of WLE QDC at 585 nm originated from electronic transition ($^4T_1$-$^6A_1$) of Mn^{2+} dopants of Qdots, whereas, the greenish blue emission of WLE QDC at 480 nm originated from the electronic transition of the newly formed surface $Zn(QS)_2$ complex.[5-7, 23-26] It is to be noted here that the synchronous contributions of orange emission of Qdots and greenish blue emission of surface $Zn(QS)_2$ complex led to the generation of white light from the QDC upon excitation by 335 nm light. The results clearly indicated the formation of $Zn(QS)_2$ complex on the surface of Qdots.[23-24] The WLE QDC exhibited color chromaticity of (0.33, 0.35) and hue mean value of 99.47 whereas (0.54, 0.44) color chromaticity and 20.66 hue mean value were observed for Qdots (Fig 3.1C, D). Importantly, the chromaticity and hue are essential optical parameters to define the exact photoluminescence colors in CIE-1931 and Hue, saturation and value (HSV) color spaces, correspondingly.[27] Further, there was no morphological changes observed as based on the size (4.4 $\pm$ 0.2 nm) and lattice fringe (0.3 nm due to (111) plane of ZnS) in the transmission electron microscopy (TEM) images and characteristics peaks of X-ray diffraction pattern (due to (111), (220) and (311) planes of cubic ZnS) when HQS had reacted with Qdots (Fig A.3.3, Appendix, Fig 3.1E-H).[5,7, 25-26] The results clearly demonstrated the preservation of morphology and dimension of Qdots during the formation of WLE QDC. The affirmative photostability of WLE QDC was measured with respect to the individual emission peaks under continuous irradiation of 335 nm light (Fig A.3.4, Appendix).

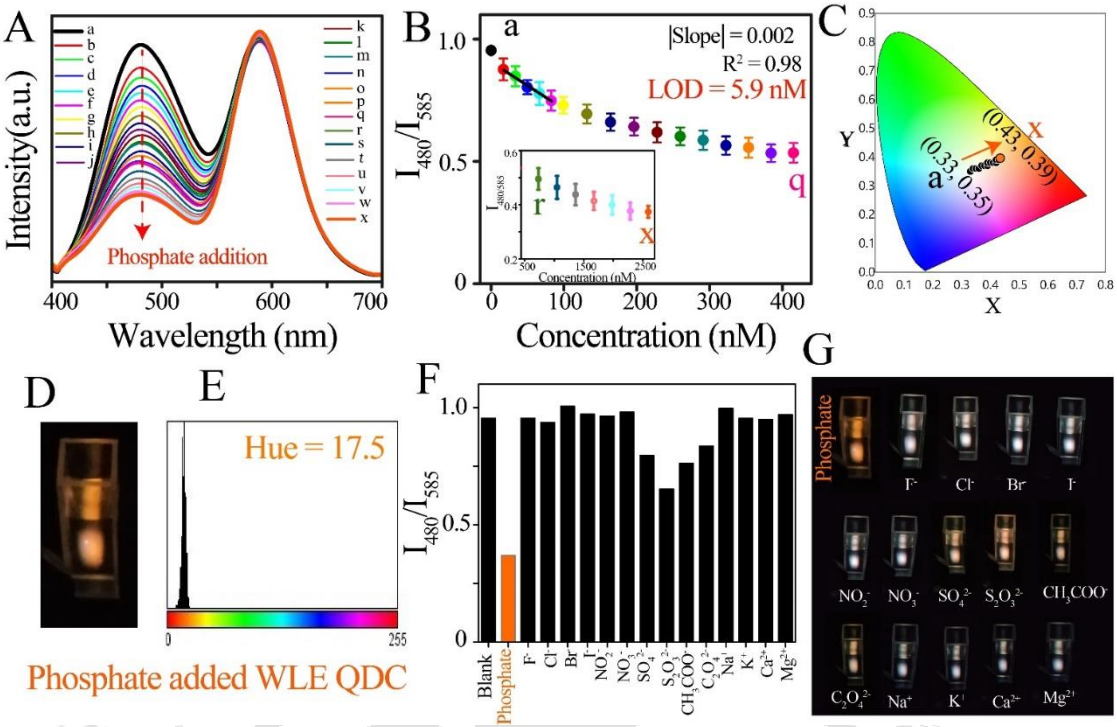

Fig 3.2 (A) Emission spectra (λ_{ex} = 335 nm), (B) alterations in photoluminescence intensity ratio (I_{480}/I_{585}) in the range of 0.0-415.3 nM; inset: alterations in photoluminescence intensity ratio (I_{480}/I_{585}) in the range of 732.5 nM-2.6 µM and (C) corresponding color chromaticity coordinates in CIE diagram of WLE QDC recorded following addition of different concentrations of phosphate: ((a) 0.0, (b) 16.6, (c) 33.2, (d) 49.8, (e) 66.2, (f) 82.6, (g) 99.0, (h) 131.6, (i) 163.9, (j) 196.1, (k) 228.0, (l) 259.7, (m) 291.3, (n) 322.6, (o) 353.7, (p) 384.6, (q) 415.3, (r) 732.5, (s) 1047.6, (t) 1360.8, (u) 1671.9, (v) 1981.1, (w) 2288.4 and (x) 2593.8 nM).The experiments were performed in triplicate. A linear relationship between photoluminescence intensity ratio (I_{480}/I_{585}) of WLE QDC and concentrations of phosphate (in the range of 16.6-82.6 nM) was considered to calculate limit of detection (LOD). (D) Photograph (λ_{ex} = 335 nm) of WLE QDC following treatment of phosphate (2.6 µM). (E) Hue histogram of phosphate added WLE QDC acquired by analyzing the digital photograph as showed in Fig 3.2A using Image-J software. (F) Bar diagram of the comparison of the photoluminescence intensity ratio (I_{480}/I_{585}) and (G) photographs (λ_{ex} = 335 nm) of WLE QDC following addition of the above-mentioned interfering ions with 10 times higher concentration i.e., of 26.0 µM, compared to phosphate at 2.6 µM.

The successive addition of the phosphate (in the range of 0.0–2.6 μM) to WLE QDC (at pH = 5.8) led to steady decrease in the photoluminescence intensity at 480 nm of WLE QDC while no significant changes in the photoluminescence intensity at 585 nm, was noticed (Fig 3.2A). The photoluminescence intensity ratio (I_{480}/I_{585}) was altered with the increasing concentration of phosphate (Fig 3.2B and inset of Fig 3.2B). For example, the photoluminescence intensity ratio (I_{480}/I_{585}) changed from 0.95 to 0.37, when WLE QDC (pH-5.8, having absorbance of 0.18 at 335 nm) was treated with 2.6 μM of phosphate (which accompanied a change in pH from 5.8 to 5.85). The pH of WLE QDC medium following addition of phosphate (NaH_2PO_4) did not change significantly and thus the effect of pH on the changes in photoluminescence intensity ratio (I_{480}/I_{585}) of WLE QDC upon phosphate (NaH_2PO_4) addition was ruled out. It is to be noted here that at pH=5.8, $H_2PO_4^-$ is considered as the main form of the phosphate and the experiments were performed using sodium salt of $H_2PO_4^-$.[16] However, the same experiments were also performed using Na_3PO_4 to study the effect of PO_4^{3-} (Fig A.3.5A-B, Appendix). Upon addition of PO_4^{3-}, WLE QDC showed changes in the photoluminescence intensity ratio (I_{480}/I_{585}) from 0.95 to 0.47 along with the changes in the pH from 5.8 to 6.4. When the pH of WLE QDC was adjusted from 5.8 to 6.4, the photoluminescence intensity ratio (I_{480}/I_{585}) changes from 0.95 to 0.82. Further, the effect of pH (in the range of 3-10) on the photoluminescence intensity ratio (I_{480}/I_{585}) of WLE QDC was verified (Fig A.3.5C-D, Appendix). Notably, the adjustment to acidic pH (<pH-5.8) resulted in abrupt reductions in the photoluminescence intensities and thus the ratio (I_{480}/I_{585}) while the adjustment to higher pH values (>pH-5.8) resulted in the decrease in the photoluminescence intensity ratio (I_{480}/I_{585}) of WLE QDC. However, the decrease in the photoluminescence intensity ratio (I_{480}/I_{585}) of WLE QDC was higher for phosphate (Na_3PO_4) addition compared to the pH adjusted dispersion of WLE QDC (as depicted in Fig A.3.5A-B, Appendix). Thus, the phosphate (Na_3PO_4) has additional effect on the changes in the photoluminescence intensity ratio (I_{480}/I_{585}) of WLE QDC compared to the pH effect of the medium. This supplementary effect of the change in the photoluminescence intensity ratio (I_{480}/I_{585}) of WLE QDC may be due to the consequence of interactions between the phosphate ion present in the medium and WLE QDC. This clearly indicated that phosphate (irrespective of their forms) had altered the emission characteristics of WLE QDC although the pH of the medium played an important role in it. In addition, a linear dependence of photoluminescence

intensity ratio (I_{480}/I_{585}) on the concentration of phosphate (in the range of 16.6-82.6 nM was observed (Fig 3.2B). The LOD was estimated to be 5.9 nM – which is highly sensitive and reasonably suitable towards sensing of phosphate, compared to previously reported ratiometric nanoprobes even if one does not consider other drawbacks related to cost-effectiveness, complicated fabrication method and sensitivity (Table A.3.1, Appendix).[8-16] No substantial alteration in the absorption spectrum of WLE QDC, upon addition of phosphate, was noticed (Fig A.3.6, Appendix). Interestingly, the color chromaticity coordinates of WLE QDC changed from (0.33, 0.35) to (0.43, 0.39) when treated with the increasing concentration of phosphate (Fig 3.2C). Upon addition of phosphate, the WLE QDC showed the changes in the photoluminescence color from white to orange (Fig 3.2D). The hue mean value of WLE QDC changed from 99.47 to 17.5 following addition of phosphate (Fig 3.2E). Thus, WLE QDC could be a new ratiometric and visual optical nanoprobe for sensing of phosphate. Notably, the selectivity of the WLE QDC for sensing of phosphate was verified in the presence of interfering anions such as F^-, Br^-, Cl^-, I^-, NO^{2-}, NO_3^-, SO_4^{2-}, $S_2O_3^{2-}$, CH_3COO^- and $C_2O_4^{2-}$ and the cations such as Na^+, K^+, Ca^{2+} and Mg^{2+} (which are usually present in water) with typically 10 times higher concentration in comparison to phosphate. No significant alteration in the I_{480}/I_{585} of WLE QDC in the presence of the mentioned interfering ions was observed. Similar observations based on the visual white color of WLE QDC were made when treated with interfering ions (Fig 3.2F-G and Table A.3.2, Appendix). Thus, high selectivity of WLE QDC toward the detection of phosphate was observed.

According to our earlier observations, $Zn(QS)_2$ might be bonded to the surface of Qdot through the dangling sulfide ions during the formation of WLE QDC.[10] Particularly, the fifth and sixth coordinations of $Zn(QS)_2$ were bonded to dangling sulfide bond (present on the surface of Qdot) and solvent molecule, respectively.[5-7, 23-24] When phosphate interacted with WLE QDC, the change in the photoluminescence intensity ratio (I_{480}/I_{585}) of WLE QDC was observed and thus provided an indication toward chemical interaction of phosphate with WLE QDC. This might be due to the bonding of the phosphate with the sixth coordination of $Zn(QS)_2$ replacing the existing solvent molecule. As a result, the quenching in the photoluminescence of $Zn(QS)_2$ was observed when WLE QDC was treated with phosphate. The coordination of phosphate

to the surface $Zn(QS)_2$ is also supported by the observed changes in the surface charge (measured by zeta potential), incorporation of characteristics peaks of functional phosphate groups in the Fourier transformed infrared (FTIR) spectrum for sample collected upon treatment of phosphate and followed by centrifugation. Notably, the change in the surface charge of WLE QDC from +4.8 mV to -10.6 mV for WLE QDC, upon treatment with phosphate, supported the modulation of the surface of the QDC through the electrostatic interaction with negative charges of phosphate (Fig A.3.7, and Table A.3.3, Appendix). The new peaks at 888 cm^{-1} (due to O–P asymmetric stretching /$P(OH)_2$ symmetric stretching (A1), P-OH stretching) and 998 cm^{-1} (due to O–P–O symmetric stretching and asymmetric with O_{nb}) – in addition to peaks of the functional groups of $Zn(QS)_2$ –appeared in the FTIR spectrum (Fig A.3.8, Table A.3.4, Appendix).[16, 28-30] The presented FTIR results clearly demonstrated the incorporation of phosphate on the surface of WLE QDC. When phosphate added WLE QDC mixture was centrifuged and redispersed, the pellet displayed quenched photoluminescence and intensity ratio (I_{480}/I_{585}) similar to that of mixture of WLE QDC and phosphate before centrifugation while no substantial photoluminescence was noticed for supernatant (Fig A.3.9, Appendix). This result also supported the chemical interaction of phosphate with the WLE QDC. Thus, the attachment of phosphate on the sixth coordinate of $Zn(QS)_2$ might be possible – which is further supported by literature.[16] As per an earlier report, the coordination of phosphate to metal quinolate complex is possible and is also responsible for the photoluminescence change of metal quinolate complex.[16] On the other hand, H-bonding moiety, present adjacent to Zn^{2+} in an inorganic complex, increases the coordination possibility of phosphate toward Zn^{2+} when present as metal center in an inorganic complex.[31] In the present case, the presence of SO_3H group of the quinolate ring of $Zn(QS)_2$ enhances the chance of coordination of phosphate in their sixth coordinate by forming an H-bonding with -SO_3H. This might have led to the quenching in the emission of $Zn(QS)_2$ (of WLE QDC) with phosphate addition. This is further supported by the evidence that when $Zn(QS)_2$ attached ZnS Qdots were treated with phosphate similarly, the quenching in their greenish blue emission (similar to that of phosphate addition to WLE QDC) was observed (Fig A.3.10, Appendix). No substantial changes in the photoluminescence intensity of only Mn^{2+}-doped ZnS Qdots following addition of phosphate was noticed (Fig A.3.10, Appendix). The results overall suggest the quenching of emission of the complex by phosphate and with no

change in emission peak due to Qdot that acted as the reference. Time resolved photoluminescence results showed that upon addition of phosphate to WLE QDC, no substantial change in the average lifetime of WLE QDC with regard to the photoluminescence of $Zn(QS)_2$ (Fig A.3.11, Table A.3.5, Appendix). This clearly showed the static quenching behavior of WLE QDC, following phosphate addition, with regard to the photoluminescence of $Zn(QS)_2$. Similarly, no significant changes in the average lifetime of WLE QDC, following phosphate addition, with regard to the photoluminescence of Qdots was noticed (Fig A.3.11, Table A.3.5, Appendix). This also supported the observed results in Fig 3.2A and demonstrated that photoluminescence of Qdots (of WLE QDC) acted as a reference signal during the sensing of phosphate. The plausible coordination of phosphate to $Zn(QS)_2$ complex (being present in the WLE QDC) might have led to quenching of emission intensity at 480 nm, while no substantial change in the emission intensity at 585 nm due to Qdots was noticed. Thus the specific interaction of phosphate with $Zn(QS)_2$ complex (being present in the WLE QDC) may be the reason for altering the photoluminescence intensity ratio (I_{480}/I_{585}) of WLE QDC. The observed results helped to further consolidate ratiometrical and visual detection of phosphate in water. The presented mechanism for phosphate sensing by WLE QDC is described and illustrated in Scheme 3.1.

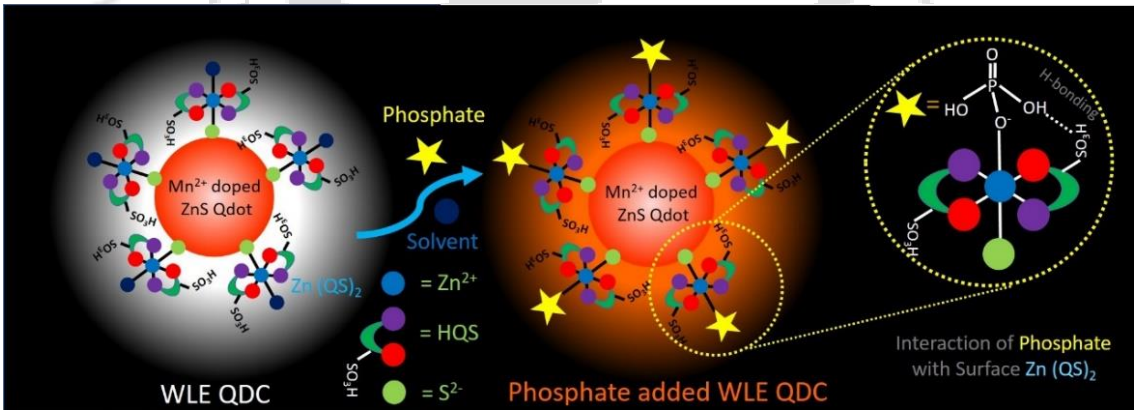

Scheme 3.1 Schematic representation of the mechanism of ratiometric and visual detection of inorganic phosphate using the WLE QDC.

Importantly, the practicability of the WLE QDC was verified following the detection of phosphate in three water samples (which were river, tap and

mineral water) and a commercial fertilizer. The recovery rate (%) of spiked phosphate in these samples ranged from 95.67% to 112.5% (Table 3.1), with relative standard deviations (RSDs) in the range of 1.88-7.91%, and thus indicated no significant interference from other ions during the determination of phosphate in the mentioned samples. The presented results indicated that WLE QDC exhibited excellent reliability in the detection of phosphate in real sample analysis.

Table 3.1. Results for detection of phosphate in environmental water samples and commercial fertilizer (Mean ± SD, n = 3). Each experiment was performed in triplicate.

Samples	Blank (μM)	Spiked (μM)	Calculated (μM)	Recovery (%)	RSD (%)
River Water	19.87	6	25.61	95.67	7.89
Tap Water	17.20	6	23.95	112.50	7.91
Mineral Water	6.89	9	16.56	107.44	6.56
Fertilizer	51.17	6	57.18	100.17	1.88

3.5 Conclusion:

In conclusion, the $Zn(QS)_2$ surface complex on Mn^{2+}-doped ZnS Qdot – that emits white light and termed as WLE QDC – served as a ratiometric and visual sensor of inorganic phosphate in the aqueous medium. The addition of phosphate to WLE QDC led to changes in the photoluminescence color from white to orange, intensity ratio (I_{480}/I_{585}), chromaticity and hue. These helped to detect phosphate with LOD of 5.9 nM in the liner range of 16.6-82.6 nM. High selectivity and sensitivity of WLE QDC toward phosphate ion was noticed even in the presence of interfering chemical species. The chemical interaction of phosphate with the zinc quinolate complex (of WLE QDC) might be considered to be the primary reason behind the presented photoluminescence changes of WLE QDC upon phosphate addition. Hence, the presented results of the ratiometric, visual, sensitive and selective detection phosphate by WLE QDC may provide a new optical nanoprobe for application such as in clinical diagnosis and water quality management. Finally, a quantitative determination of

phosphate in real environmental water and commercial fertilizer was tested using the presented WLE QDC.

3.6 Bibliography:

1. S. Silvi and A. Credi, *Chem. Soc. Rev.*, 2015**, 44**, 4275-4289.
2. L. He, W. Lin, Q. Xu and H. Wei, *Chem. Commun.*, 2015, **51**, 1510-1513.
3. Y.-N. Chen, P.-C. Chen, C.-W. Wang, Y.-S. Lin, C.-M. Ou, L.-C. Ho and H.-T. Chang, *Chem. Commun.*, 2014, **50**, 8571-8574.
4. A. Bonanno, I. Pérez-Herráez, E. Zaballos-García and J. Pérez-Prieto, *Chem. Commun.*, 2020, **56**, 587-590.
5. M. Manna, S. Roy, S. Bhandari and A. Chattopadhyay, *J. Mater. Chem. C*, 2020**, 8**, 6972-6976.
6. S. Pramanik, S. Bhandari, U. N. Pan, S. Roy and A. Chattopadhyay, *Small*, 2018, **14**, 1800323.
7. S. Pramanik, S. Roy, A. Mondal and S. Bhandari, *Chem. Commun.*, 2019**, 55**, 4331-4334.
8. L. Han, S. G. Liu, Y. Z. Yang, Y. Z. Fan, J. Zhou, X. Y. Zhang, N. B. Li and H. Q. Luo, *J. Mater. Chem. C*, 2020**, 8**, 13063-13071.
9. X. Li, P. Liu, X. Niu, K. Ye, L. Ni, D. Du, J. Pan and Y. Lin, *Nanoscale*, 2020**, 12**, 19383-19389.
10. Y. Ma, Y. Zhang, X. Li, P. Yang, J.-Y. Yue, Y. Jiang and B. Tang, *Anal. Chem.*, 2020**, 92**, 3722-3727.
11. X. Li, X. Niu, P. Liu, X. Xu, D. Du and Y. Lin, *Sensors and Actuators B: Chemical*, 2020**, 321**, 128546.
12. G. Li and C. Tong, *Anal. Chim. Acta*, 2020**, 1133**, 11-19.
13. N. Gao, J. Huang, L. Wang, J. Feng, P. Huang and F. Wu, *Appl. Surf. Sci.*, 2018**, 459**, 686-692.
14. C. Dai, C.-X. Yang and X.-P. Yan, *Anal. Chem.*, 2015**, 87**, 11455-11459.
15. D. Yan, Y. He, Y. Ge and G. Song, *J. Fluores.*, 2017**, 27**, 227-233.
16. Z. Zhang, J. Feng, P. Huang, S. Li and F.-Y. Wu, *Sensors and Actuators B: Chemical*, 2019**, 298**, 126891.
17. J. Qin, D. Li, Y. Miao and G. Yan, *RSC Advances*, 2017, **7**, 46657-46664.

18. J.-M. Bai, L. Zhang, R.-P. Liang and J.-D. Qiu, *Chem. Euro. J.*, 2013**, 19**, 3822-3826.
19. S. Pathak, N. Sakai, F. Wisnivesky Rocca Rivarola, S. D. Stranks, J. Liu, G. E. Eperon, C. Ducati, K. Wojciechowski, J. T. Griffiths, A. A. Haghighirad, A. Pellaroque, R. H. Friend and H. J. Snaith, *Chem. Mater.*, 2015, **27**, 8066–8075.
20. T. E. Rosson, S. M. Claiborne, J. R. McBride, B. S. Stratton and S. J. Rosenthal, *J. Am. Chem. Soc*. 2012, **134**, 8006−8009.
21. D. K. Maiti, S. Roy, A. Baral and A. Banerjee, *J. Mater. Chem. C*, 2014, **2**, 6574-6581.
22. S. Tanwar, B. Sharma, V. Kaur and T. Sen, *RSC Advances*, 2019, **9**, 15997-16006.
23. S. Bhandari, S. Roy, S. Pramanik and A. Chattopadhyay, *Langmuir*, 2019, **35**, 14399-14413.
24. S. Pramanik, S. Bhandari, S. Roy and A. Chattopadhyay, *J. Phys. Chem. Lett.*, 2015**, 6**, 1270-1274.
25. B. B. Srivastava, S. Jana, N. S. Karan, S. Paria, N. R. Jana, D. D. Sarma and N. Pradhan, *J. Phys. Chem. Lett.,* 2010**, 1**, 1454-1458.
26. H.-C. Pan, F.-P. Liang, C.-J. Mao, J.-J. Zhu and H.-Y. Chen, *J. Phys. Chem. B*, 2007**, 111**, 5767-5772.
27. A. Hakonen and J. E. Beves, *ACS Sens.*, 2018**, 3**, 2061-2065.
28. A. A. Ahmed, S. Gypser, P. Leinweber, D. Freese and O. Kühn, *Phys. Chem. Chem. Phys.*, 2019**, 21**, 4421-4434.
29. B. J. M. Rajkumar and V. Ramakrishnan, *Spectrochim. Act. Part A*, 2001**, 57**, 247-254.
30. S. Bhandari, S. Roy and A. Chattopadhyay, *RSC Advances*, 2014, **4**, 24217-24221.
31. J. C. Mareque-Rivas, R. Torres Martín de Rosales and S. Parsons, *Chem. Commun.*, 2004, 610-611.

Chapter 4

Recognition and Ratiometric Visual Sensing of Long-Chain Unsaturated Fatty Acids by a White-Light-Emitting Quantum-Dot Complex

4.1 Abstract: This chapter reports the twin advantages of a white-light-emitting quantum-dot complex (WLE-QDC), comprising Mn^{2+}-doped ZnS quantum dots (Qdots) and a zinc quinolato (ZnQ_2) complex, towards the selective recognition of long-chain unsaturated fatty acids (LCUFAs; e.g., Na-salt of oleic acid) from their corresponding saturated forms (e.g., Na-salt of stearic acid). Importantly, the WLE-QDC provided the unique ratiometric visual detection of LCUFAs with a detection limit of 0.127 μM in the linear range of 4.2–16.6 μM. This was pursued by monitoring alterations in the photoluminescence color from white to cyan, the hue, the chromaticity and the emission intensity ratio (I_{480}/I_{590}) of WLE-QDC upon interaction with LCUFAs. The concurrent hydrophobic and π–π interactions between the ZnQ_2 complex (present in WLE-QDC) and LCUFAs might play an important role in this regard. Remarkably, the high selectivity of WLE-QDC towards LCUFAs led to their practical utilization in the quantification of LCUFAs in commercial vegetable oils.

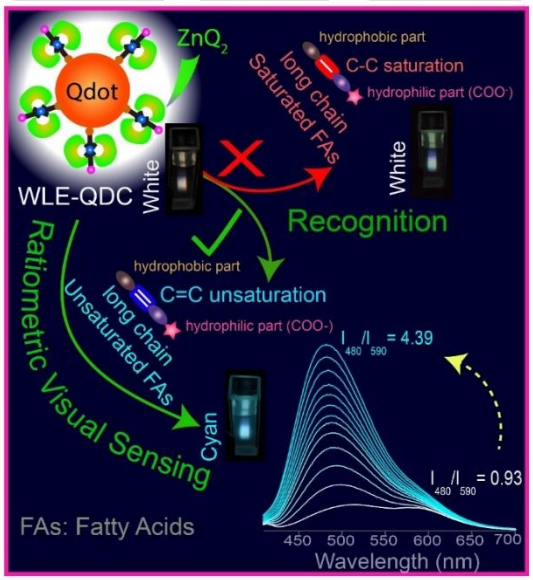

* [Manna et al. *J. Mater. Chem. C*, 2021, **9**, 13810-13817.] - Reproduced by permission from the Royal Society of Chemistry.

4.2 Introduction:

The importance of long-chain unsaturated fatty acids (LCUFAs) in biological processes such as the cell membrane activity, metabolic regulation, responses in the hypothalamus, gene expressions and the functioning of anaerobic digesters is well-established.[1–14] Furthermore, LCUFAs also play a vital role in the production quality of pharmaceuticals, cosmetics and dietary food products, particularly vegetable oils.[1–14] An abnormal content of LCUFAs may lead to diseases in humans such as fatal diseases with symptoms akin to multiple sclerosis, coronary heart disease, chronic pain, depression and weight issues.[1–14] The length of LCUFAs plays a vital role in the emulsification of several pharmaceutical and cosmetic products. On the other hand, the presence of LCUFAs, which cannot be synthesized by the human body, in dietary food products (mainly vegetable oils), compared with their saturated forms that have the same carbon chain length, is essential for lowering the serum cholesterol level (by promoting antioxidant defenses and lessening inflammatory mediators and oxidative stress) and governing cell membrane fluidity.[1–14] Notably, vegetable oils (such as sunflower, edible and soybean oils) that are composed of LCUFAs, such as oleic, linoleic and erucic acids, are important day-to-day food products due to their capability of providing energy and nutritional supplements to the human body.[12–14] However, the quality of vegetable oils as available commercially has a great impact on human health.[12–14] A way of ascertaining this is to check for the contents of LCUFAs, such as oleic, linoleic and erucic acids, as compared with their saturated counterparts in vegetable oils.

The chemical recognition of LCUFAs from their corresponding saturated forms is challenging, owing to their flexible and long hydrocarbon chains with the limited presence of CQC group(s), surface complementarity and water insolubility.[1–5] In this aspect, natural biological recognition moieties such as fatty acid-binding proteins (FABP) and cavities (e.g., FABP4 and FABP5) are known for their use in selectively recognizing LCUFAs (e.g., oleic acid, linoleic acid, etc.).[1–5] Synthetic molecular receptors, such as polyaromatic receptors, polymerized liposomes, organic molecular tubes, supramolecular nanocapsules and cavitands, have displayed their usability towards the recognition of LCUFAs.[1–5] For example, a polyaromatic receptor recognized oleic acid from a mixture of oleic and stearic acids while long-chain unsaturated o-fatty acids could be recognized by different forms of cavitands.[1,2] However, the mentioned receptors

need complicated fabrication strategies, timeconsuming procedures and costly instruments to recognize LCUFAs, which limit their application potential. Thus, it is important to search for new and specific synthetic platforms to discriminate LCUFAs from their corresponding saturated forms through chemical interactions.

Techniques such as gas chromatography, colorimetric assays, nuclear magnetic resonance (NMR) spectroscopy, and liquid/gas chromatography coupled with mass spectrometry (LCMS/GCMS) have been used for the detection of LCUFAs.[6–11] However, the recent development of chemical recognition-based fluorometric methods provides easier, faster and cost-effective options for real sample analysis.[6–11] There are several single-emitting luminescent sensors (for example, calixnaphthalene-based molecular tubes) that sense LCUFAs through luminescence quenching.[8] However, their application is limited due to the drawbacks associated with singlewavelength-based optical sensors such as the variation in intensity based on the local concentration of analytes, the light source and the detector.[15–18] On the other hand, the fast, precise and consistent optical detection ability of ratiometric luminescent sensors, with the supplementary benefit of a visual color change, make ratiometric luminescent sensors unique for the detection of LCUFAs.[15–18] However, such ratiometric luminescent sensors – with the option of chemical interaction-based sensing – are still being developed. For example, (i) a luminescent fatty acid-binding protein has been used to ratiometrically sense oleic acid in the concentration range of 0.02–4.7 μM,[9] (ii) a duplex pyrene–cyclodextrin-based fluorescent sensor has shown its utility for the detection of oleic acid in the concentration range of 0–7.0 equivalents[10] and (iii) a quantum dot–protein composite was able to sense oleic acid in the range of 10–1000 nM.[11] Thus, the exploration of new ratiometric visual sensors, with two emission maxima, is of great value towards the detection of LCUFAs, mainly in dietary vegetable oils.

Incidentally, the surface engineering of bright and photostable quantum dots (Qdots), with various chemical and biological agents, has provided options for fabricating nanomaterials for white-light emission-based optical sensing and imaging.[15–20] For example, modifying the surface of Qdots with an inorganic complex has led to the formation of a nanocomposite – named a quantum dot complex (QDC) – that emits bright and photostable white light.[15–20] The white-light emitting QDCs (WLE-QDCs) have shown their application potential towards the ratiometric visual detection of neurotransmitter agents like dopamine, in vitro pH, heavy metal ions (for example, Hg^{2+}

and Cu^{2+} ions), and phosphate ions in commercial fertilizer.[15–18] However, the utilization of WLEQDCs towards the recognition of LCUFAs from a mixture with their corresponding saturated forms – in addition to their ratiometric visual detection – has not been explored yet. Thus, the idea of using a WLE-QDC for the combined purposes of a molecular recognition nano-platform and a turn-on ratiometric visual sensor for LCUFAs will bring newer avenues in molecular recognition and optical sensing purposes.

Herein we report the twin applications of a bright and photostable WLE-QDC, composed of Mn^{2+}-doped ZnS Qdots and a ZnQ_2 inorganic complex, towards the selective recognition of LCUFAs from their corresponding saturated forms and the turn-on ratiometric visual detection of LCUFAs in commercial vegetable oils. This was pursued by observing the variations in the luminescence characteristics (such as color, hue, emission intensity ratio (I_{480}/I_{590})) of WLE-QDC upon interaction with LCUFAs. Importantly, WLE-QDC exhibited the turn-on and ratiometric visual sensing of LCUFAs (such as Na-salt of oleic acid) with a detection limit of 0.127 μM in the linear range of 4.2–16.6 μM. Notably, WLE-QDC selectively recognized LCUFAs (such as the Na-salt of oleic acid) from a mixture with their corresponding saturated forms (i.e., the Na-salt of stearic acid). The concurrent hydrophobic and π–π interactions of LCUFAs with the quinoline moieties of the surface ZnQ_2 complex (present in WLE-QDC) might play a significant role towards the observed specific luminescence changes of the WLE-QDC upon interaction with LCUFAs. Interestingly, the high selectivity of the WLE-QDC towards LCUFAs in the presence of interfering FAs (such as stearate, palmitate, laurate and geranate), anions (such as citrate, tartrate, oxalate, and fluoride) and metal ions (such as Ca^{2+}, Mg^{2+}, Na^{+} and K^{+}) was noticed. The molecular structures of the mentioned FAs are given in Fig. A.4.1 (Appendix). Finally, the practical utilization of the WLE-QDC was investigated via the quantification of LCUFAs in commercial vegetable oils (such as sunflower, edible and soybean oils). The environmentally friendly synthesis, cost-effectiveness, low toxicity and possible specific chemical interaction of WLE-QDCs make them a preferable choice for the recognition and ratiometric sensing of LCUFAs.[16–20] The obtained results represent the first report showing the advantages of WLE-QDCs towards the selective recognition of LCUFAs from their corresponding saturated forms and the turn-on ratiometric visual detection of LCUFAs in vegetable oils through monitoring the changes in their luminescence properties.

4.3 Experimental Section:

4.3.1 Materials: Zinc acetate dihydrate (Merck, assay = 99.5–101.0 %), manganese acetate tetrahydrate (Merck, assay ≥ 99.0 %), sodium sulphide flakes purified (Merck, assay > 50.0 %), 8-hydroxyquinoline (HQ: Merck, assay ≥ 99.0 %), sodium carbonate (Merck, assay ≥ 99.9 %), sodium hydroxide (Merck, assay ≥ 99.0 %), sodium fluoride (Merck, assay ≥ 99.5 %), di-sodium oxalate (Merck, assay ≥ 99.8 %), tri-sodium citrate dihydrate (Merck, assay = 99.0-101.0 %), di-sodium tartrate dihydrate (Merck, assay ≥ 99.5 %), calcium chloride (Merck, assay ≥ 98.0 %), potassium chloride (Merck, assay ≥ 99.5 %), magnesium chloride (Merck, assay ≥ 98.0 %), sodium chloride (Merck, assay ≥ 99.5 %), methanol (Merck, assay ≥ 99.9 %), sodium oleate (Merck, assay ≥ 82.0 %), sodium stearate (Merck, assay ≥ 99.0 %), linoleic acid (Merck, assay ≥ 99.0 %), palmitic acid (Merck, assay ≥ 99.0 %), geranic acid (Merck, assay = 85.0 %), erucic acid (Merck, assay ≥ 99.0 %), sunflower oil (Fortune company), soybean oil (Fortune company), edible oil (Saffola company) were purchased and directly used without further purification. Water of Milli-Q grade was used for all experiments.

4.3.2 Fabrication of white light emitting quantum dot complex (WLE-QDC):

(i) Synthesis of Mn^{2+}-doped ZnS quantum dots (Qdots): Mn^{2+}-doped ZnS Qdots were synthesized using a previously reported procedure.[16,17,19a] In short, an aqueous solution of sodium sulfide was added to an aqueous mixture of zinc acetate dihydrate and manganese acetate tetrahydrate in such a way that the concentrations of S^{2-}, Zn^{2+} and Mn^{2+} ions in the reaction mixture were 5.0 mM, 5.0 mM and 0.75 mM, respectively. The reaction mixture was heated at 100 °C and refluxed for 4 h with continuous stirring. To separate synthesized colloidal particles from aqueous phase, (i) at first, the milky white reaction mixture was centrifuged for 10 min with speed of 20,000 rpm and (ii) then, the separated colloidal particles (i.e., pellet after centrifugation) were redispersed into same amount of water and centrifuged with same experimental condition in order to remove the unreacted reactants. The separation process was repeated again and finally the solid pellet was dispersed into 200.0 mL of water using sonication. The colloidal dispersion was used as stock for all other experiments.

(ii) Preparation of 8-hydroxyquinoline (HQ) solution: 7.3 mg of solid HQ was dissolved in 10.0 mL of methanol by sonication at room temperature to prepare 5.0 mM methanolic solution of HQ.

(iii) Fabrication of WLE-QDC: The WLE-QDC was prepared by adding 15.0 µL of 5.0 mM methanolic solution of HQ into 3.0 mL of as-prepared aqueous dispersion of Qdots (with absorbance of 0.04 at 357 nm). Then, the aforementioned mixture of HQ and Qdots was centrifuged at 20,000 rpm for 10 min. The pellet obtained from centrifugation was redispersed into same volume of water and centrifuged under same condition and then the pellet was washed as before. Finally, the pellet was dispersed into same volume of water, which was then used for further experiments. For the preparation of WLE-QDC, the optimum concentration of HQ used was calculated to be 25.0 µM.

4.3.3 Sensing of LCUFAs: The sensing of LCUFA was performed by adding 2.5 mM aqueous solution of sodium oleate sequentially to 3.0 mL of aqueous dispersion of WLE QDC (with absorbance of 0.06 at 357 nm) followed by recording of their photoluminescence spectra and other optical properties. The experiment was carried out in triplicate. The intensity ratio (I_{480}/I_{590}) of WLE QDC against concentration of oleate was plotted to find out the linear range and to calculate the limit of detection (LOD). Equation $3\sigma/k$ was used for the calculation of LOD. Similarly, the sensing of other LCUFAs (like linoleate and erucate) by WLE-QDC was also carried out.

4.3.4 Recognition of long chain unsaturated fatty acid (LCUFA) from their saturated form: The different responses of WLE-QDC towards LCUFA (e.g., oleic acid) and their corresponding saturated form (i.e., stearic acid) were examined by adding mixture of sodium salt of oleic acid and stearic acid with different ratio of concentrations (with keeping total concentration of fatty acids to a fixed amount) into the solution of WLE-QDC. Accordingly, five different ratiometric mixtures were prepared with oleate and stearate ratio of 0:1, 1:3, 1:1, 3:1 and 1:0 (keeping the total fatty acid concentration equal to 2.5 mM). The highest amount of oleate added to WLE-QDC (with absorbance of 0.06 at 357 nm) for this experiment was 80.6 µM and the photoluminescence properties of oleate added WLE-QDC were monitored. Similar experiment was performed for stearate (of 80.6 µM). The experiments were performed in triplicate.

4.3.5 Selectivity of Sensing by WLE-QDC towards LCUFAs: Selectivity of sensing by WLE-QDC towards LCUFAs was examined by adding sodium salt of different

saturated and unsaturated fatty acids (like oleic acid, linoleic acid, erucic acid, palmitic acid, lauric acid, geranic acid and stearic acid), anions (like citrate tartrate, oxalate and fluoride) and metal ions (like Ca^{2+}, Mg^{2+}, Na^{+} and K^{+}). The mentioned interfering substances were added to 3.0 mL of aqueous dispersion of WLE QDC (with absorbance of 0.06 at 357 nm) separately such that their concentration became 80.6 µM (same as the highest concentration used in sensing experiment as in Fig. 4.2 of the Chapter 4). The experiments were carried out executed in triplicate. The change in intensity ratio ($\Delta (I_{480}/I_{590}) = (I_{480}/I_{590})_{\text{after addition}} - (I_{480}/I_{590})_{\text{before addition}}$) of WLE-QDC after addition of each substance was plotted in bar diagram for comparative study. It is to be noted here that linoleic acid, erucic acid, palmitic acid, lauric acid and geranic acid were converted to their corresponding sodium salts by following a previously reported method.[6] In short, excess amount of solid sodium carbonate was added to 5.0 mL of 100 mM methanolic solution of above mentioned fatty acids separately and stirred for 20 min at 40 °C. The reaction mixtures were then filtered to remove unreacted Na_2CO_3 and were dried in vacuum to get sodium salt of corresponding fatty acids.[6]

4.3.6 Commercial Vegetable Oil Analysis. For real sample analysis commercial sunflower, edible and soybean oils were purchased from local market and saponified with 20% aqueous NaOH solution following a well-known procedure.[6] In short, 5.0 mL of 20% aqueous NaOH was added to 5.0 mL of each of above-mentioned oils separately and stirred for 30 min at 80 °C. The formed sodium salts of fatty acids were precipitated out by cooling the reaction mixture in an ice cold condition. Then the precipitate was filtered and washed with ice cold water followed by drying in vacuum. Dried solid salt of sunflower, edible and soybean oil were dissolved in water to make 0.2, 0.5 and 0.3 mg/mL solutions, respectively. LCUFAs in those solutions were determined following above-mentioned sensing procedure by adding 20.0 µL of each solution to 3.0 mL of WLE QDC (with absorbance of 0.06 at 357 nm) separately and monitoring the photoluminescence properties. Notably, a linear relationship between I_{480}/I_{590} of WLE-QDC and concentrations of equivalent mixture of (i) oleate, (ii) linoleate and (ii) erucate was measured (Fig. A.4.15, Appendix) and used for the quantification of LCUFAs in commercial vegetable oils such as sunflower, edible and soybean oils (Table 4.1 of Chapter 4).

4.3.7 Instruments: To characterize the samples and to probe the recognition and sensing phenomena, HORIBA Jobin Yvon FluoroMax-4 spectrofluorimeter was mainly used to record photoluminescence. Digital photographs were taken using Realme Mobile (Realme 5) under spectrofluorimeter excitation source. OSRAM color calculator (CIE-1931) software was used to calculate chromaticity coordinates from photoluminescence spectra and Image-J software was used to calculate hue from digital photograph. PerkinElmer Lambda 35 UV–vis spectrophotometer was used to record the absorption spectra of the samples. Transmission electron microscopy (TEM; Model: JEOL JEM 2100F, maximum accelerating voltage: 200 kV) was used to analyze the size and lattice parameters of the nanoparticles. Gatan Digital Micrograph software was used to analyze TEM image, High resolution TEM image and corresponding inverse fast Fourier transformation. X-ray diffraction patterns of the samples were recorded by using Rigaku TTRAX-III X-ray diffractometer.

4.4 Result and Discussion:

The QDC was prepared using the complexation reaction between Mn^{2+}-doped ZnS Qdots and 8-hydroxyquinoline (HQ).[19] The step-wise details of the synthesis are available in the Experimental Section. Briefly, (i) water-soluble Qdots were synthesized using an established procedure,[16–20] (ii) an alcoholic solution of HQ was prepared using sonication, and (iii) finally, the complexation reaction between Qdots and HQ was performed to synthesize the QDC nanocomposite that was followed by monitoring the photoluminescence properties. The HQ-complexed Qdot is called herein the QDC. The preservation of the morphology (in terms of diameter of 4.6 ± 0.4 nm, lattice fringe (0.3 nm due to the 111 plane and characteristic diffraction patterns) of the host cubic ZnS was observed when the Qdot was transformed into the QDC. This was concluded by comparing the transmission electron microscopy (TEM) images, the high-resolution TEM images and the X-ray diffraction (XRD) patterns of the Qdots and QDC (Fig. 4.1A–D). When excited using 357 nm light, the aqueous dispersions of Qdots and QDC displayed orange and white luminescence colors, respectively (Fig. 4.1E). The white-light-emitting QDC is termed hereafter as WLE-QDC.

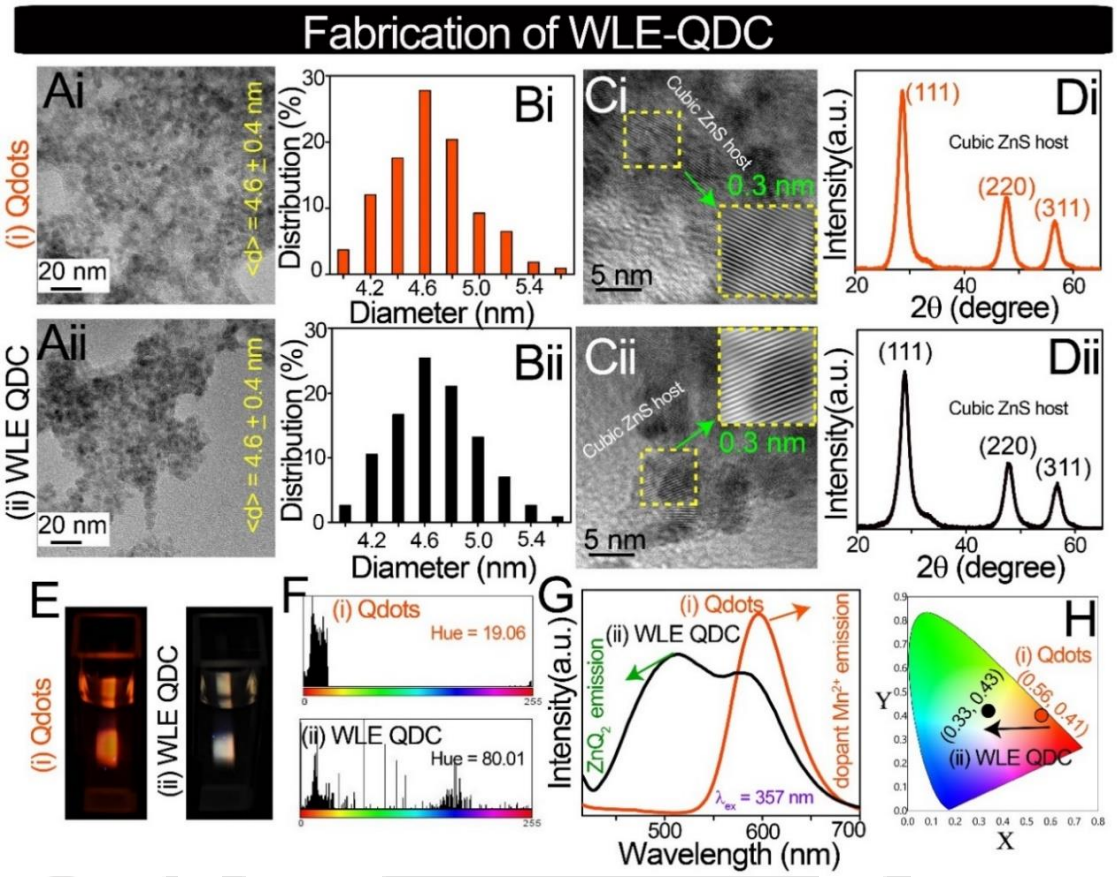

Fig. 4.1 (A) Transmission electron microscopy (TEM) images (scale bar = 20 nm), (B) corresponding particle size distributions, (C) high-resolution TEM images (scale bar = 5 nm) and corresponding inverse fast Fourier transform (IFFT) analyses (inset), (D) powder X-ray diffraction patterns, (E) photographs (λ_{ex} = 357 nm), (F) hue histograms (acquired by analysing digital photographs using Image-J software), (G) emission spectra (λ_{ex} = 357 nm), and (H) corresponding color chromaticity coordinates in the CIE diagram of (i) Qdots and (ii) WLE-QDC.

The alteration in the hue value from 19.06 to 80.01 also supported the transformation of an orange-light-emitting Qdot to a WLE-QDC (Fig. 4.1F). The WLE-QDC exhibited an extinction peak at 365 nm in addition to the original peak of the Qdots at 325 nm (Fig. A.4.2, Appendix). The WLE-QDC (with λ_{ex} = 357 nm) showed the appearance of a new green emission peak at 512 nm – along with the Mn^{2+}-dopant's orange emission peak of the Qdots at 590 nm (Fig. 4.1G). Notably, the green emission (at 512 nm) arose due to the intrinsic molecular electronic transition of the surface ZnQ_2 complex when the Qdots were reacted with HQ to form WLE-QDC, while the orange

emission peak at 590 nm was due to the $^4T_1$–$^6A_1$ electronic transition of the Mn^{2+} dopants of the Qdots (present in the WLE-QDC).[16–20] The synchronous contribution of the dual emitting species (i.e., ZnQ_2 and Qdots) led to the generation of white light from the QDC. This clearly demonstrated the successful fabrication of the WLE-QDC. Furthermore, the orange- and white-light nature of the Qdots and QDC were supported by observing the chromaticity coordinates of (0.56, 0.41) and (0.33, 0.43), respectively, in the CIE diagram (Fig. 4.1H). The WLE-QDC displayed a photoluminescence quantum yield (PLQY%; using quinine sulphate as the reference at an excitation wavelength of 357 nm) of 0.28, while a PLQY% of 0.45 was measured for the as-synthesized Qdots.[19]

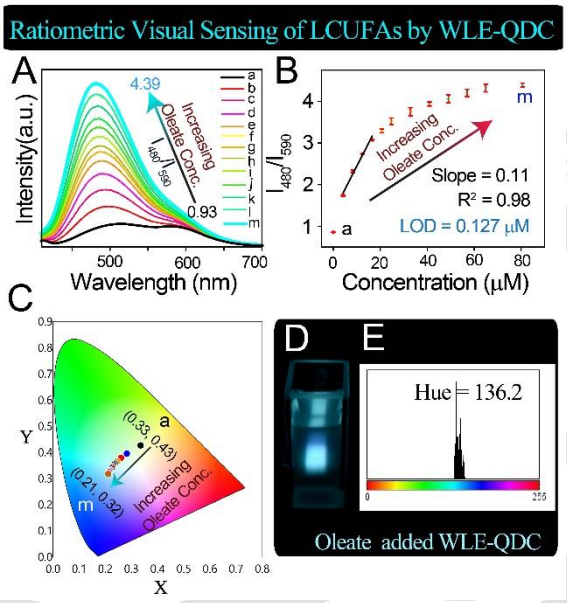

Fig. 4.2 (A) Representative emission spectra (λ_{ex} = 357 nm), (B) changes in the emission intensity ratio (I_{480}/I_{590}) and (C) corresponding color chromaticity coordinates of WLE-QDC recorded following the addition of different concentrations of LCUFA (that is, oleate): ((a) 0.0, (b) 4.2, (c) 8.3, (d) 12.4, (e) 16.6, (f) 20.7, (g) 24.8, (h) 32.9, (i) 41.0, (j) 49.0, (k) 57.0, (l) 64.9, and (m) 80.6 μM). The experiments were carried out in triplicate. A linear relationship between the I_{480}/I_{590} value of the WLE-QDC and the concentration of oleate (4.2–16.6 μM) was measured to estimate limit of detection (LOD). (D) Photograph (λ_{ex} = 357 nm) and corresponding (E) hue histogram (acquired by analysing digital photographs using ImageJ software) of the WLE-QDC following the addition of 80.6 μM of oleate.

The decrease in PLQY of the Qdots upon conversion to WLE-QDC might be due to the presence of ZnQ_2 (which typically acts as a quencher of the orange emission of the Qdots

– as supported by our earlier observations)[16,18,19] on the surface of the Qdots. The stability of the WLE-QDC in terms of the emission intensity ratio (I_{512}/I_{590}) at different time intervals (up to 48 h) in a water medium was observed (Fig. A.4.3, Appendix). Additionally, the WLE-QDC was found to be photostable under continuous irradiation of 357 nm light for 20 min. The observation was made with respect to the emission maxima of the Qdots (590 nm) and the surface ZnQ_2 complex (512 nm; Fig. A.4.4, Appendix). These results clearly demonstrated the usability of the WLE-QDC for recognition and optical sensing purposes.[16,17]

The turn-on ratiometric visual sensing of LCUFAs (particularly, the Na-salt of oleic acid) by the WLE-QDCs (having absorbance of 0.06 at 357 nm) was demonstrated by first observing the alterations in their emission characteristics (such as the intensity ratio, change in emission wavelength, chromaticity and hue). The sequential addition of oleate (in the range of 0.0–80.6 μM) to the WLE-QDCs led to high and slight enhancements in their emission intensities at 480 and 590 nm, respectively (Fig. 4.2A). Notably, the emission intensity ratio (I_{480}/I_{590}) of WLE-QDCs increased from 0.93 to 4.39 with the increasing concentration of oleate in the range of 0.0–80.6 μM (Fig. 4.2B and Table A.4.1, Appendix). Furthermore, the gradual shift in the emission maximum from 512 to 480 nm of the ZnQ_2 complex (present in WLE-QDC) with the increasing concentration of oleate was observed and thus indicated the specific chemical interaction of oleate with the WLE-QDCs (Fig. A.4.5, Appendix). The extinction of the WLE-QDC, upon the addition of oleate, remained unaltered (Fig. A.4.6, Appendix). A linear relationship between the emission intensity ratio (I_{480}/I_{590}) of WLE-QDC and the concentration of oleate in the range of 4.2–16.6 μM was noticed (Fig. 4.2B). The limit of detection (LOD) was calculated to be 0.127 μM, which is quite reasonable for the detection of oleate and is comparable to earlier reported luminescent nanoprobes (Table A.4.2, Appendix).[1–11] Further, a gradual shift in the color chromaticity coordinates of the WLE-QDC from (0.33, 0.43) to (0.21, 0.32) was observed when the WLE-QDC was titrated with an increasing concentration of oleate in the range of 0.0–80.6 μM (Fig. 4.2C). The treatment of oleate on the WLE-QDC resulted in an alteration of the luminescence color (λ_{ex} = 357 nm) from white to cyan, and this was also supported by the changes observed in their hue values from 80.01 to 136.2 (Fig. 4.2D and E). Notably, the enhancement in the average emission fluorescence lifetime ((λ_{ex} = 375 nm laser; (λ_{em} = 480 nm) from 8.3 to 13.0 ns with regard to the emission of ZnQ_2 was noticed when

WLE-QDC was treated with oleate (Fig. A.4.7 and Table A.4.3, Appendix). It is to be noted here that the enhancement in the fluorescence lifetime of the ZnQ_2 complex (being present in WLE-QDC) in the presence of oleate might be due to the attainment of structural rigidity and activation of the surface states.[24–26] This is in support of the luminescence-enhancement-based ratiometric sensing of oleate by WLE-QDC. On the other hand, the average emission phosphorescence lifetime (λ_{ex} = 330 nm; λ_{em} = 590 nm, which is due to the $^4T_1$–$^6A_1$ electronic transition of the Mn^{2+} dopants of the Qdots)[16–20] of WLE-QDC with regard to the emission of the Qdots remained unaltered even after oleate treatment (Fig. A.4.7 and Table A.4.3, Appendix). Thus, the presented results clearly demonstrate the usability of WLE-QDC as a turn-on ratiometric visual sensor of LCUFAs (especially the Na-salt of oleic acid).

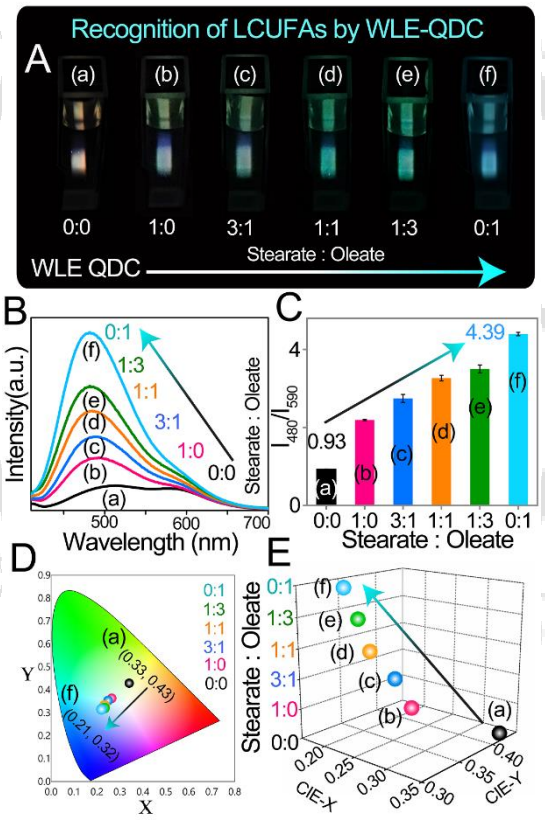

Fig. 4.3 Comparative changes in (A) digital photographs (λ_{ex} = 357 nm), (B) emission spectra (λ_{ex} = 357 nm), (C) bar diagram of the emission intensity ratio (I_{480}/I_{590}), (D) color chromaticity coordinates and (E) 3-D chromaticity plot of the WLE-QDC in presence of a mixture of LCUFAs and corresponding saturated forms (for example, mixture of the Na-salts of oleic and stearic acids): ((a) 0 : 0, (b) 0 : 1, (c) 1 : 3, (d) 1 : 1, (e) 3 : 1, and (f) 1 : 0. The experiments were performed in triplicate.

The selective recognition of an LCUFA (for example, the Na-salt of oleic acid) from a mixture with the corresponding saturated form (i.e., the Na-salt of stearic acid) was demonstrated by observing the changes in the photoluminescence properties (such as the visual luminescence color, the hue, the emission intensity ratio, the shift in the emission wavelength, and the chromaticity) of the WLE-QDC (having an absorbance of 0.06 at 357 nm). Notably, only the oleate-induced luminescence color change from white to cyan of the WLE-QDC was noted, while a blueish white luminescence color was noticed for only stearate (under 357 nm light; Fig. 4.3A). With an increasing concentration of oleate in the mixture of oleate and stearate, the white luminescence of the WLE-QDC (under 357 nm light) changed towards the cyan color as depicted in Fig. 4.3A. As the concentration of oleate was increased in the mixture, the enhancement in the emission intensity due to the ZnQ_2 complex, with a shift in the emission maximum from 512 to 480 nm, of the WLE-QDC was noticed (Fig. 4.3B). This indicated the specific chemical interaction of oleate with the ZnQ_2 complex present in the WLE-QDC. Fig. 4.3C clearly shows the changes in the emission intensity ratio (I_{480}/I_{590}) of the WLE-QDC in the presence of a ratiometric mixture of stearate and oleate. The emission intensity ratio (I_{480}/I_{590}) of the WLE-QDC changed from 0.93 to 2.19 upon the addition of a 1 : 0 mixture of stearate and oleate, while the addition of a 0 : 1 ratiometric mixture of stearate and oleate to the WLE-QDC led to a change in the emission intensity ratio (I_{480}/I_{590}) from 0.93 to 4.39 (Fig. 4.3C). Thus, the oleate induced enhancement in the emission intensity ratio (I_{480}/I_{590}) of WLE-QDC was noticed. This clearly indicated the selective binding/interaction of oleate with the WLE-QDC and its effect on the emission due to the surface complex. Similarly, changes in the chromaticity coordinates in the CIE diagram and a 3-D chromaticity plot were observed when the WLE-QDC was reacted with different ratiometric mixtures of oleate and stearate (Fig. 4.3D and E and Table A.4.4, Appendix). For example, the change in the chromaticity values from (0.33, 0.43) to (0.26, 0.37) was observed for the WLE-QDC when reacted with a 1 : 0 mixture of stearate and oleate, while the addition of a 0 : 1 ratiometric mixture of stearate and oleate to the WLE-QDC led to a change in the chromaticity from (0.33, 0.43) to (0.21, 0.32) (Fig. 4.3D and E and Table A.4.4, Appendix). The results further supported the observed changes in the photoluminescence of the WLE-QDC, which may be attributed to the specific interaction of oleate with the ZnQ_2 complex present in the WLE-QDC. Thus, WLE-QDC could be useful as a nanoprobe to discriminate LCUFAs from their corresponding saturated forms through monitoring luminescence changes, and further

indicating the usability of the WLE-QDC as a ratiometric visual sensor of LCUFAs in commercial vegetable oils. The advantages of environmentally friendly synthesis, cost-effectiveness, lower toxicity and possible specific chemical interaction of the WLE-QDC make it a preferable recognition luminescent platform for the recognition of LCUFAs in comparison with other reported molecular receptors, which need complicated fabrication strategies, time-consuming procedures and costly instrumentation (Table A.4.2, Appendix).[1–11]

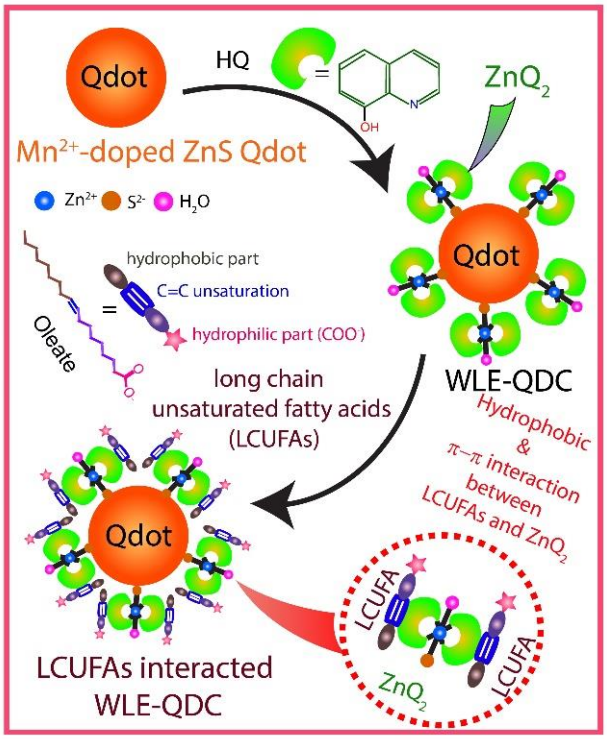

Scheme 4.1 Schematic illustration of the fabrication of WLE-QDCs followed by the reaction between Qdot and HQ and proposed mechanism of recognition and ratiometric visual sensing of LCUFAs by WLE-QDC nanoprobe.

The mechanism of the presented recognition and sensing of LCUFAs (here, oleate is used as a model sample) was verified with the help of the combined results obtained from luminescence-based control experiments, Fourier transform infrared (FTIR), zeta potential measurements and supportive observations acquired from earlier reports. Notably, the aqueous dispersion of only oleate and a mixture of oleate with Zn^{2+} and Mn^{2+} ions did not exhibit any fluorescence when excited using 357 nm light (Fig. A.4.8, Appendix). This clearly excluded the possibility of any luminescence from oleate

and its metal complexes. The change in the pH from 5.8 to 7.9 of the WLE-QDC was observed when treated with 80.6 μM oleate (i.e., the concentration at which the maximum enhancement in the emission intensity ratio (I_{480}/I_{590}) of the WLE-QDC was observed, as depicted in Fig. 4.2B). The pH adjustment of the WLE-QDC from 5.8 to 7.9 resulted in a decrease in the emission intensity ratio (I_{480}/I_{590}), which is opposite to the results of oleate addition to WLE-QDC (Fig. A.4.9, Appendix). This clearly ruled out the effect of pH during the recognition and sensing of oleate by the WLE-QDC. At pH of 7.9 (i.e., the same value of oleate added to WLE-QDC in water), oleic acid/oleate existed as an oil–water emulsion (as per earlier reports) and thus ruling out the chance of micelle formation (which generally occurs at the higher pH of 10.6).[21] This is further supported by the fact that the oleate concentration used (in the range of 0.0–80.6 μM) is lower compared to the critical micelle concentration, which is around 2.5 mM at room temperature (as supported by earlier observations).[21] Fig. A.4.10 (Appendix) shows that the addition of oleate to only Qdots resulted in a slight enhancement in the emission intensity at 590 nm (akin to the observed oleate-induced change in the emission of Qdots, present in WLE-QDC as depicted in Fig. 4.2B). This may be either due to the oleate-induced surface passivation of Qdots (irrespective of their bare form as well their WLE-QDC form) or due to the increase in pH of the medium when oleate interacted with WLE-QDC/only Qdots.[22,23] Importantly, the enhancement in the emission intensity at 480 nm was noticed when the ZnQ_2 complex attached ZnS Qdots were treated with oleate (Fig. A.4.10, Appendix). These results clearly supported the observation made when oleate was treated with WLE-QDC (depicted in Fig. 4.2A) and also the claim that oleate specifically interacted with the surface ZnQ_2 complex (present in WLE-QDC). Thus, the specific interaction between oleate and the ZnQ_2 complex (present in WLE-QDC) played a vital role in the observed luminescence changes of WLE-QDC. Notably, the higher and specific binding affinity of oleate towards the surface ZnQ_2 complex (of WLE-QDC) may be due to concurrent hydrophobic and π–π interactions between quinoline moieties of the ZnQ_2 complex (present in WLE-QDC) and oleate molecules, which led to the structural rigidity of the ZnQ_2 complex and thus the oleate-induced enhancement of luminescence of ZnQ_2 was noticed. According to the literature, the structural rigidity and activation of the surface states of the ZnQ_2 complex are the key factors for enhancing their emission features.[24,25] For example, the protein- and surfactant-induced structural rigidity of the ZnQ_2 complex (either in its bare form or attached to ZnS Qdots) led to the enhancement of their luminescence.[24–26] Also, reports have shown that the π–π interaction is important in order

to discriminate LCUFAs from their corresponding saturated forms.[1] These earlier results also supported the current oleate-induced structural rigidity of the ZnQ_2 complex (being present in WLE-QDC). Now, when the oleate-treated WLE-QDC was centrifuged and redispersed into the same amount of water, the pellet showed an enhanced emission and an intensity ratio (I_{480}/I_{590}) similar to that of their reaction mixture (i.e., oleate-treated WLE-QDC before centrifugation) while no emission was noticed for the supernatant of that medium (Fig. A.4.11, Appendix). This clearly indicated the incorporation of oleate on the surface of the WLE-QDC and thus might have been the reason for the observed enhancement in the emission intensity ratio of the WLE-QDC. The incorporation of oleate on the surface of WLE-QDC was further confirmed from the main functional group's characteristic peaks that are attributed to the symmetric and asymmetric stretching of –CH2 (at 2850 and 2918 cm^{-1}) and COO^{-} (at 1542 cm^{-1}) – along with the characteristic peaks of the main functional groups of ZnQ_2 – in the FTIR spectrum of oleate-treated WLE-QDC (recorded following centrifugation; Fig. A.4.12 and Table A.4.5, Appendix).[27] Further, the decrease in the zeta potential value of WLE-QDC from +28.5 mV to +7.9 mV, following the addition of oleate, clearly indicated the oleate-induced surface modification of the WLE-QDC (Fig. A.4.13 and Table A.4.6, Appendix). On the other hand, the addition of Na-salts of aromatic compounds (such as benzoate and cinnamate) and Na-salts of shorter chain UFAs (such as geranate), with the capability of forming π–π interactions, to WLE-QDC did not show any significant change in the emission intensity ratio (I_{480}/I_{590}) and luminescence color (Fig. A.4.14, Appendix). While medium- and long-chain saturated FAs (such as laurate and palmitate, with the possibility of hydrophobic interactions) showed a slight enhancement in the emission intensity ratio (I_{480}/I_{590}) (which was not like the observed change in emission intensity ratio (I_{480}/I_{590}) from 0.93 to 4.39 in case of oleate added WLE-QDC), no significant change, however, was noticed in terms of the luminescence color of the WLE-QDC in the presence of laurate or palmitate (Fig. A.4.14, Appendix). Importantly, when other long-chain UFAs (such as linoleate and erucate, which have the capability of forming hydrophobic and π–π interactions akin to oleate) were treated with WLE-QDC, similar observations in the enhancement of the emission intensity ratio, as well as the luminescence color change from white to cyan (akin to oleate-treated WLE-QDC), were observed (Fig. A.4.15, Appendix). Thus, the presence of a long hydrocarbon chain along with unsaturated C=C bond(s) are needed to alter the luminescence color and intensity ratio (I_{480}/I_{590}) of the WLE-QDC. This clearly indicated that the specific and concurrent

effect of hydrophobic and π–π interactions between the quinoline moieties of the ZnQ_2 complex (present in WLE-QDC) and LCUFAs might play an essential role towards the selective recognition and turn-on ratiometric visual sensing of LCUFAs including oleate, linoleate and erucate by the WLE-QDC. It should be further mentioned here that the synchronous contribution of the ZnQ_2 complex (λ_{em}-480 nm) and Qdots (λ_{em}-590 nm) led to the generation of the white-light emission from the as-fabricated QDC.[16,18,19] The specific chemical interaction (i.e., the concurrent effect of hydrophobic and π–π interactions) of the LCUFAs (such as oleate, linoleate, erucate and their equivalent mixture) with the ZnQ_2 complex (λ_{em} = 480 nm; being present in the WLE-QDC) led to the structural rigidity of the ZnQ_2 complex with an enhancement in the emission intensity, the average life time and the blue-shift in the emission maximum. On the other hand, the emission intensity, the average lifetime and the emission maximum of the other component of WLE-QDC (i.e., Mn^{2+} doped-ZnS Qdots with λ_{em} = 590 nm) remained unaltered in the presence of LCUFAs. As a result, when LCUFAs interacted with the WLE-QDC, the change in the emission intensity ratio (I_{480}/I_{590}) of the WLE-QDC was noticed and thus led to the change in the luminescence color from white to cyan. The fabrication of the WLE-QDC (based on the reaction between Qdot and HQ) and the mechanism (based on the concurrent hydrophobic and π–π interactions) for the recognition and sensing of LCUFAs by the WLE-QDC is clearly demonstrated in Scheme 4.1.

Furthermore, the selective detection of a mixture of LCUFAs in commercial oils (such as sunflower, edible and soybean oils) was successfully verified through changes in the luminescence of the WLE-QDC nanoprobe. The selectivity of the WLE-QDC towards the Na-salts of LCUFAs (such as oleate, linoleate, erucate and their equivalent mixture) was tested in the presence of interfering Na-salts of FAs (such as stearate, palmitate, laurate and geranate), anions (which are basically used as interfering anions during spot tests of FAs; such as citrate, tartrate, oxalate, and fluoride)[28] and metal ions (which are commonly present in water; such as Ca^{2+}, Mg^{2+}, Na^{+} and K^{+}). The molecular structures of the FAs are given in the Appendix (Fig. A.4.1). There were no significant changes in the emission intensity ratio (I_{480}/I_{590}) and the white-light luminesce of the WLE-QDC in the presence of the mentioned interfering substances (Fig. 4.4A and B and Table A.4.7, Appendix). This clearly indicated the high selectivity of the WLE-QDC towards the Na-salts of LCUFAs (such as oleate, linoleate and erucate).

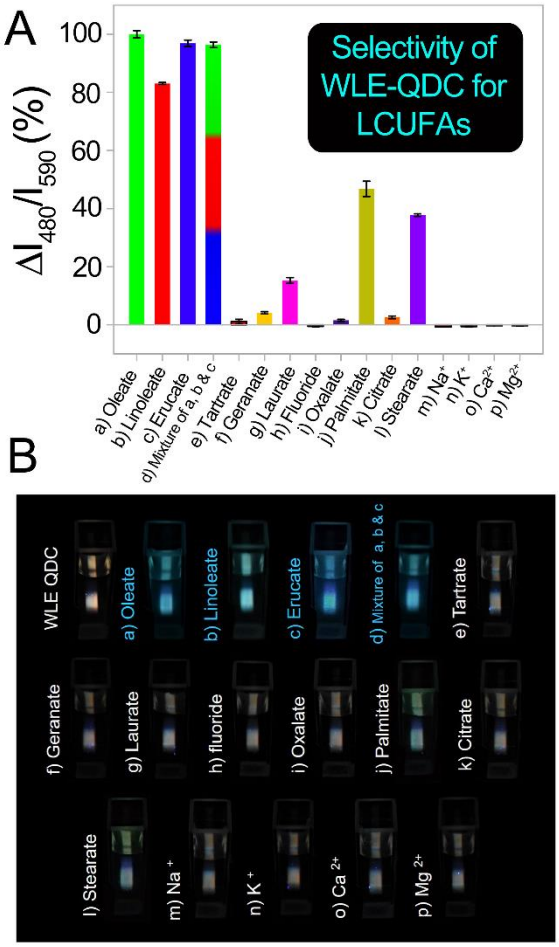

Fig. 4.4 (A) Bar diagram of the comparison of emission intensity ratios (I_{480}/I_{590}) and corresponding (B) photographs (λ_{ex} = 357 nm) of WLE-QDC obtained following the addition of the above-mentioned interfering substances (as in the legends) with the concentration of 80.6 μM (for each substance).

In addition, the WLE-QDC showed LODs of 0.126 μM and 0.103 μM (in the linear range of 4.2–16.6 μM) for linoleate and erucate (which are generally present in commercial vegetable oils in addition to oleate) respectively (Fig. A.4.15, Appendix). This further supported the prescribed mechanism of concurrent hydrophobic and π–π interactions between the quinoline moieties of the ZnQ_2 complex (present in the WLE-QDC) and the LCUFAs including oleate, linoleate and erucate. Importantly, the practical utilization of the WLE-QDC was tested for the detection of LCUFAs in the commercial vegetable oils (such as sunflower, edible and soybean oils), which mostly contain LCUFAs including oleate, linoleate and erucate.[1–14] The quantification of the mixture of long-chain UFAs in the above-mentioned vegetable oils was demonstrated using the linear equation obtained

from the plot of I_{480}/I_{590} (of the WLE-QDC) vs. the concentration of the equivalent mixture of Na-salts of LCUFAs in the range of 4.2–16.6 μM (Fig. A.4.16, Appendix). The representative emission spectra (λ_{ex} = 357 nm) of the WLE-QDC followed by the addition of saponified commercial vegetable oils such as sunflower, edible and soybean oils are given in Fig. A.4.17A–C, Appendix. The digital photographs of the commercial vegetable oils, such as sunflower, edible and soybean oils, used for the experiments are given in Fig. A.4.17D, Appendix. Notably, recovery rates in the range of 97.04–102.96%, with relative standard deviations (RSDs) below 6%, were noticed for a spiked equivalent mixture of Na-salts of LCUFAs (i.e., oleate, linoleate and erucate) in the mentioned vegetable oils (Table 4.1). This clearly demonstrated that other substances present in the mentioned vegetable oil samples did not show any significant interference. Hence, the presented WLE-QDC could be useful for the detection of LCUFAs in real and commercial vegetable oils with excellent reliability. It should be mentioned here that the recognition of LCUFAs in comparison with their saturated forms and their quantification is important towards monitoring the quality of the vegetable oils, although their sensitivity towards the detection of LCUFAs is incidental.

Table 4.1 Results for the detection of LCUFAs in commercial vegetable oils such as sunflower, edible and soybean oils (mean ± SD, n = 3). The representative emission spectra (λ_{ex} = 357 nm) of WLE-QDC recorded following the addition of different concentrations of mentioned saponified commercial oils are given in Fig. A.4.17, Appendix. The extracted concentrations against the data are described and tabulated. The recovery rates (%), with relative standard deviations (RSDs), were tabulated for a spiked equivalent mixture of Na-salts of LCUFAs (i.e., oleate, linoleate and erucate) in the mentioned vegetable oils. Each experiment was performed in triplicate.

Samples	Blank (mM)	Spiked (mM)	Calculated (mM)	Recovery (%)	RSD (%)
Sunflower Oil	0.29	1.35	1.68	102.96	4.37
Edible Oil	0.69	1.35	2.00	97.04	2.02
Soybean Oil	0.40	1.35	1.75	100.00	5.69

4.5 Conclusion:

In summary, the WLE-QDC, which is comprised of Mn^{2+}-doped ZnS Qdots and the ZnQ_2 inorganic complex, exhibited the twin advantages in terms of the selective recognition of LCUFAs from their corresponding saturated forms and the turn-on ratiometric visual detection of LCUFAs in commercial vegetable oils. This was demonstrated by monitoring the variations in the luminescence characteristics (such as color, hue, emission intensity ratio (I_{480}/I_{590})) of the WLE-QDC upon interaction with LCUFAs. Importantly, the WLE-QDC demonstrated its use as a turn-on and ratiometric visual sensor for the detection of LCUFAs (for example, the Na-salt of oleic acid) with a detection limit of 0.127 μM in the linear range of 4.2–16.6 μM. Notably, the WLE-QDC selectively recognized LCUFAs (such as the Na-salt of oleic acid) from a mixture with their corresponding saturated forms (i.e., the Na-salt of stearic acid). The concurrent hydrophobic and π–π interactions between the quinoline moieties of the surface ZnQ_2 complex and LCUFAs may account for the observed specific luminescence changes of the WLE-QDC when interacted with LCUFAs. Finally, the high selectivity of the WLE-QDC nanoprobe towards LCUFAs led to its practical utilization in the quantification of LCUFAs in commercial vegetable oils (such as sunflower, edible and soybean oils).

4.6 Bibliography:

1. K. Niki, T. Tsutsui, M. Yamashina, M. Akita and M. Yoshizawa, *Angew. Chem., Int. Ed.*, 2020, **59**, 10489-10492.
2. (a) S. Mosca, D. Ajami and J. Rebek, *Proc. Natl. Acad. Sci. U. S. A.*, 2015, **112**, 11181-11186. (b) K. D. Schierbaum, T. Weiss, E. U. Thoden Van Velzen, J. F. J. Engbersen, D. N. Reinhoudt and W. Göpel, *Science*, 1994, **265**, 1413-1415.
3. K. Wang, J. H. Jordan and B. C. Gibb, *Chem. Commun.*, 2019, **55**, 11695-11698.
4. K. Yazaki, Y. Sei, M. Akita and M. Yoshizawa, *Nat. Commun.*, 2014, **5**, 5179.
5. J. N. Lee, H. Kim, H. Yao, Y. Chen, K. Weng and J. Ye, *Proc. Natl. Acad. Sci. U. S. A.*, 2010, **107**, 21424.
6. Y.-S. Cho, D. H. Ma and K. H. Ahn, *J. Mater. Chem. C*, 2016, **4**, 2871-2876.
7. F. Zhang, X. Wang, H. Tang, X. Jie, X. Jiang and W. Wei, *Nanotechnology*, 2018, **30**, 065502.

8. B. J. Shorthill, C. T. Avetta and T. E. Glass, *J. Am. Chem. Soc.*, 2004, **126**, 12732-12733.
9. A. Bartolome, C. Bardliving, G. Rao and L. Tolosa, *Anal. Biochem.*, 2005, **345**, 133-139.
10. K. Fujimoto, S. Yamada and M. Inouye, *Chem. Commun.*, 2009, 7164-7166.
11. S. V. Dezhurov, I. Y. Volkova and M. S. Wakstein, *Bioconjugate Chem.*, 2011, **22**, 338-345.
12. (a) A. R. Saltiel and C. R. Kahn, *Nature*, 2001, **414**, 799-806. (b) E. Honoré, J. Barhanin, B. Attali, F. Lesage and M. Lazdunski, *Proc. Natl. Acad. Sci. U. S. A.*, 1994, **91**, 1937. (C) X. Chen, K. M. Lee and J. Yoon, *Bull. Korean Chem. Soc.*, 2011, **32**, 3775. (D) S. C. Smolinske, *Handbook of Food, Drug, and Cosmetic Excipients* 1992, pp. 1–448.
13. (a) C. D. Funk, *Science*, 2001, **294**, 1871. (b) D. Mozaffarian, M. B. Katan, A. Ascherio, M. J. Stampfer and W. C. Willett, *N. Engl. J. Med.*, 2006, **354**, 1601-1613.
14. L. Zhang, P. Li, X. Sun, X. Wang, B. Xu, X. Wang, F. Ma, Q. Zhang and X. Ding, *J. Agric. Food Chem.*, 2014, **62**, 8745-8751.
15. S. Pramanik, S. Bhandari, U. N. Pan, S. Roy and A. Chattopadhyay, *Small*, 2018, **14**, 1800323.
16. S. Pramanik, S. Roy, A. Mondal and S. Bhandari, *Chem. Commun.*, 2019, **55**, 4331-4334.
17. M. Manna, S. Roy, S. Bhandari and A. Chattopadhyay J. Mater. Chem. C, 2020, **8**, 6972-6976.
18. M. Manna, S. Roy, S. Bhandari and A. Chattopadhyay, *Langmuir*, 2021, **37**, 5506-5512.
19. (a) S. Pramanik, S. Bhandari, S. Roy and A. Chattopadhyay, *J. Phys. Chem. Lett.*, 2015, **6**, 1270-1274. (b) S. Pramanik, M. Manna, B. Hudait, S. Roy, and S. Bhandari, *Phys. Chem. Chem. Phys.*, 2021, **23**, 9860-9866.
20. S. M. Shet, M. Bisht, S. Pramanik, S. Roy, S. Kumar T, S. K. Nataraj, D. Mondal and S. Bhandari, *Adv. Opt. Mater.*, 2020, **8**, 1902022.
21. (a) K. Suga, D. Kondo, Y. Otsuka, Y. Okamoto and H. Umakoshi, *Langmuir*, 2016, **32**, 7606-7612. (b) J. Chen, B. Yang, C. Li, K. Zheng, K. Žídek and T. Pullerits, *ACS Omega*, 2017, **2**, 1922-1929.
22. A. Hildebrand, P. Garidel, R. Neubert and A. Blume, *Langmuir*, 2004, **20**, 320-328.

23. D. Zherebetskyy, M. Scheele, Y. Zhang, N. Bronstein, C. Thompson, D. Britt, M. Salmeron, P. Alivisatos and L.-W. Wang, *Science*, 2014, **344**, 1380.
24. S. Bhandari, S. Pramanik, N. K. Biswas, S. Roy and U. N. Pan, *ACS Appl. Nano Mater.*, 2019, **2**, 2358-2366.
25. H.-C. Pan, F.-P. Liang, C.-J. Mao, J.-J. Zhu and H.-Y. Chen, *J. Phys. Chem. B*, 2007, **111**, 5767-5772.
26. (a) A. Sanz-Medel, R. F. de la Campa and J. I. G. Alonso, *Analyst*, 1987, **112**, 493-497. (b) D. A. Phillips, K. Soroka, R. S. Vithanage and P. K. Dasgupta, *Microchim. Acta*, 1986, **88**, 207-220.
27. (a) L. C. Cass, M. Malicki and E. A. Weiss, *Anal. Chem.*, 2013, **85**, 6974-6979. (b) Y. Wang, L. Jiang, Q. Shen, J. Shen, Y. Han and H. Zhang, *RSC adv.*, 2017, **7**, 41561-41572.
28. E. J. Singh, *J. Chem. Educ.*, 1973, **50**, 669.

Chapter 5

5.1 Summary

The present thesis described three different quantum dot complex (QDC)-based ratiometric visual sensors using a simple complexation reaction on the surface of Mn^{2+}-doped ZnS Qdots with external organic ligands like (i) N-methyl salicylaldimine (MSA), (ii) 8-hydroxyquinoline-5-sulfonic acid (HQS), and (iii) 8-hydroxyquinoline (HQ) for the detection of (i) Hg^{2+} and Cu^{2+}, (ii) phosphate, and (iii) LCUFAs, respectively. All the above-mentioned ratiometric sensors have dual emission properties, one emission from Qdots and the other one from surface complex, which make them suitable for ratiometric applications. In the case of Hg^{2+} and Cu^{2+} detection, the ratiometric sensor QDC (composed of Mn^{2+}-doped ZnS Qdots and MSA**)** exhibited one blue emission at λ_{em} = 430 nm (from surface complex) and another orange emission at λ_{em} = 600 nm (from Qdots). In presence of Hg^{2+} or Cu^{2+} the orange emission had been quenched whereas the blue emission was enhanced resulting in a visual color change from purple to blue (at λ_{ex} = 355 nm). This ratiometric sensor showed high selectivity towards Hg^{2+} and Cu^{2+} ions among other interfering metal ions and a high sensitivity with a LOD of 85.5 nM for Hg^{2+} and 34.9 nM for Cu^{2+}. The second ratiometric sensor i.e., the phosphate sensor exhibited an orange emission at λ_{em} = 585 nm (from Qdots) and a greenish blue emission at λ_{em} = 480 nm (from $Zn(QS)_2$ complex) making the WLE-QDC (composed of Mn^{2+}-doped ZnS Qdots and HQS) an excellent sensor for phosphate detection. In presence of phosphate ions, the greenish blue emission of the QDC had been quenched keeping the orange one unchanged. As a result, a visual color of QDC that changed from white to orange had been observed during phosphate sensing. The WLE-QDC ratiometric sensor responded selectively towards phosphate ions among other ions normally present in environmental water. The LOD was found to be 5.9 nM, which proved the high sensitivity of the sensor towards phosphate. Furthermore, the ratiometric sensor successfully displayed its detection ability in environmental water samples also. In the third ratiometric sensor (composed of Mn^{2+}-doped ZnS Qdots and HQ), a green emission at λ_{em} = 512 nm (from ZnQ_2 complex) and an orange emission at λ_{em} = 590 nm (from Qdots) together made the sensor a WLE nanoprobe. Simultaneous turn-on photoluminescence and blue-shift of the emission maximum were observed with respect to green emission in the presence of LCUFAs while the orange emission remained

unchanged in the same condition. As a result, a visual color change from white to cyan had been observed during the detection of LCUFAs. This current ratiometric sensor selectively responded towards LCUFAs among some common unsaturated fatty acids, saturated fatty acids, amino acids, and cations with a LOD of 0.127, 0.126, and 0.103 μM for sodium salt of oleic acid, linoleic acid, and erucic acid, respectively. Furthermore, the current ratiometric sensor accurately measured the concentration of spiked LCUFAs in saponified daily-used vegetable oils such as sunflower, edible, and soybean oils. The fabrication of different dual emitting/WLE ratiometric sensors using simple complexation reactions on the surface of Qdots helped to accurately detect environmental pollutant ions, major components of commercialized fertilizers, and vegetable oils.

5.2 Future Prospects

The present thesis will guide in the path of fabricating non-toxic Qdot-based ratiometric sensors to detect various types of molecules. The proposed concept of ratiometric sensing may be designed to further detect pesticides, amino acids, nucleic acids, explosives, gas that are usually dissolved in water, etc. This may lead us towards the advancement of portable, cost-effective, and environment-friendly sensing devices for visual detection of environmental pollutants, various molecules that are responsible for human diseases, the molecules which dictate the quality of our daily life, food products, important biomolecules, and toxic explosives, etc. Nowadays, the multi-analyte optical sensor is getting more priority to explore, which may be possible using QDC. Thus, researchers can try to design a suitable complex on the surface of Qdots in order to make QDC-based multi-analyte ratiometric visual sensors. Naked eye detection of the above-mentioned molecules/ions by QDC-based ratiometric sensors will bring a new paradigm towards developing sensing technology and unravelling the chemistry of ratiometric sensors as well as the surface chemistry of quantum dots.

Appendix

A.2: Chapter 2

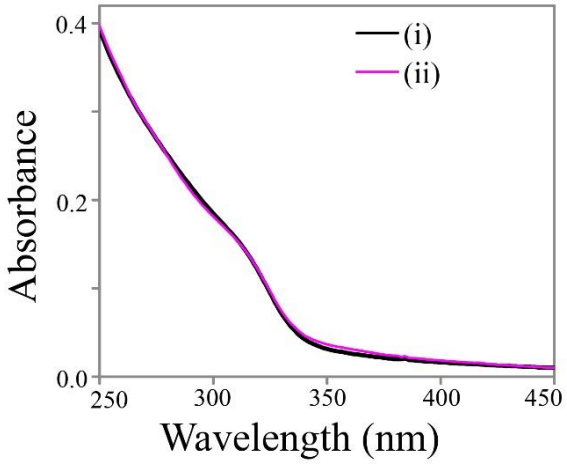

Fig. A.2.1 UV-vis absorption spectra of (i) Mn^{2+} doped ZnS Qdots and (ii) the dual-emitting QDC.

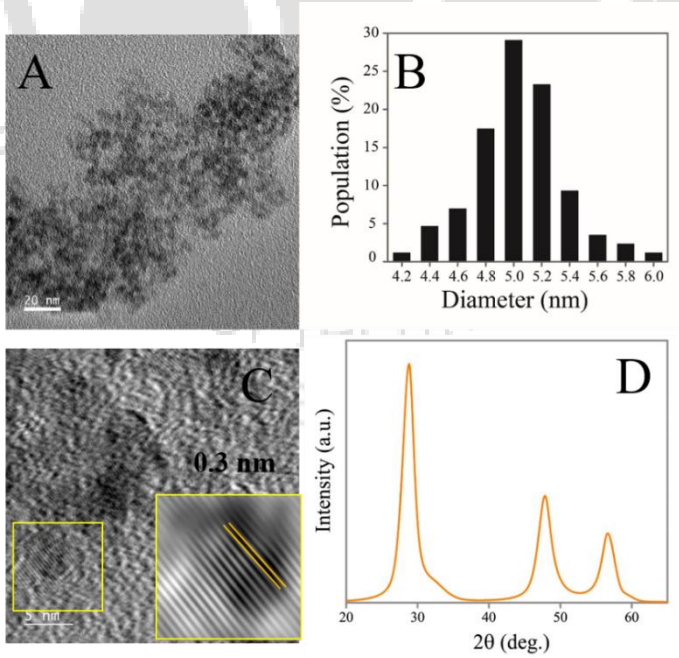

Fig. A.2.2 (A) Transmission electron microscopy (TEM) image (scale bar-20 nm), **(B)** particle size distribution, **(C)** high resolution TEM image (scale bar = 5 nm) and corresponding inverse fast Fourier transformed image (inset), and **(D)** powder X-ray diffraction (XRD) pattern of Mn^{2+} doped ZnS Qdots.

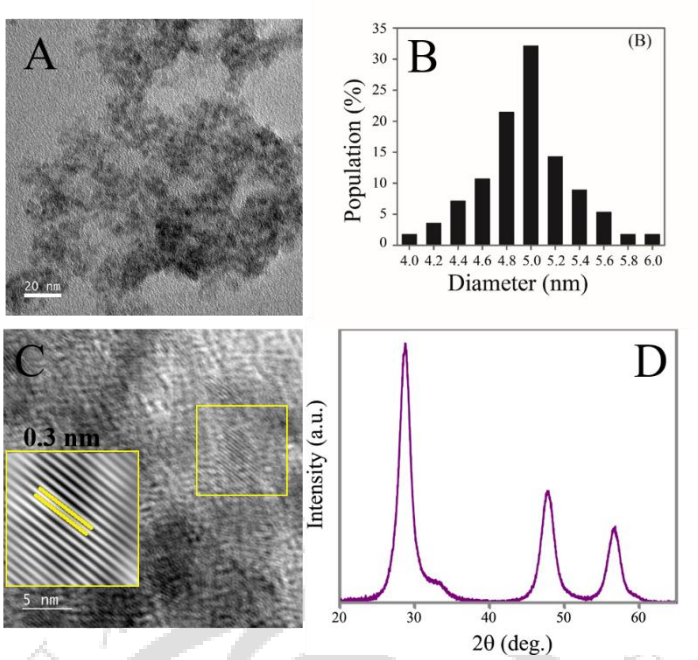

Fig. A.2.3 (A) Transmission electron microscopy (TEM) image (scale bar = 20 nm), **(B)** particle size distribution, **(C)** high resolution TEM image (scale bar = 5 nm) and corresponding inverse fast Fourier transformed image (inset), and **(D)** powder X-ray diffraction (XRD) pattern of the dual-emitting QDC.

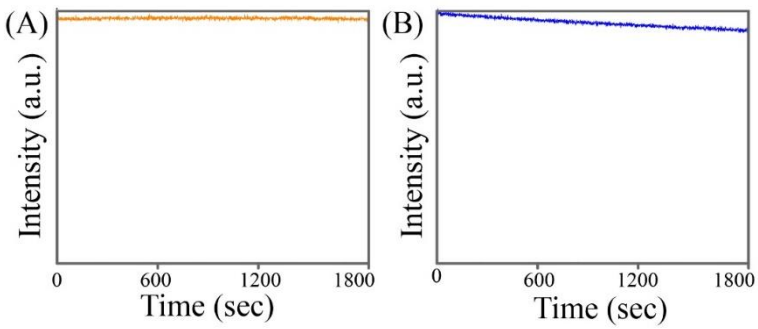

Fig. A.2.4 Photostability results of the dual-emitting QDC as monitored by the variation of intensity (Y-axes) with time with respect to emission maxima at (A) 600 nm and (B) 430 nm.

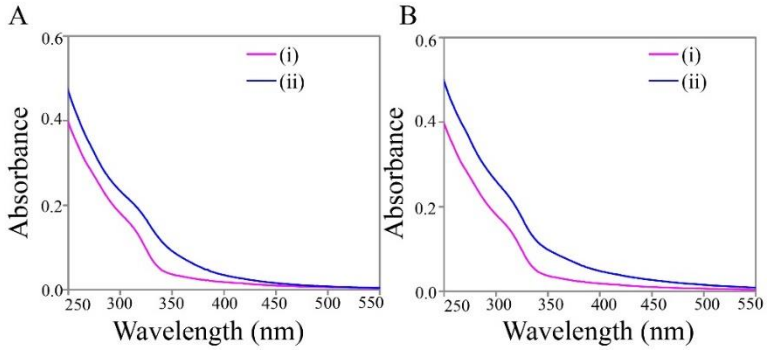

Fig. A.2.5 UV-vis absorption spectra of QDC **(A)** (i) in absence and (ii) presence of Hg^{2+} and **(B)** (i) in absence and (ii) presence of Cu^{2+} ions.

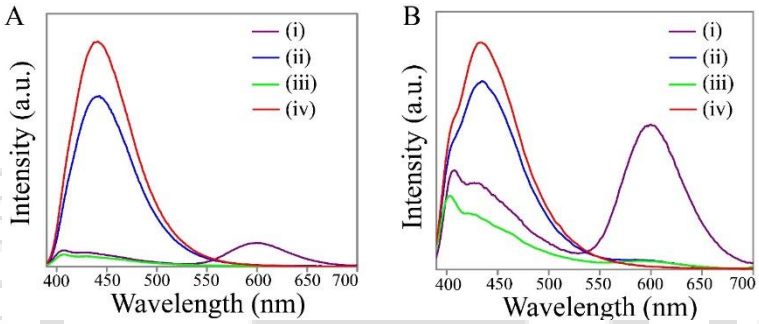

Fig. A.2.6 (A) Emission spectra (λ_{ex} = 355 nm) of (i) QDC and (ii) Hg^{2+} ion added dual-emitting QDC before centrifugation, (iii) the pellet obtained after centrifugation and redispersion into same amount of solvent and (iv) of the supernatant after centrifugation. **(B)** Emission spectra (λ_{ex} = 355 nm) of (i) QDC and (ii) Cu^{2+} ion added dual-emitting QDC before centrifugation, (iii) the pellet obtained after centrifugation and redispersion into same amount of solvent and (iv) of the supernatant after centrifugation.

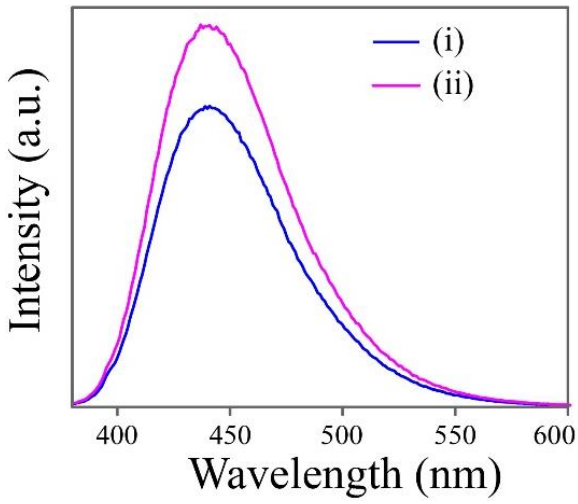

Fig. A.2.7 Emission spectra of MSA in (i) absence and (ii) presence of Zn^{2+} ions.

Table A.2.1 Tabulated form of the comparison of different optical nanoprobes for ratiometric sensing of Hg^{2+} and Cu^{2+} ions.

Ref. No.	*Used optical nanoprobe*	*Detected ion*	*Linear range/LOD*	*Advantages*	*Disadvantages*
This Work	Dual emitting QDC	Hg^{2+} Cu^{2+}	0.67-3.33 µM/ 85.5 nM 0.67-5.33 µM/ 34.9 nM	Ratiometric (I_{430}/I_{600}), luminescence color, chromaticity and hue based detection of Hg^{2+} and Cu^{2+} ions	-----
*J. Hazard. Mater. 2019, **367**, 437.*	Au-Ag NCs	Cu^{2+} Hg^{2+}	20-600 nM/7 nM 20-2000/ 5 nM	Ratiometric detection	Expensive and complicated fabrication
*Sens. Actuators B Chem. 2017, **245**, 386.*	CD/CD conjugates	Cu^{2+} Hg^{2+}	0–3.2 µM/0.05 µM 0–8.5 µM/0.08 µM	Ratiometric detection	Non-radiative energy transfer and complicated fabrication
*Anal. Bioanal. Chem. 2017, **409**, 6655.*	CDs mixed with CdTe/CdS QDs	Cu^{2+}	0-2.5 µM/ 38 nM	Ratiometric detection	Toxicity and Non-radiative energy transfer
*ACS Appl. Mater. & Interfaces, 2014, **6**, 21270.*	C-NP and rhodamine B dye hybrid	Hg^{2+}	0-6 µM /45 nM	Ratiometric detection	Toxicity and Non-radiative energy transfer
*Chem. Commun. 2018, **54**, 4955.*	Coumarin derivatives	Hg^{2+}	0–5 mM/ 27 nM	Ratiometric detection	Toxicity and complicated fabrication

A.3: Chapter 3

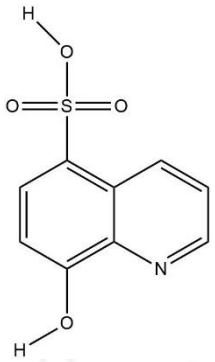

Fig. A.3.1 The molecular structure of 8-hydroxyquinoline-5-sulphonic acid (HQS).

Table A.3.1 Tabulated form of the comparison of ratiometric optical sensors for ratiometric and visual sensing of phosphate.

Ref. No.	Used optical nanoprobe	Linear range/LOD	Advantages
This work	White light emitting quantum dot complex (WLE QDC)	0-82.6 nM / 5.9 nM	Ratiometric, luminescence color, chromaticity and hue based detection of phosphate
J. Mater. Chem. C, 2020, 8, 13063-13071.	Lanthanide coordination polymers (NH_2-BDC–TbGMP CPs)	0.5 to 100 µM/ 0.13 µM	Ratiometric detection
Nanoscale, 2020, **12**, 19383-19389.	Tri-functional Fe-Zr bi-metal–organic frameworks (MOF)	0.2–266.7 µM/ 85 nM	Ratiometric detection
Anal. Chem., 2020, **92**, 3722-3727.	Porphyrin-based NMOF, PCN-224	0−10 µM/ 54 nM	Ratiometric detection
Sens. Act. B, 2020, **321**, 128546.	Ce-Zr bimetal-organic frameworks	3.3-666.7 µM/ 1.1 µM	Ratiometric detection
Anal. Chim. Acta, 2020, **1133**, 11-19.	Dual-functional lanthanide MOFs CIP-Eu^{3+} complex	100-250 µM/ 4.4 nM	Ratiometric detection
Appl. Surf. Sci., 2018, **459**, 686-692.	Rhodamine B (RhB), incorporated Zr-based MOF, UiO-66-NH_2	80-400 µM/ 2.0 µM	Ratiometric detection
Anal. Chem., 2015, **87**, 11455-11459.	AgNCs/MOF	1-100 µM/ 0.06 µM	Ratiometric detection
J. Fluores., 2017, **27**, 227-233.	Ag_2S QDs/MOF	0.7–4.2 µM/ 0.006 µM	Ratiometric detection
Sens. Act. B, 2019, **298**, 126891.	AuNCs- 8-hydroxyquinoline-5-sulfonate-Mg^{2+} composite	0-50 µM / 0.14 µM	Ratiometric detection

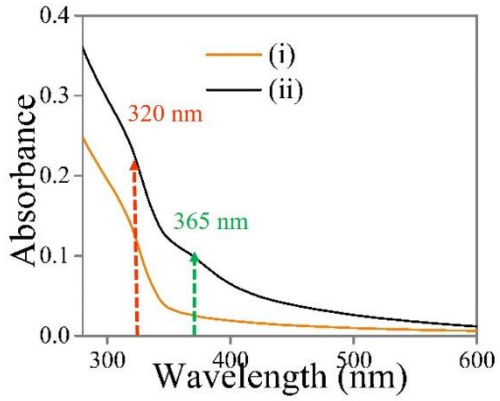

Fig. A.3.2 UV-vis absorption spectra of (i) Mn^{2+} doped ZnS Qdots and (ii) WLE QDC.

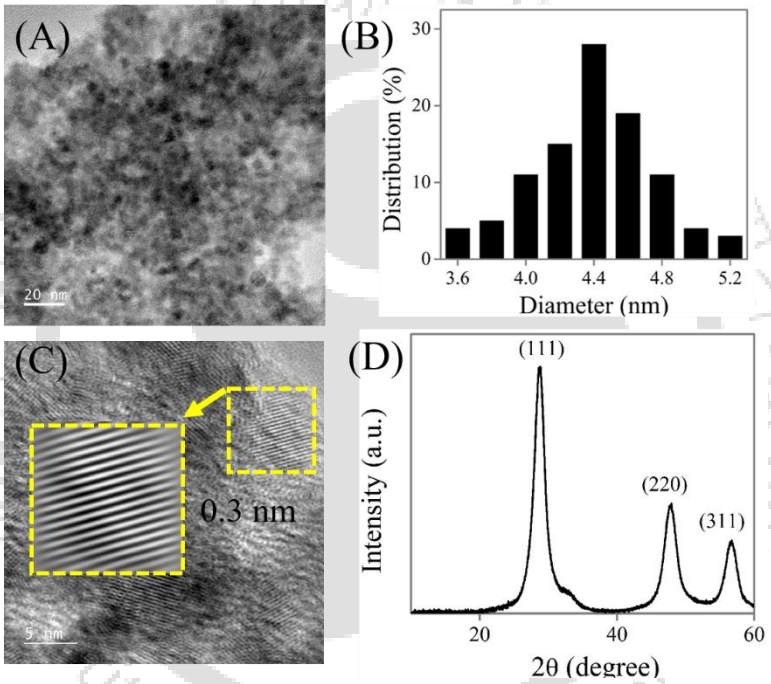

Fig. A.3.3 (A) Transmission electron microscopy (TEM) image (scale bar = 20 nm), **(B)** particle size distribution, **(C)** high resolution TEM image (scale bar = 5 nm) and corresponding inverse fast Fourier transformed image (inset), and **(D)** powder X-ray diffraction (XRD) pattern of Mn^{2+} doped ZnS Qdots.

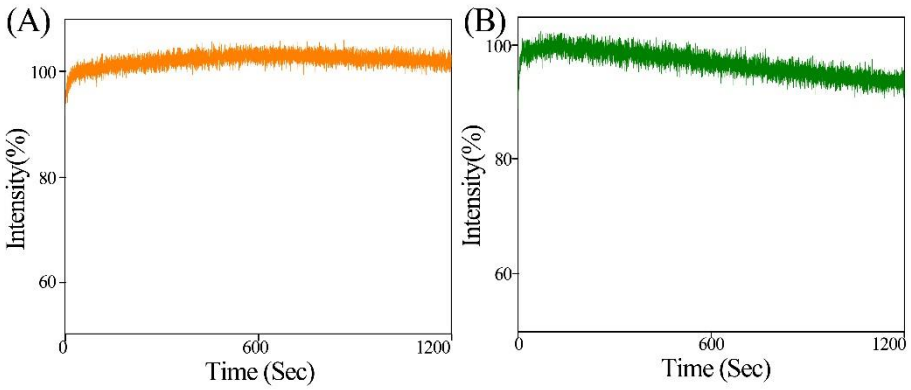

Fig. A.3.4 Photostability of WLE QDC as observed by the variation of luminescence intensity with time with regard to emission maxima at (A) 585 and (B) 480 nm.

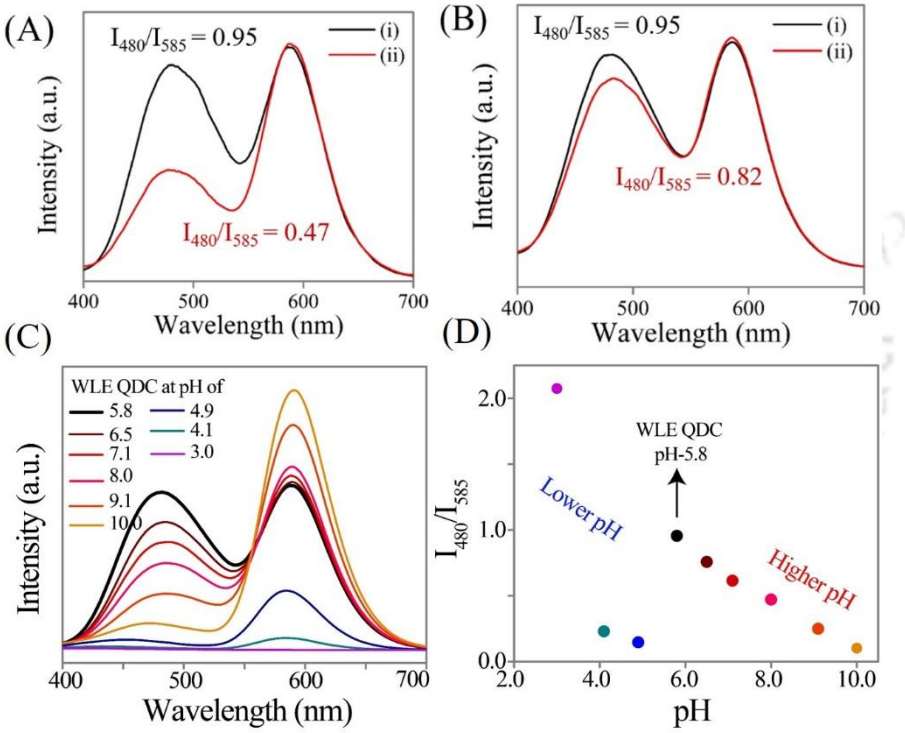

Fig. A.3.5 (A) Emission spectra (λ_{ex} = 335 nm) of WLE QDC (having absorbance of 0.18 at 335 nm) (i) before and (ii) after addition of 20 µL of 0.1 mM of Na_3PO_4. The WLE QDC showed pH of 5.8 while pH of 6.4 was observed Na_3PO_4 added WLE QDC. **(B)** Emission spectra (λ_{ex} = 335 nm) of (i) WLE QDC (pH-5.8), (ii) WLE QDC recorded following adjustment of pH from 5.8 to 6.4. **(C)** Emission spectra (λ_{ex} = 335 nm) and **(D)** alterations in photoluminescence intensity ratio (I_{480}/I_{585}) of WLE QDC at different pH of the medium (in the range of 3-10).

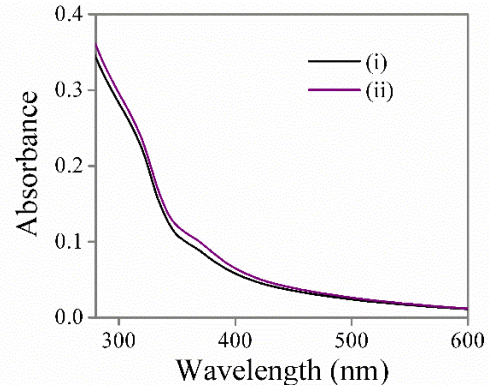

Fig. A.3.6 UV-vis absorption spectra of WLE QDC (i) in absence and (ii) presence of phosphate.

Table A.3.2 Tabulated % changes in intensity ratio (I_{480}/I_{585}) of WLE QDC in presence of interfering ions.

Interfering Substances	% changes in intensity ratio (I_{480}/I_{585}) of WLE QDC	Interfering Substances	% changes in intensity ratio (I_{480}/I_{585}) of WLE QDC
Blank	00.00	SO_4^{2-}	16.54
NaH_2PO_4	61.31	$S_2O_3^{2-}$	31.56
F^-	-0.19	CH_3COO^-	20.13
Br^-	1.77	$C_2O_4^{2-}$	12.23
Cl^-	-5.45	Na^+	-4.55
I^-	-1.91	K^+	-0.04
NO_2^-	-1.06	Ca^{2+}	0.44
NO_3^-	-2.87	Mg^{2+}	-1.63

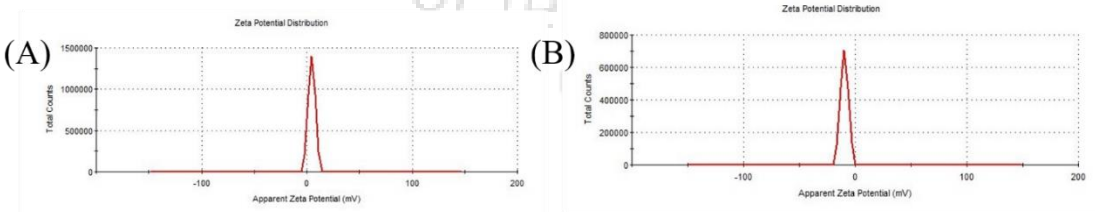

Fig. A.3.7 Zeta potential curves of WLE QDC in **(A)** absence and **(B)** presence of phosphate.

Table A.3.3 Tabulated form of zeta potentials of (i) WLE QDC and (ii) WLE QDC following addition of phosphate.

	Samples	Zeta potential (mV)
(i)	WLE QDC	+4.8
(ii)	Phosphate added WLE QDC	-10.6

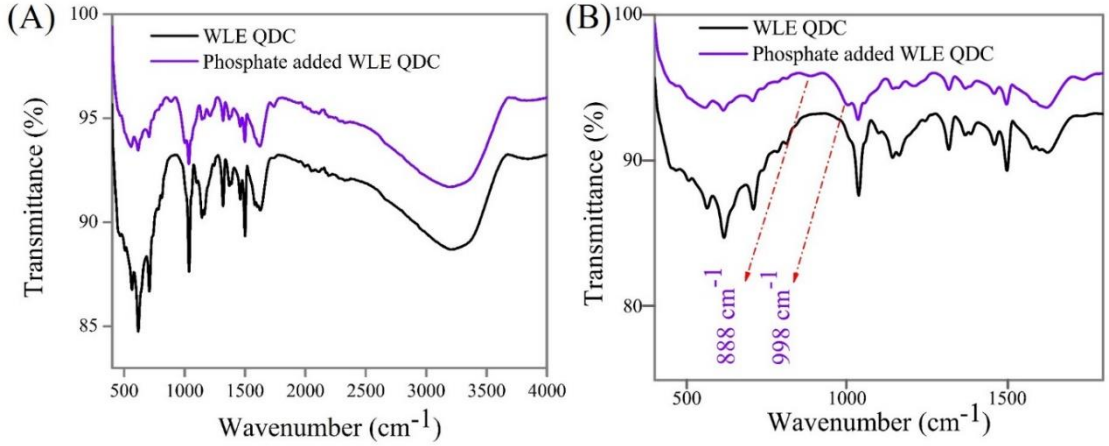

Fig. A.3.8 (A) FTIR spectra of WLE QDC and phosphate added WLE QDC. **(B)** FTIR spectra of WLE QDC and phosphate added WLE QDC in the range of 400-1700 cm^{-1}.

Table A.3.4 Tabulated form of the peaks against possible functional groups in the FTIR spectra in Fig. A.3.8.

Wave number (cm^{-1})	Functional Groups	Ref.
888	O–P asymmetric stretching /$P(OH)_2$ symmetric stretching (A_1), P-OH stretching	*Phys. Chem. Chem. Phys.*, 2019, **21**, 4421-4434.
998	O–P–O symmetric stretching and asymmetric with O_{nb}	

The presence of phosphate in the WLE QDC was verified by observing the characteristics peaks of phosphate in the FTIR spectra of phosphate added WLE QDC (following centrifugation). The new peaks at 888 cm^{-1} (due to O–P asymmetric stretching /$P(OH)_2$ symmetric stretching (A1), P-OH stretching) and 998 cm^{-1} (due to O–P–O symmetric stretching and asymmetric with O_{nb}) – in addition to peaks of the functional groups of $Zn(QS)_2$ complex – appeared when phosphate was reacted with WLE QDC. This clearly demonstrated the incorporation of phosphate on the surface of WLE QDC.

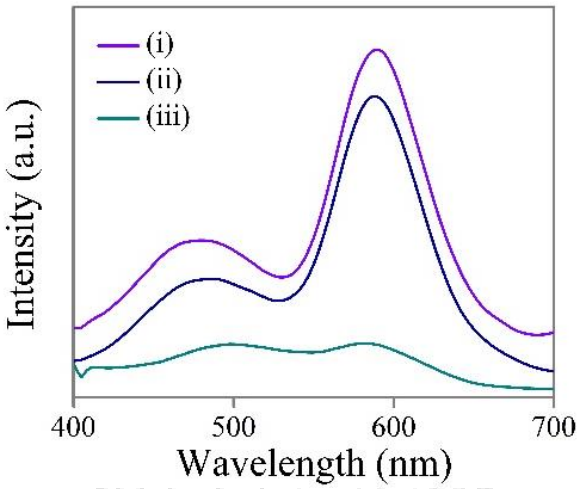

Fig. A.3.9 Emission spectra (λ_{ex} = 335 nm) of (i) phosphate added WLE QDC before centrifugation, (ii) the pellet obtained following centrifugation and redispersion into same amount of water and (iii) of the supernatant following centrifugation.

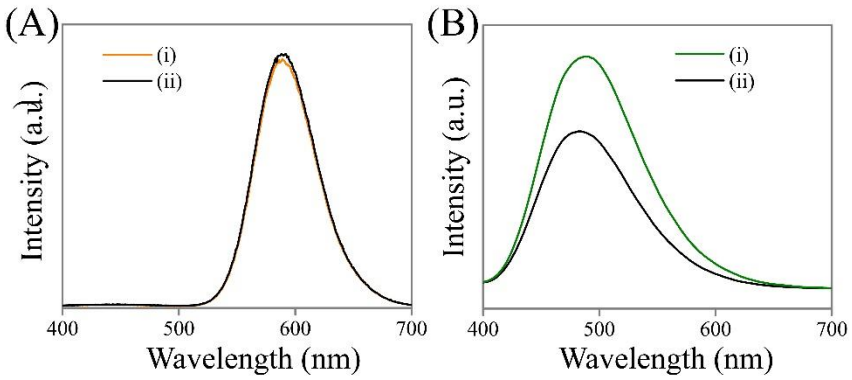

Fig. A.3.10 (A) Emission spectra (λ_{ex} = 335 nm) of Mn^{2+}- doped ZnS Qdots (i) before and (ii) after phosphate addition. **(B)** Emission spectra (λ_{ex} = 335 nm) of $Zn(QS)_2$ attached ZnS Qdots (i) before and (ii) after addition of phosphate.

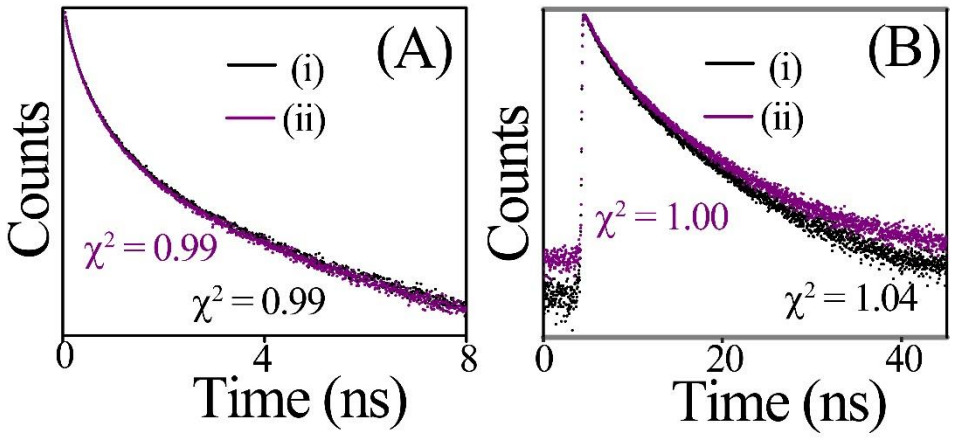

Fig. A.3.11 (A) Time-resolved photoluminescence spectra (λ_{ex} = 330 nm) of WLE QDC monitored at 585 nm (i) before and (ii) after addition of phosphate. The decay curves were fitted with tri-exponential function. **(B)** Time-resolved photoluminescence spectra (λ_{ex} = 375 nm laser) of WLE QDC monitored at 480 nm (i) before and (ii) after addition of phosphate. The decay curves were fitted with tri-exponential function.

Table A.3.5 Tabulated form of the average life times monitored at **(A)** 585 and **(B)** 480 nm of (i) WLE QDC and (ii) WLE QDC following addition of phosphate.

(A) Samples at λ_{em} = 585 nm	α_1 (%)	τ_1 (ms)	α_2 (%)	τ_2 (ms)	α_3 (%)	τ_3 (ms)	τ_{av} (ms)	χ^2
(i) WLE QDC	36.73	0.05	50.18	0.30	13.09	1.48	0.91	0.99
(ii) WLE QDC + Phosphate	36.62	0.07	50.78	0.32	12.60	1.53	0.92	0.99
(B) Samples at λ_{em} = 480 nm	α_1 (%)	τ_1 (ns)	α_2 (%)	τ_2 (ns)	α_3 (%)	τ_3 (ns)	τ_{av} (ns)	χ^2
(i) WLE QDC	18.05	1.49	48.87	4.77	33.08	11.52	8.65	1.00
(ii) WLE QDC + Phosphate	15.64	1.51	46.38	4.59	37.98	10.99	8.56	1.04

The decay profiles were fitted to a multi-exponential model based on the use of following equation

$$I(t) = \sum_i \alpha_i \exp\left(-t/\tau_i\right) \qquad (1)$$

Where, tri exponential functions were used to fit respective decay curve with obtaining χ^2 close to 1.0. The averaged life times (τ_{av}) in Table A.3.5, determined from the results of three exponential model using

$$\tau_{av} = \frac{\sum_i \alpha_i \tau_i^2}{\sum_i \alpha_i \tau_i} \qquad (2)$$

Where, α_i and τ_i are the pre-exponential factors and excited-state luminescence decay time associated with the *i*-th component, respectively. The respective decay curve was fitted with a tri-exponential function. It is to be mentioned here that although there are slight changes in the respective life times (τ_1, τ_2 and τ_3) of three components (α_1, α_2 and α_3) of WLE QDC in presence of phosphate; however the average life time (τ_{av}) of WLE QDC did not show any significant change in presence of phosphate.

A.4: Chapter 4

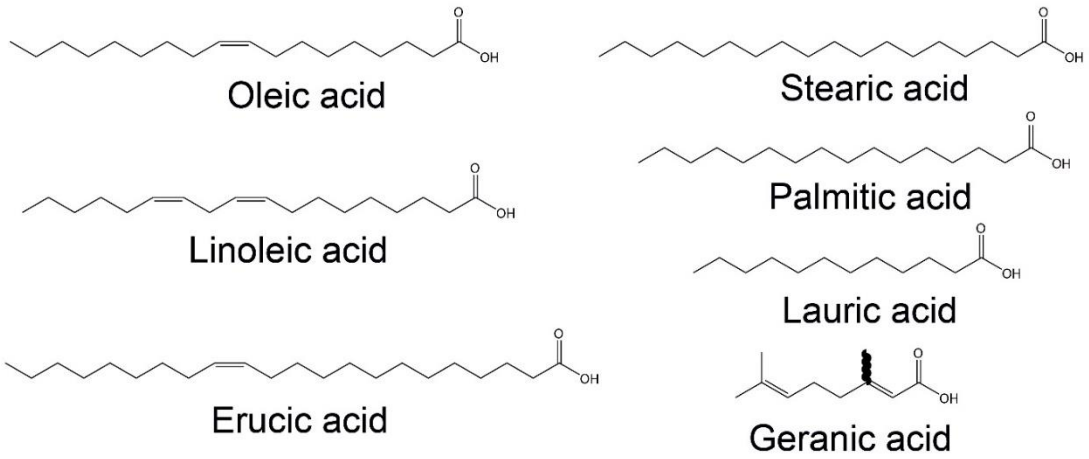

Fig. A.4.1 The molecular structures of the unsaturated and saturated fatty acids that have been used for experiments reported in this work.

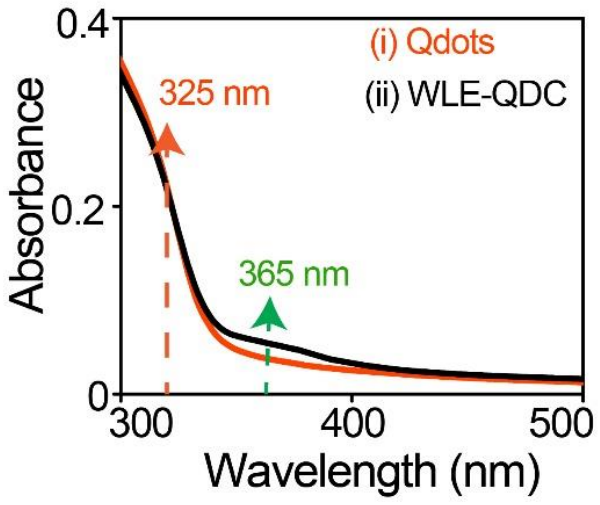

Fig. A.4.2 UV-vis spectra of (i) Qdots and (ii) WLE-QDC.

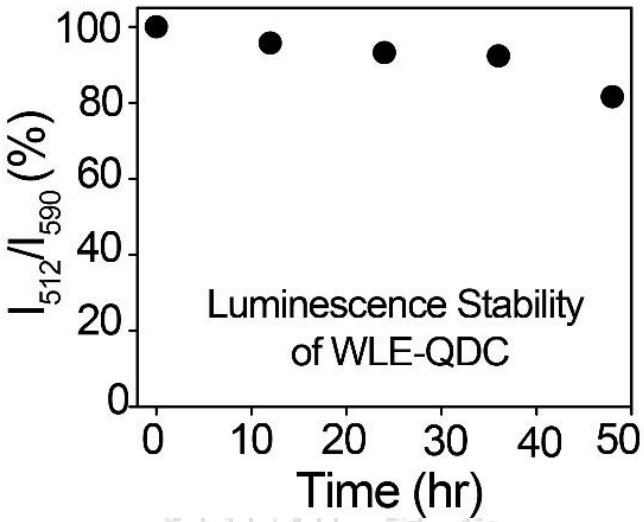

Fig. A.4.3 Time dependent luminescence stability of WLE-QDC (in water). The stability of WLE−QDC in terms of the emission intensity ratio (I_{512}/I_{590}) at different time intervals (upto 48 h) in a water medium was monitored at an excitation wavelength of 357 nm.

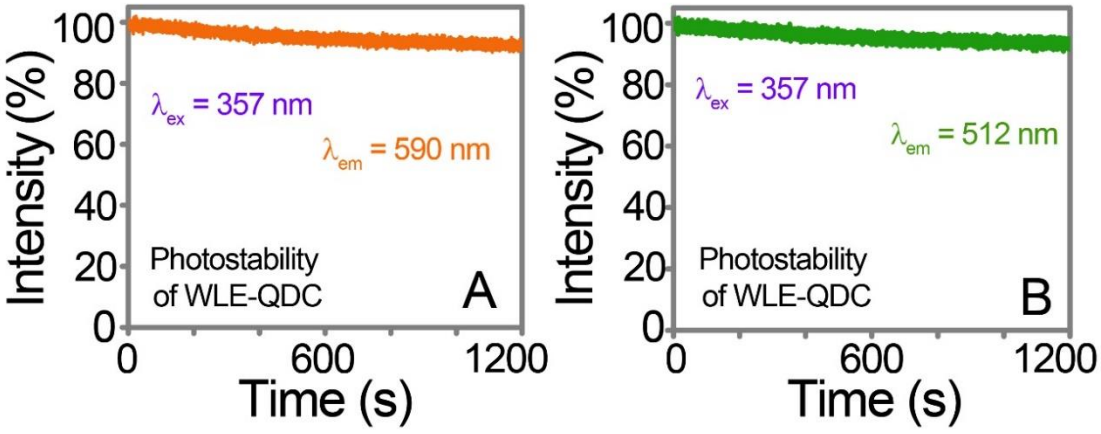

Fig. A.4.4 Photostability of WLE-QDC (in water) with regard to λ_{em} at (A) 590 and (B) 512 nm. The photostability of WLE-QDC was monitored under a continuous irradiation of 357 nm light for 20 minutes and with respect to emission maxima of Qdots (590 nm) and surface ZnQ_2 complex (512 nm).

Table A.4.1 Tabulated form of the photoluminescence intensity ratios and chromaticity values of WLE-QDC following the addition of different amount of oleate. The data were extracted from Fig. 4.2 (Chapter 4).

Conc. of Oleate (μM)	I_{480}/I_{590}	Chromaticity	
		CIE-X	CIE-Y
a) 0	0.93	0.33	0.43
b) 4.2	1.74	0.28	0.40
c) 8.3	2.32	0.26	0.38
d) 12.4	2.73	0.25	0.37
e) 16.6	3.07	0.24	0.36
f) 20.7	3.29	0.23	0.35
g) 24.8	3.52	0.23	0.35
h) 32.9	3.75	0.22	0.34
i) 41.0	3.94	0.22	0.33
j) 49.0	4.06	0.22	0.33
k) 57.0	4.20	0.21	0.33
l) 64.9	4.32	0.21	0.32
m) 80.6	4.39	0.21	0.32

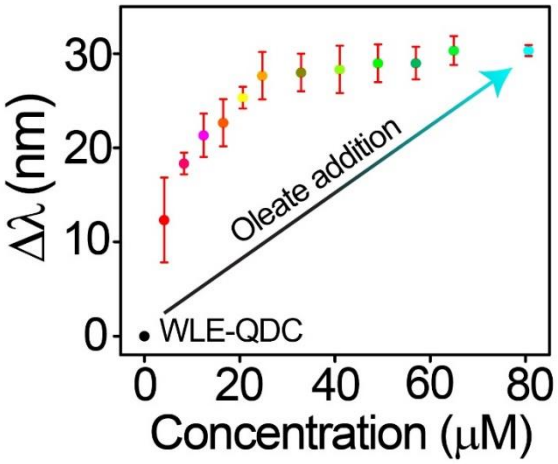

Fig. A.4.5 Change in λ_{max} (at 512 nm) of WLE-QDC with increasing concentration of oleate in the range of 0.0-80.6 μM.

Table A.4.2 Tabulated form of the comparison of (A) recognition systems and (B) optical sensors for recognition and ratiometric visual sensing of long chain unsaturated fatty acids.

(A) References for Recognition	Used Recognition Probes	Selective Recognition Ability	Analytical Method Used
This work	White light emitting quantum dot complex (WLE-QDC)	Long chain unsaturated fatty acids (LCUFAs; e.g. Na-salt of oleic acid) from their corresponding saturated forms (Na-salt of stearic acid)	Fluorescence
Angew. Chem., Int. Ed., 2020, **59**, 10489-10492.	Polyaromatic receptor	Oleic acid over stearic acid	NMR + Mass
Proc. Natl. Acad. Sci. U. S. A., 2015, **112**, 11181-11186	Cavitand receptor	Unsaturated ω-3, -6, and -9 fatty acids	NMR
Chem. Commun., 2019, **55**, 11695-11698.	Polyaromatic molecular tube	Oleic acid methyl ester (cis-5c)	NMR
Nat. Commun., 2014, **5**, 5179.	Supramolecular nano-capsule	Molecular protection of C18 fatty acid methyl esters	NMR
Proc. Natl. Acad. Sci. U. S. A., 2010, **107**, 21424.	Ubxd8 membrane protein	Long chain unsaturated fatty acids (Oleate)	Circular dichroism
(B) References for Ratiometric Sensing	Used Optical Probes	Optical Sensing Ability	Analytical Method Used
This work	White light emitting quantum dot complex (WLE-QDC)	Ratiometric visual detection, with a detection limit of 0.127 μM in the linear range of 4.2-16.6 μM and its practical utilization in quantification of LCUFAs in commercial vegetable oils (such as sunflower, edible and soybean oils)	Fluorescence
J. Mater. Chem. C, 2016, **4**, 2871-2876.	Polymerized liposome	Colorimetric sensing of oleic acid and linoleic acid in μM scale	Colorimetric response
Nanotechnology, 2018, **30**, 065502.	A multichannel Au nanosensor	Colorimetric sensing of in the oleic acid concentration range of 0.0–10.0 μM	Colorimetric response
J. Am. Chem. Soc., 2004, **126**, 12732-12733.	Calix-naphthalene based molecular tubes	Cis-fatty acids Octanoic acid (1-10 *m*M)	Fluorescence
Anal. Biochem., 2005, **345**, 133-139.	Fluorescent fatty acid binding protein (FABP)	Ratiometric fluorescence sensing of oleic acid in the concentration range of 0.02–4.7 μM	Fluorescence
Chem. Commun., 2009, 7164-7166.	Duplex-pyrene-cyclodextrin based fluorescent sensors	Ratiometric fluorescence sensing of oleic acid in the concentration range of (0–7.0 equiv.)	Fluorescence
Bioconjugate Chem., 2011, **22**, 338-345.	CdSe/ZnSMPA-BSARhod complex	Ratiometric fluorescence sensing of oleic acid in 10–1000 nM scale	Fluorescence

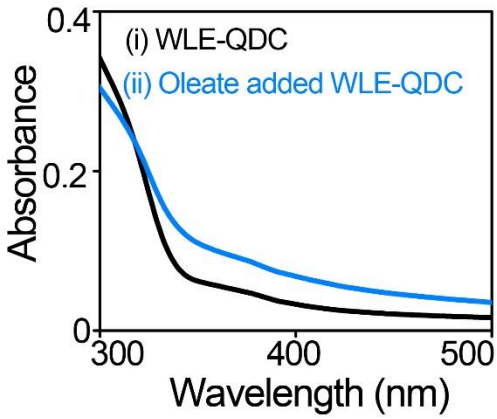

Fig. A.4.6 UV-vis spectra of (i) WLE-QDC and (ii) oleate added WLE-QDC.

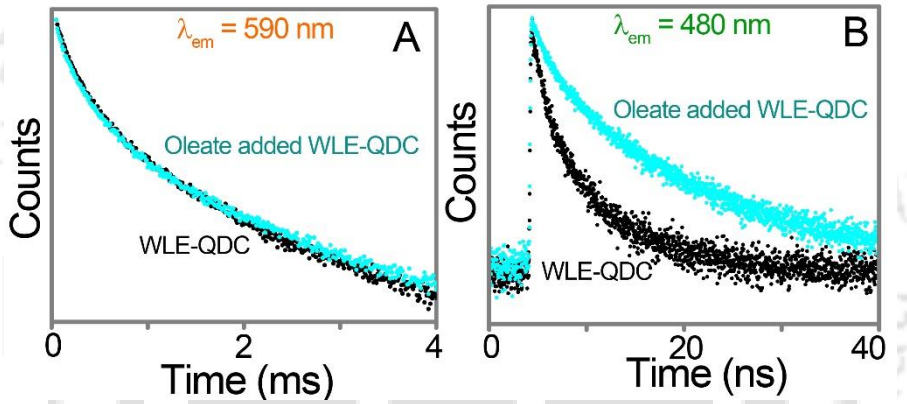

Fig. A.4.7 (A) Time-resolved photoluminescence spectra (λ_{ex} = 330 nm) of WLE-QDC monitored at 590 nm (i) before and (ii) after addition of oleate. (B) Time-resolved photoluminescence spectra (λ_{ex} = 375 nm laser) of WLE-QDC monitored at 480 nm (i) before and (ii) after addition of oleate. The decay curves were fitted with tri-exponential function.

Table A.4.3 Tabulated form of the average life times monitored at **(A)** 590 and **(B)** 480 nm of (i) WLE-QDC and (ii) oleate added WLE-QDC. The data were extracted from Fig. A.4.7, Appendix.

(A) Samples at λ_{em} = 590 nm	α_1 (%)	τ_1 (ms)	α_2 (%)	τ_2 (ms)	α_3 (%)	τ_3 (ms)	τ_{av} (ms)	χ^2
(i) WLE QDC	44.12	0.31	16.74	1.38	39.15	0.09	**0.91**	0.99
(ii) WLE QDC + oleate	56.37	0.26	72.14	0.04	19.93	1.33	**0.90**	0.99
(B) Samples at λ_{em} = 480 nm	α_1 (%)	τ_1 (ns)	α_2 (%)	τ_2 (ns)	α_3 (%)	τ_3 (ns)	τ_{av} (ns)	χ^2
(i) WLE QDC	8.10	0.57	36.74	2.93	55.16	9.47	**8.30**	1.00
(ii) WLE QDC + oleate	10.00	1.30	34.44	5.43	55.56	14.90	**13.00**	1.01

The decay curves were fitted to a multi-exponential model using following equations

$$I(t) = \sum_i \alpha_i \exp\left(-t/\tau_i\right) \qquad (1)$$

The tri exponential functions were applied to fit respective decay curve to acquire χ^2 close to 1.0. The averaged life times (τ_{av}) were determined from the results of three exponential model using

$$\tau_{av} = \frac{\sum_i \alpha_i \tau_i^2}{\sum_i \alpha_i \tau_i} \qquad (2)$$

Where, α_i = pre-exponential factors and τ_i = excited-state luminescence decay time associated with the *i*-th component.

Table A.4.4 Tabulated form of the photoluminescence intensity ratios and chromaticity values of WLE-QDC following the addition of the mixture of stearate and oleate. The data were extracted from Fig. 4.3 (Chapter 4).

Stearate : Oleate	I_{480}/I_{590}	Chromaticity	
		CIE-X	CIE-Y
0:0	0.93	0.33	0.43
1:0	2.19	0.26	0.37
3:1	2.74	0.25	0.36
1:1	3.26	0.23	0.34
1:3	3.50	0.23	0.33
0:1	4.39	0.21	0.32

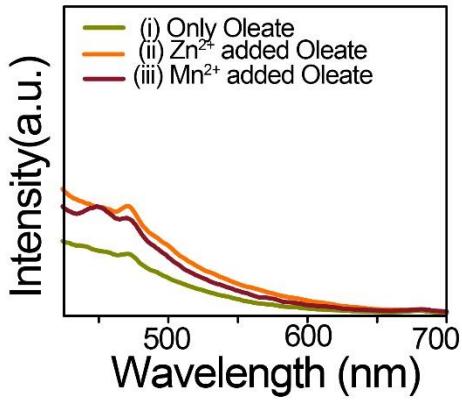

Fig. A.4.8 Emission spectra (λ_{ex}= 357 nm) of (i) oleate (80.6 µM; in water), (ii) Zn^{2+} ions added oleate (iii) Mn^{2+} ions added oleate.

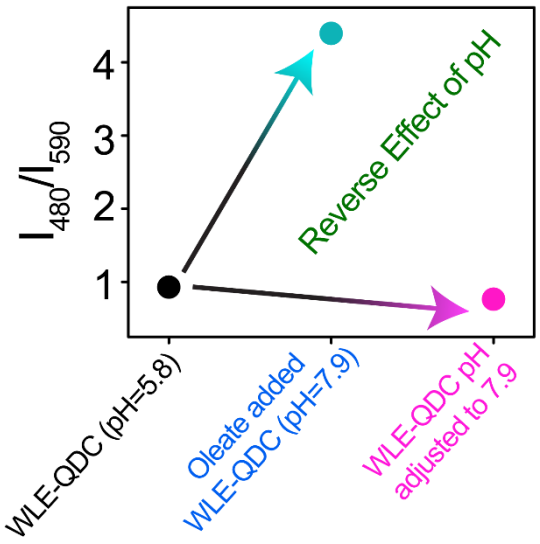

Fig. A.4.9 Change in emission intensity ratio (I_{480}/I_{590}) of (i) WLE QDC (pH= 5.8) (ii) 80.6 µM oleate added WLE-QDC (pH-7.9) and (iii) WLE-QDC adjusted to pH = 7.9 (i.e., the same pH of oleate added WLE-QDC).

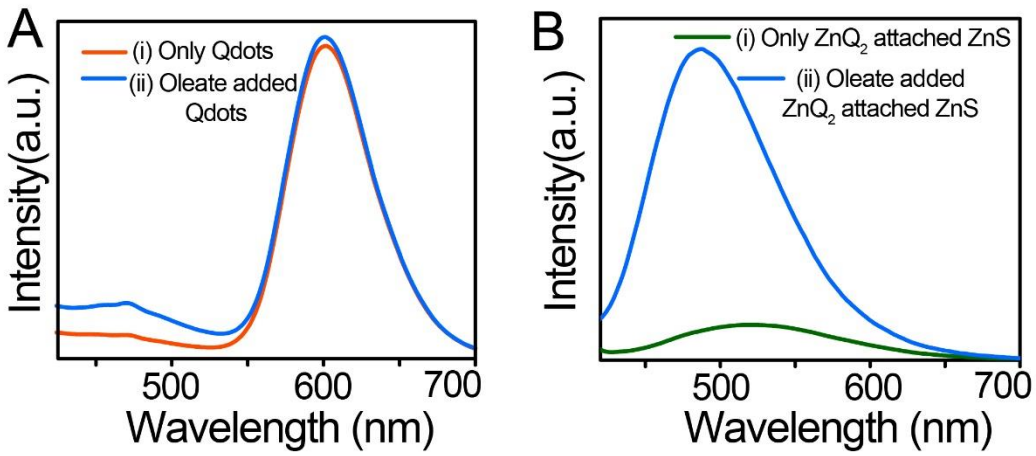

Fig. A.4.10 (A) Emission spectra (λ_{ex}= 357 nm) of the aqueous dispersion of (i) Qdots and (ii) Qdots following addition of 80.6 µM oleate. (B) Emission spectra (λ_{ex}= 357 nm) of (i) ZnQ_2 attached ZnS Qdots and (ii) ZnQ_2 attached ZnS Qdots following addition of 80.6 µM oleate.

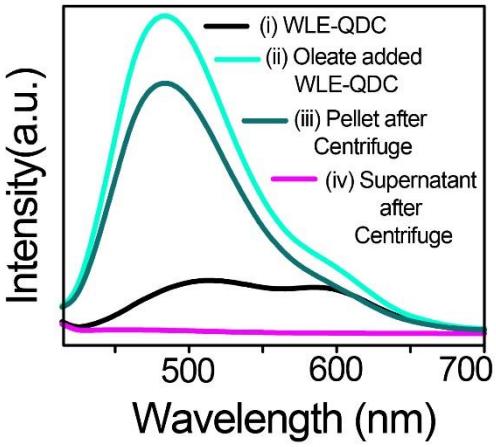

Fig. A.4.11 Emission spectra (λ_{ex} = 357 nm) of (i) WLE-QDC, (ii) 80.6 µM oleate added WLE-QDC before centrifugation, (iii) the pellet obtained following centrifugation and redispersion into same amount of water and (iv) of the supernatant following centrifugation.

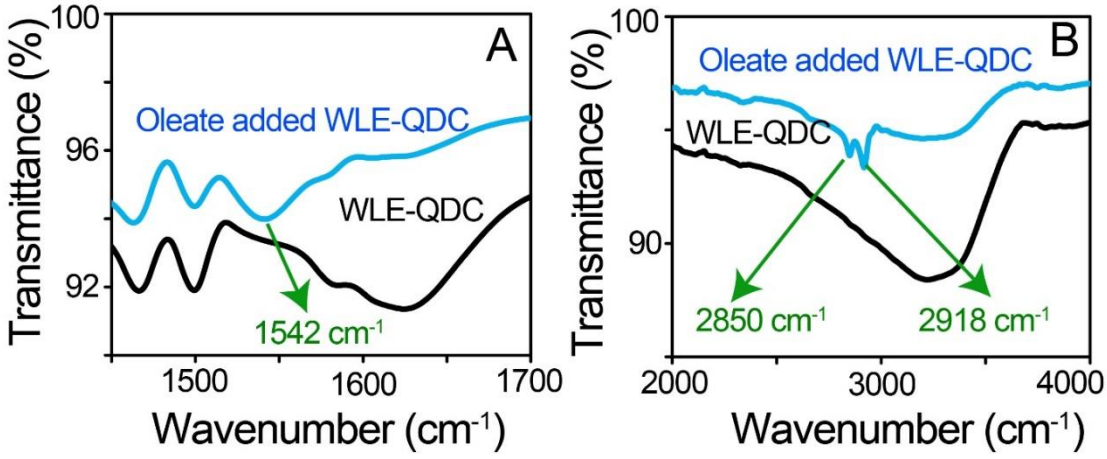

Fig. A.4.12 FTIR spectra of (i) WLE-QDC and (ii) 80.6 µM oleate added WLE-QDC (following centrifugation) in the range of (A) 1450-1700 cm^{-1} and (B) 2000-4000 cm^{-1}.

Table A.4.5 Tabulated form of FTIR peaks of (i) WLE-QDC and (ii) 80.6 µM oleate added WLE-QDC (following centrifugation). The data were extracted from Fig. A.4.12, Appendix.

Wave number (cm^{-1})	Functional Groups	Ref.
2850 & 2918	symmetric & asymmetric stretching of $-CH_2$	(a) *Anal. Chem.*, 2013, **85**, 6974-6979. (b) *RSC adv.*, 2017, **7**, 41561-41572.
1542	asymmetric stretching of COO^-	

The incorporation of oleate on the surface of WLE-QDC was further confirmed by observing their main functional group's characteristic symmetric and asymmetric stretching peaks of -CH_2 (at 2850 and 2918 cm^{-1}) and that of -COO^- (at 1542 cm^{-1}) – along with the main functional groups of ZnQ_2 - in the FTIR spectra of oleate treated WLE-QDC (Fig. A.4.12, Table A.4.5, Appendix**)**. This clearly confirmed the incorporation of oleate on the surface of WLE-QDC.

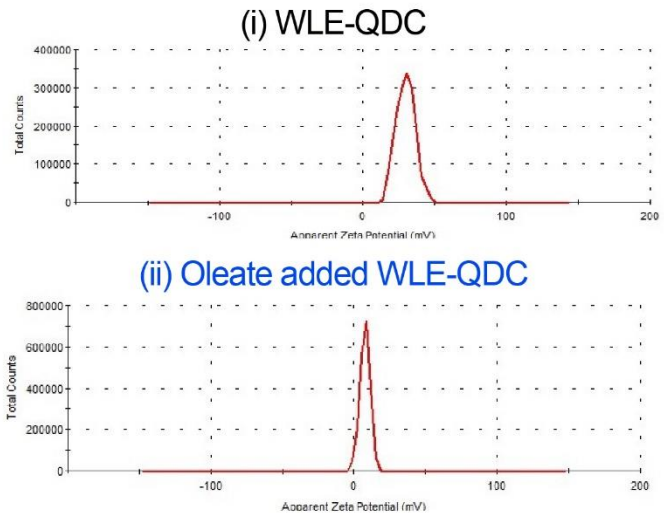

Fig. A.4.13 Zeta potential curves of (i) WLE-QDC and (ii) 80.6 µM oleate added WLE-QDC (following centrifugation).

Table A.4.6 Tabulated form of zeta potentials of (i) WLE-QDC and (ii) 80.6 µM oleate added WLE-QDC (following centrifugation). The data were extracted from Fig. A.4.13, Appendix.

	Samples	Zeta potential (mV)
(iii)	WLE QDC	28.53
(iv)	Oleate added WLE QDC	7.42

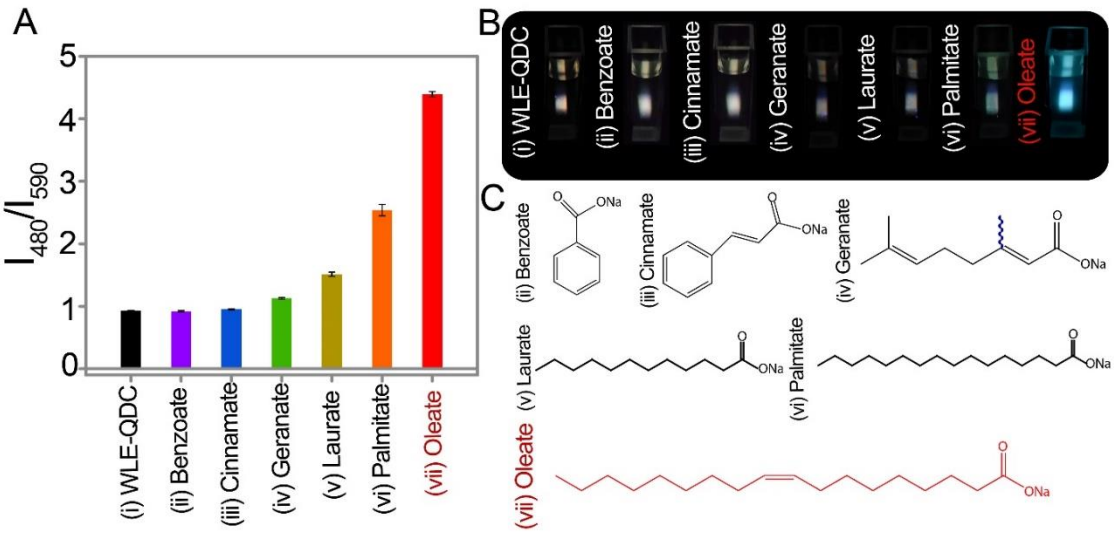

Fig. A.4.14 (A) Bar diagram of the comparison of emission intensity ratio (I_{480}/I_{590}) and **(B)** corresponding photographs (λ_{ex}= 357 nm) of (i) WLE-QDC obtained following addition of (ii) benzoate (80.6 μM, aromatic compound that favours π–π interaction), (iii) cinnamate (80.6 μM; aromatic compound that favours π–π interaction), (iv) geranate (80.6 μM; short chain unsaturated fatty acid that favours π–π interaction), (v) laurate (80.6 μM; medium chain saturated fatty acid that favours hydrophobic interaction), (vi) palmitate (80.6 μM; long chain saturated fatty acid that favours hydrophobic interaction) and (vii) oleate (80.6 μM; long chain unsaturated fatty acid that favours hydrophobic and π–π interaction). Each experiment was performed in triplicate. **(C)** The molecular structures of the Na-salts of benzoate, cinnamate, geranate, laurate, palmitate and oleate that have been used for experiments reported in this work.

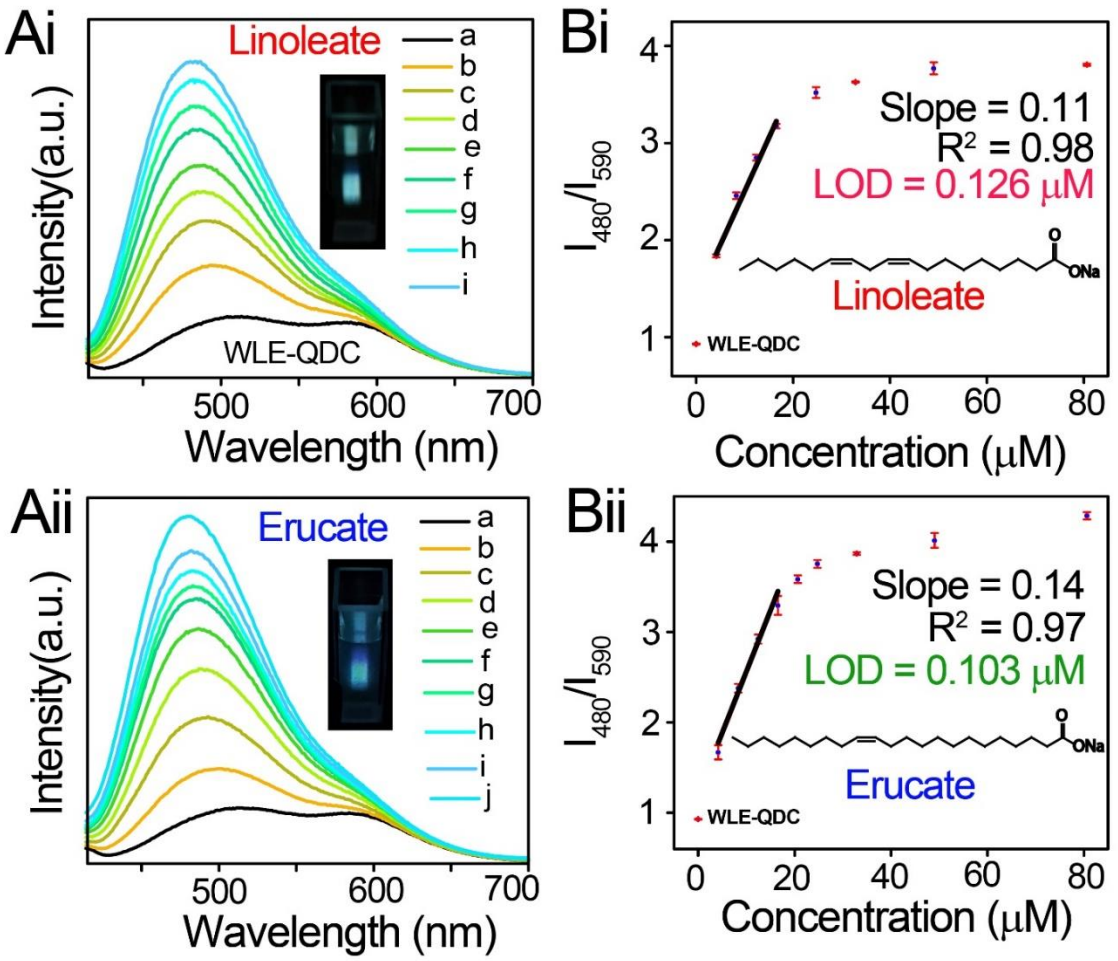

Fig. A.4.15 (A) Emission spectra (λ_{ex}= 357 nm), **(B)** changes in emission intensity ratio (I_{480}/I_{590}) of WLE-QDC noted following addition of different concentrations of (i) linoleate: ((a) 0.0, (b) 4.2, (c) 8.3, (d) 12.4, (e) 16.6, (f) 24.8, (g) 32.9, (h) 49.0 and (i) 80.6 μM) and (ii) erucate ((a) 0.0, (b) 4.2, (c) 8.3, (d) 12.4, (e) 16.6, (f) 20.7, (g) 24.8, (h) 32.9, (i) 49.0 and (j) 80.6 μM). The experiments were carried out in triplicate. A linear relationship between I_{480}/I_{590} of WLE-QDC and concentrations of (i) linoleate or (ii) erucate was used to estimate limit of detection (LOD). The digital photographs of WLE-QDC following addition of linoleate and erucate, which are LCUFAs and has capability of concurrent hydrophobic and π–π interactions similar to oleate. (inset; Fig. A.4.15A, Appendix).

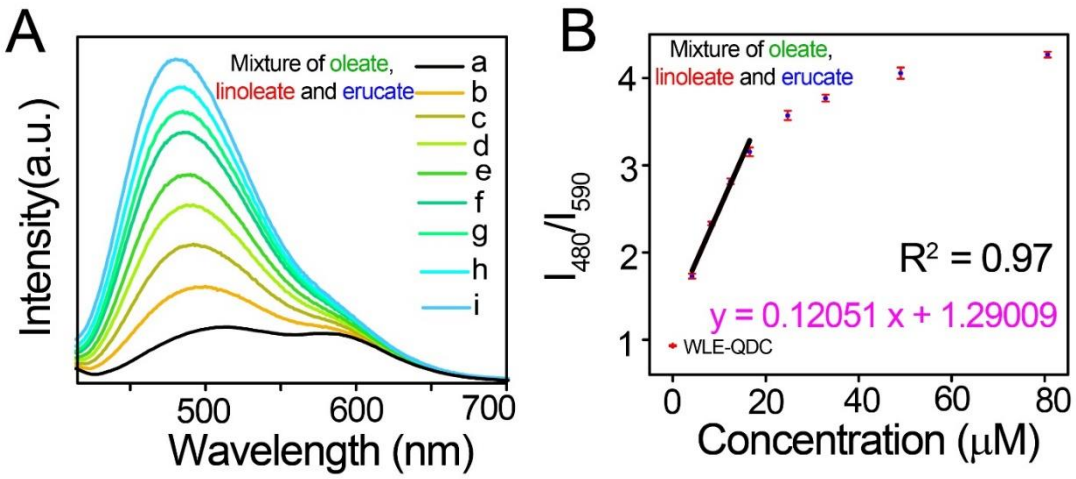

Fig. A.4.16 (A) Emission spectra (λ_{ex}= 357 nm), **(B)** changes in emission intensity ratio (I_{480}/I_{590}) of WLE-QDC noted following addition of different concentrations of equivalent mixture of (i) oleate, (ii) linoleate and (ii) erucate ((a) 0.0, (b) 4.2, (c) 8.3, (d) 12.4, (e) 16.6, (f) 24.8, (g) 32.9, (h) 49.0, (i) 80.6 μM). The experiments were carried out in triplicate. A linear relationship between I_{480}/I_{590} of WLE-QDC and concentrations of equivalent mixture of (i) oleate, (ii) linoleate and (iii) erucate was obtained and used for the quantification of LCUFAs in commercial vegetable oils such as sunflower, edible and soybean oils (Table 4.1 of Chapter 4).

Table A.4.7 Tabulated form of the change in intensity ratio of WLE-QDC following addition of the mentioned interfering substances in Fig. 4.4 (Chapter 4). The data were extracted from Fig. 4.4 (Chapter 4). The Δ (I_{480}/I_{590}) was considered as 100% for oleate added WLE-QDC.

Interfering Substances	Δ (I_{480}/I_{590}) (%)
Oleate	100.00
Linoleate	83.03
Erucate	96.85
Equivalent mixture oleate, linoleate and erucate	96.34
Tartrate	1.12
Geranate	4.13
Laurate	15.29
Fluoride	-0.52
Oxalate	1.57
Palmitate	46.80
Citrate	2.57
Stearate	37.73
Na^+	-0.68
K^+	-0.59
Ca^{2+}	-0.32
Mg^{2+}	-0.33

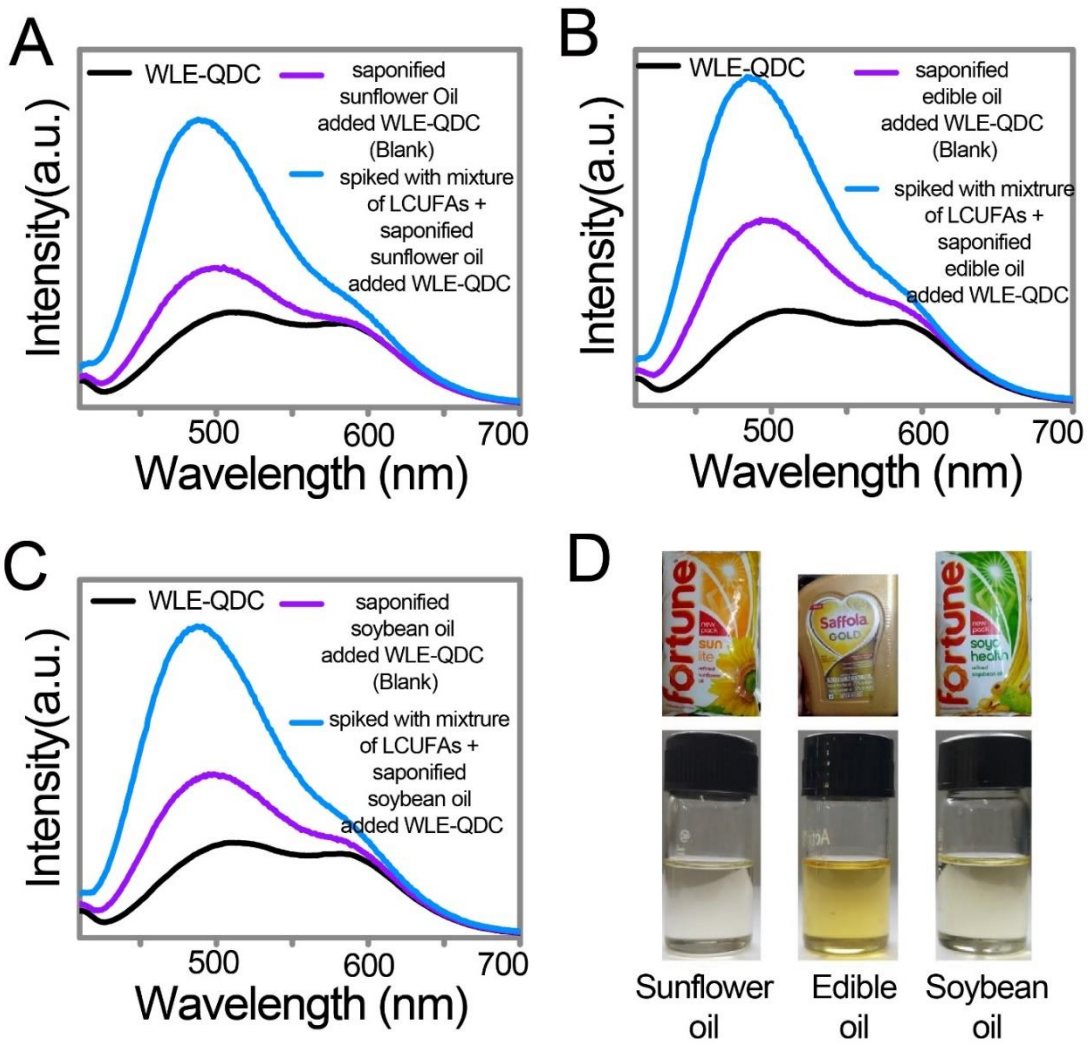

Fig. A.4.17 (A, B & C) Representative emission spectra (λ_{ex}= 357 nm) of WLE-QDC recorded following addition of different concentrations of saponified commercial sunflower, edible and soybean oils, respectively. The extracted concentrations aganist the data from Fig. A.4.17 (A-C) are clearly described and tabulated in Table 4.1 (Chapter 4). **(D)** The digital photographs of the commercial vegetable oils such as sunflower, edible and soybean oils that were used for experiments in this work.

List of Publications

In Peer Reviewed Journals

1. **M. Manna**, S. Bhandari, and A. Chattopadhyay, *J. Mater. Chem. C*, 2021, **9**, 13810-13817.
2. **M. Manna**, S. Roy, S. Bhandari and A. Chattopadhyay, *Langmuir*, 2021, 37, **18**, 5506-5512.
3. **M. Manna**, S. Roy, S. Bhandari and A. Chattopadhyay, *J. Mater. Chem. C*, 2020, **8**, 6972-6976.
4. S. Pramanik, **M. Manna**, B. Hudait, S. Roy and S. Bhandari, *Phys. Chem. Chem. Phys.*, 2021, **23**, 9860-9866.
5. S. Roy, S. Bhandari, **M. Manna**, S. De and A. Chattopadhyay, *Phys. Chem. Chem. Phys.*, 2019, **21**, 589-596.
6. S. Roy, S. Pramanik, P. Mandal, **M. Manna** and S. Bhandari, *Chemistry–An Asian Journal*, 2019, 14, **21**, 3823-3829.
7. S. Roy, **M. Manna** and A. Chattopadhyay, *J. Phys. Chem. C*, 2018, 122, **18**, 9939-9946.

Conferences Attended

1. Presented a poster in International Conference on Advanced Nanomaterials and Nanotechnology, ICANN- 2019 held at Indian Institute of Technology Guwahati, India.
2. Presented an oral talk in International Conference on Advanced Nanomaterials and Nanotechnology, ICANN- 2021 held at Indian Institute of Technology Guwahati, India.
3. Presented an oral talk in Research and Industrial Conclave (RIC) - INTEGRATION 2022 held at Indian Institute of Technology Guwahati, India.

Permissions

Quantum Dots Still Shining Strong 30 Years On

Author: Andrey Rogach
Publication: ACS Nano
Publisher: American Chemical Society
Date: Jul 1, 2014

PERMISSION/LICENSE IS GRANTED FOR YOUR ORDER AT NO CHARGE

This type of permission/license, instead of the standard Terms and Conditions, is sent to you because no fee is being charged for your order. Please note the following:

- Permission is granted for your request in both print and electronic formats, and translations.
- If figures and/or tables were requested, they may be adapted or used in part.
- Please print this page for your records and send a copy of it to your publisher/graduate school.
- Appropriate credit for the requested material should be given as follows: "Reprinted (adapted) with permission from {COMPLETE REFERENCE CITATION}. Copyright {YEAR} American Chemical Society." Insert appropriate information in place of the capitalized words.
- One-time permission is granted only for the use specified in your RightsLink request. No additional uses are granted (such as derivative works or other editions). For any uses, please submit a new request.

If credit is given to another source for the material you requested from RightsLink, permission must be obtained from that source.

BACK CLOSE WINDOW

TH-2661_166122014

Rainbow Emission from an Atomic Transition in Doped Quantum Dots

Author: Abhijit Hazarika, Anshu Pandey, D. D. Sarma
Publication: Journal of Physical Chemistry Letters
Publisher: American Chemical Society
Date: Jul 1, 2014

PERMISSION/LICENSE IS GRANTED FOR YOUR ORDER AT NO CHARGE

This type of permission/license, instead of the standard Terms and Conditions, is sent to you because no fee is being charged for your order. Please note the following:

- Permission is granted for your request in both print and electronic formats, and translations.
- If figures and/or tables were requested, they may be adapted or used in part.
- Please print this page for your records and send a copy of it to your publisher/graduate school.
- Appropriate credit for the requested material should be given as follows: "Reprinted (adapted) with permission from {COMPLETE REFERENCE CITATION}. Copyright {YEAR} American Chemical Society." Insert appropriate information in place of the capitalized words.
- One-time permission is granted only for the use specified in your RightsLink request. No additional uses are granted (such as derivative works or other editions). For any uses, please submit a new request.

If credit is given to another source for the material you requested from RightsLink, permission must be obtained from that source.

BACK CLOSE WINDOW

Tuning the Emission of CdSe Quantum Dots by Controlled Trap Enhancement

Author: David R. Baker, Prashant V. Kamat
Publication: Langmuir
Publisher: American Chemical Society
Date: Jul 1, 2010

PERMISSION/LICENSE IS GRANTED FOR YOUR ORDER AT NO CHARGE

This type of permission/license, instead of the standard Terms and Conditions, is sent to you because no fee is being charged for your order. Please note the following:

- Permission is granted for your request in both print and electronic formats, and translations.
- If figures and/or tables were requested, they may be adapted or used in part.
- Please print this page for your records and send a copy of it to your publisher/graduate school.
- Appropriate credit for the requested material should be given as follows: "Reprinted (adapted) with permission from {COMPLETE REFERENCE CITATION}. Copyright {YEAR} American Chemical Society." Insert appropriate information in place of the capitalized words.
- One-time permission is granted only for the use specified in your RightsLink request. No additional uses are granted (such as derivative works or other editions). For any uses, please submit a new request.

If credit is given to another source for the material you requested from RightsLink, permission must be obtained from that source.

BACK CLOSE WINDOW

Order Date	23-Jan-2022	**Type of Use**	Republish in a thesis/dissertation
Order License ID	1181141-1		
ISSN	2046-2069	**Publisher**	RSC Publishing
		Portion	Image/photo/illustration

LICENSED CONTENT

Publication Title	RSC advances	**Publication Type**	e-Journal
Article Title	Enhanced photoluminescence and thermal stability of zinc quinolate following complexation on the surface of quantum dots	**Start Page**	24217
		Issue	46
		Volume	4
		URL	http://pubs.rsc.org/en/Journals/JournalIssues/RA
Date	01/01/2011		
Language	English		
Country	United Kingdom of Great Britain and Northern Ireland		
Rightsholder	Royal Society of Chemistry		

REQUEST DETAILS

Portion Type	Image/photo/illustration	**Distribution**	Worldwide
Number of images / photos / illustrations	1	**Translation**	Original language of publication
Format (select all that apply)	Print, Electronic	**Copies for the disabled?**	No
		Minor editing privileges?	No
Who will republish the content?	Academic institution	**Incidental promotional use?**	No
Duration of Use	Life of current edition	**Currency**	USD
Lifetime Unit Quantity	Up to 499		
Rights Requested	Main product		

NEW WORK DETAILS

Title	Complexation on the Surface of Quantum Dots for Ion and Molecular Sensing	**Institution name**	IIT Guwahati
		Expected presentation date	2022-01-31
Instructor name	Mihir Manna		

ADDITIONAL DETAILS

TH-2661_166122014

Order reference number	N/A	**The requesting person / organization to appear on the license**	MIHIR MANNA

REUSE CONTENT DETAILS

Title, description or numeric reference of the portion(s)	54	**Title of the article/chapter the portion is from**	Enhanced photoluminescence and thermal stability of zinc quinolate following complexation on the surface of quantum dots
Editor of portion(s)	Bhandari, Satyapriya; Roy, Shilaj; Chattopadhyay, Arun	**Author of portion(s)**	Bhandari, Satyapriya; Roy, Shilaj; Chattopadhyay, Arun
Volume of serial or monograph	4	**Issue, if republishing an article from a serial**	46
Page or page range of portion	24217	**Publication date of portion**	2014-06-09

CCC Terms and Conditions

1. Description of Service; Defined Terms. This Republication License enables the User to obtain licenses for republication of one or more copyrighted works as described in detail on the relevant Order Confirmation (the "Work(s)"). Copyright Clearance Center, Inc. ("CCC") grants licenses through the Service on behalf of the rightsholder identified on the Order Confirmation (the "Rightsholder"). "Republication", as used herein, generally means the inclusion of a Work, in whole or in part, in a new work or works, also as described on the Order Confirmation. "User", as used herein, means the person or entity making such republication.

2. The terms set forth in the relevant Order Confirmation, and any terms set by the Rightsholder with respect to a particular Work, govern the terms of use of Works in connection with the Service. By using the Service, the person transacting for a republication license on behalf of the User represents and warrants that he/she/it (a) has been duly authorized by the User to accept, and hereby does accept, all such terms and conditions on behalf of User, and (b) shall inform User of all such terms and conditions. In the event such person is a "freelancer" or other third party independent of User and CCC, such party shall be deemed jointly a "User" for purposes of these terms and conditions. In any event, User shall be deemed to have accepted and agreed to all such terms and conditions if User republishes the Work in any fashion.

3. Scope of License; Limitations and Obligations.

    3.1. All Works and all rights therein, including copyright rights, remain the sole and exclusive property of the Rightsholder. The license created by the exchange of an Order Confirmation (and/or any invoice) and payment by User of the full amount set forth on that document includes only those rights expressly set forth in the Order Confirmation and in these terms and conditions, and conveys no other rights in the Work(s) to User. All rights not expressly granted are hereby reserved.

    3.2. General Payment Terms: You may pay by credit card or through an account with us payable at the end of the month. If you and we agree that you may establish a standing account with CCC, then the following terms apply: Remit Payment to: Copyright Clearance Center, 29118 Network Place, Chicago, IL 60673-1291. Payments Due: Invoices are payable upon their delivery to you (or upon our notice to you that they are available to you for downloading). After 30 days, outstanding amounts will be subject to a service charge of 1-1/2% per month or, if less, the maximum rate allowed by applicable law. Unless otherwise specifically set forth in the Order Confirmation or in a separate written agreement signed by CCC, invoices are due and payable on "net 30" terms. While User may exercise the rights licensed immediately upon issuance of the [illegible] Confirmation, the license is automatically revoked and is null and void, as if it had never been

issued, if complete payment for the license is not received on a timely basis either from User directly or through a payment agent, such as a credit card company.

3.3. Unless otherwise provided in the Order Confirmation, any grant of rights to User (i) is "one-time" (including the editions and product family specified in the license), (ii) is non-exclusive and non-transferable and (iii) is subject to any and all limitations and restrictions (such as, but not limited to, limitations on duration of use or circulation) included in the Order Confirmation or invoice and/or in these terms and conditions. Upon completion of the licensed use, User shall either secure a new permission for further use of the Work(s) or immediately cease any new use of the Work(s) and shall render inaccessible (such as by deleting or by removing or severing links or other locators) any further copies of the Work (except for copies printed on paper in accordance with this license and still in User's stock at the end of such period).

3.4. In the event that the material for which a republication license is sought includes third party materials (such as photographs, illustrations, graphs, inserts and similar materials) which are identified in such material as having been used by permission, User is responsible for identifying, and seeking separate licenses (under this Service or otherwise) for, any of such third party materials; without a separate license, such third party materials may not be used.

3.5. Use of proper copyright notice for a Work is required as a condition of any license granted under the Service. Unless otherwise provided in the Order Confirmation, a proper copyright notice will read substantially as follows: "Republished with permission of [Rightsholder's name], from [Work's title, author, volume, edition number and year of copyright]; permission conveyed through Copyright Clearance Center, Inc. " Such notice must be provided in a reasonably legible font size and must be placed either immediately adjacent to the Work as used (for example, as part of a by-line or footnote but not as a separate electronic link) or in the place where substantially all other credits or notices for the new work containing the republished Work are located. Failure to include the required notice results in loss to the Rightsholder and CCC, and the User shall be liable to pay liquidated damages for each such failure equal to twice the use fee specified in the Order Confirmation, in addition to the use fee itself and any other fees and charges specified.

3.6. User may only make alterations to the Work if and as expressly set forth in the Order Confirmation. No Work may be used in any way that is defamatory, violates the rights of third parties (including such third parties' rights of copyright, privacy, publicity, or other tangible or intangible property), or is otherwise illegal, sexually explicit or obscene. In addition, User may not conjoin a Work with any other material that may result in damage to the reputation of the Rightsholder. User agrees to inform CCC if it becomes aware of any infringement of any rights in a Work and to cooperate with any reasonable request of CCC or the Rightsholder in connection therewith.

4. Indemnity. User hereby indemnifies and agrees to defend the Rightsholder and CCC, and their respective employees and directors, against all claims, liability, damages, costs and expenses, including legal fees and expenses, arising out of any use of a Work beyond the scope of the rights granted herein, or any use of a Work which has been altered in any unauthorized way by User, including claims of defamation or infringement of rights of copyright, publicity, privacy or other tangible or intangible property.

5. Limitation of Liability. UNDER NO CIRCUMSTANCES WILL CCC OR THE RIGHTSHOLDER BE LIABLE FOR ANY DIRECT, INDIRECT, CONSEQUENTIAL OR INCIDENTAL DAMAGES (INCLUDING WITHOUT LIMITATION DAMAGES FOR LOSS OF BUSINESS PROFITS OR INFORMATION, OR FOR BUSINESS INTERRUPTION) ARISING OUT OF THE USE OR INABILITY TO USE A WORK, EVEN IF ONE OF THEM HAS BEEN ADVISED OF THE POSSIBILITY OF SUCH DAMAGES. In any event, the total liability of the Rightsholder and CCC (including their respective employees and directors) shall not exceed the total amount actually paid by User for this license. User assumes full liability for the actions and omissions of its principals, employees, agents, affiliates, successors and assigns.

6. Limited Warranties. THE WORK(S) AND RIGHT(S) ARE PROVIDED "AS IS". CCC HAS THE RIGHT TO GRANT TO USER THE RIGHTS GRANTED IN THE ORDER CONFIRMATION DOCUMENT. CCC AND THE RIGHTSHOLDER DISCLAIM ALL OTHER WARRANTIES RELATING TO THE WORK(S) AND RIGHT(S), EITHER EXPRESS OR IMPLIED, INCLUDING

WITHOUT LIMITATION IMPLIED WARRANTIES OF MERCHANTABILITY OR FITNESS FOR A PARTICULAR PURPOSE. ADDITIONAL RIGHTS MAY BE REQUIRED TO USE ILLUSTRATIONS, GRAPHS, PHOTOGRAPHS, ABSTRACTS, INSERTS OR OTHER PORTIONS OF THE WORK (AS OPPOSED TO THE ENTIRE WORK) IN A MANNER CONTEMPLATED BY USER; USER UNDERSTANDS AND AGREES THAT NEITHER CCC NOR THE RIGHTSHOLDER MAY HAVE SUCH ADDITIONAL RIGHTS TO GRANT.

7. Effect of Breach. Any failure by User to pay any amount when due, or any use by User of a Work beyond the scope of the license set forth in the Order Confirmation and/or these terms and conditions, shall be a material breach of the license created by the Order Confirmation and these terms and conditions. Any breach not cured within 30 days of written notice thereof shall result in immediate termination of such license without further notice. Any unauthorized (but licensable) use of a Work that is terminated immediately upon notice thereof may be liquidated by payment of the Rightsholder's ordinary license price therefor; any unauthorized (and unlicensable) use that is not terminated immediately for any reason (including, for example, because materials containing the Work cannot reasonably be recalled) will be subject to all remedies available at law or in equity, but in no event to a payment of less than three times the Rightsholder's ordinary license price for the most closely analogous licensable use plus Rightsholder's and/or CCC's costs and expenses incurred in collecting such payment.

8. Miscellaneous.

    8.1. User acknowledges that CCC may, from time to time, make changes or additions to the Service or to these terms and conditions, and CCC reserves the right to send notice to the User by electronic mail or otherwise for the purposes of notifying User of such changes or additions; provided that any such changes or additions shall not apply to permissions already secured and paid for.

    8.2. Use of User-related information collected through the Service is governed by CCC's privacy policy, available online here:https://marketplace.copyright.com/rs-ui-web/mp/privacy-policy

    8.3. The licensing transaction described in the Order Confirmation is personal to User. Therefore, User may not assign or transfer to any other person (whether a natural person or an organization of any kind) the license created by the Order Confirmation and these terms and conditions or any rights granted hereunder; provided, however, that User may assign such license in its entirety on written notice to CCC in the event of a transfer of all or substantially all of User's rights in the new material which includes the Work(s) licensed under this Service.

    8.4. No amendment or waiver of any terms is binding unless set forth in writing and signed by the parties. The Rightsholder and CCC hereby object to any terms contained in any writing prepared by the User or its principals, employees, agents or affiliates and purporting to govern or otherwise relate to the licensing transaction described in the Order Confirmation, which terms are in any way inconsistent with any terms set forth in the Order Confirmation and/or in these terms and conditions or CCC's standard operating procedures, whether such writing is prepared prior to, simultaneously with or subsequent to the Order Confirmation, and whether such writing appears on a copy of the Order Confirmation or in a separate instrument.

    8.5. The licensing transaction described in the Order Confirmation document shall be governed by and construed under the law of the State of New York, USA, without regard to the principles thereof of conflicts of law. Any case, controversy, suit, action, or proceeding arising out of, in connection with, or related to such licensing transaction shall be brought, at CCC's sole discretion, in any federal or state court located in the County of New York, State of New York, USA, or in any federal or state court whose geographical jurisdiction covers the location of the Rightsholder set forth in the Order Confirmation. The parties expressly submit to the personal jurisdiction and venue of each such federal or state court.If you have any comments or questions about the Service or Copyright Clearance Center, please contact us at 978-750-8400 or send an e-mail to support@copyright.com.

v 1.1

TH-2661_166122014

Surface Complexation Reaction for Phase Transfer of Hydrophobic Quantum Dot from Nonpolar to Polar Medium

Author: Satyapriya Bhandari, Shilaj Roy, Sabyasachi Pramanik, et al
Publication: Langmuir
Publisher: American Chemical Society
Date: Sep 1, 2014

PERMISSION/LICENSE IS GRANTED FOR YOUR ORDER AT NO CHARGE

Synchronous Tricolor Emission-Based White Light from Quantum Dot Complex

Author: Sabyasachi Pramanik, Satyapriya Bhandari, Shilaj Roy, et al

Publication: Journal of Physical Chemistry Letters

Publisher: American Chemical Society

Date: Apr 1, 2015

PERMISSION/LICENSE IS GRANTED FOR YOUR ORDER AT NO CHARGE

This type of permission/license, instead of the standard Terms and Conditions, is sent to you because no fee is being charged for your order. Please note the following:

- Permission is granted for your request in both print and electronic formats, and translations.
- If figures and/or tables were requested, they may be adapted or used in part.
- Please print this page for your records and send a copy of it to your publisher/graduate school.
- Appropriate credit for the requested material should be given as follows: "Reprinted (adapted) with permission from {COMPLETE REFERENCE CITATION}. Copyright {YEAR} American Chemical Society." Insert appropriate information in place of the capitalized words.
- One-time permission is granted only for the use specified in your RightsLink request. No additional uses are granted (such as derivative works or other editions). For any uses, please submit a new request.

If credit is given to another source for the material you requested from RightsLink, permission must be obtained from that source.

BACK CLOSE WINDOW

Order Date	24-Jan-2022	**Type of Use**	Republish in a thesis/dissertation
Order License ID	1181240-1		
ISSN	0003-2654	**Publisher**	ROYAL SOCIETY OF CHEMISTRY
		Portion	Image/photo/illustration

LICENSED CONTENT

Publication Title	The Analyst	**Rightsholder**	Royal Society of Chemistry
Article Title	CTAB-capped Mn-doped ZnS quantum dots and label-free aptamer for room-temperature phosphorescence detection of mercury ions.	**Publication Type**	Journal
		Start Page	4651
		Issue	20
		Volume	137
Author/Editor	ROYAL SOCIETY OF CHEMISTRY (GREAT BRITAIN), SOCIETY OF PUBLIC ANALYSTS (GREAT BRITAIN), SOCIETY OF PUBLIC ANALYSTS AND OTHER ANALYTICAL CH, SOCIETY FOR ANALYTICAL CHEMISTRY., CHEMICAL SOCIETY (GREAT BRITAIN), SOCIETY OF PUBLIC ANALYSTS (GREAT BRITAIN).		
Date	01/01/1876		
Language	English		
Country	United Kingdom of Great Britain and Northern Ireland		

REQUEST DETAILS

Portion Type	Image/photo/illustration	**Distribution**	Worldwide
Number of images / photos / illustrations	1	**Translation**	Original language of publication
Format (select all that apply)	Print, Electronic	**Copies for the disabled?**	No
		Minor editing privileges?	No
Who will republish the content?	Academic institution	**Incidental promotional use?**	No
Duration of Use	Life of current edition	**Currency**	USD
Lifetime Unit Quantity	Up to 499		

Rights Requested	Main product

NEW WORK DETAILS

Title	Complexation on the Surface of Quantum Dots for Ion and Molecular Sensing	**Institution name**	IIT Guwahati
		Expected presentation date	2022-01-31
Instructor name	Mihir Manna		

ADDITIONAL DETAILS

Order reference number	N/A	**The requesting person / organization to appear on the license**	MIHIR MANNA

REUSE CONTENT DETAILS

Title, description or numeric reference of the portion(s)	92	**Title of the article/chapter the portion is from**	CTAB-capped Mn-doped ZnS quantum dots and label-free aptamer for room-temperature phosphorescence detection of mercury ions.
Editor of portion(s)	Xie, Wan Yi; Huang, Wei Tao; Luo, Hong Qun; Li, Nian Bing	**Author of portion(s)**	Xie, Wan Yi; Huang, Wei Tao; Luo, Hong Qun; Li, Nian Bing
Volume of serial or monograph	137	**Issue, if republishing an article from a serial**	20
Page or page range of portion	4651	**Publication date of portion**	2012-09-17

CCC Terms and Conditions

1. Description of Service; Defined Terms. This Republication License enables the User to obtain licenses for republication of one or more copyrighted works as described in detail on the relevant Order Confirmation (the "Work(s)"). Copyright Clearance Center, Inc. ("CCC") grants licenses through the Service on behalf of the rightsholder identified on the Order Confirmation (the "Rightsholder"). "Republication", as used herein, generally means the inclusion of a Work, in whole or in part, in a new work or works, also as described on the Order Confirmation. "User", as used herein, means the person or entity making such republication.

2. The terms set forth in the relevant Order Confirmation, and any terms set by the Rightsholder with respect to a particular Work, govern the terms of use of Works in connection with the Service. By using the Service, the person transacting for a republication license on behalf of the User represents and warrants that he/she/it (a) has been duly authorized by the User to accept, and hereby does accept, all such terms and conditions on behalf of User, and (b) shall inform User of all such terms and conditions. In the event such person is a "freelancer" or other third party independent of User and CCC, such party shall be deemed jointly a "User" for purposes of these terms and conditions. In any event, User shall be deemed to have accepted and agreed to all such terms and conditions if User republishes the Work in any fashion.

3. Scope of License; Limitations and Obligations.

   3.1. All Works and all rights therein, including copyright rights, remain the sole and exclusive property of the Rightsholder. The license created by the exchange of an Order Confirmation (and/or any invoice) and

payment by User of the full amount set forth on that document includes only those rights expressly set forth in the Order Confirmation and in these terms and conditions, and conveys no other rights in the Work(s) to User. All rights not expressly granted are hereby reserved.

3.2. General Payment Terms: You may pay by credit card or through an account with us payable at the end of the month. If you and we agree that you may establish a standing account with CCC, then the following terms apply: Remit Payment to: Copyright Clearance Center, 29118 Network Place, Chicago, IL 60673-1291. Payments Due: Invoices are payable upon their delivery to you (or upon our notice to you that they are available to you for downloading). After 30 days, outstanding amounts will be subject to a service charge of 1-1/2% per month or, if less, the maximum rate allowed by applicable law. Unless otherwise specifically set forth in the Order Confirmation or in a separate written agreement signed by CCC, invoices are due and payable on "net 30" terms. While User may exercise the rights licensed immediately upon issuance of the Order Confirmation, the license is automatically revoked and is null and void, as if it had never been issued, if complete payment for the license is not received on a timely basis either from User directly or through a payment agent, such as a credit card company.

3.3. Unless otherwise provided in the Order Confirmation, any grant of rights to User (i) is "one-time" (including the editions and product family specified in the license), (ii) is non-exclusive and non-transferable and (iii) is subject to any and all limitations and restrictions (such as, but not limited to, limitations on duration of use or circulation) included in the Order Confirmation or invoice and/or in these terms and conditions. Upon completion of the licensed use, User shall either secure a new permission for further use of the Work(s) or immediately cease any new use of the Work(s) and shall render inaccessible (such as by deleting or by removing or severing links or other locators) any further copies of the Work (except for copies printed on paper in accordance with this license and still in User's stock at the end of such period).

3.4. In the event that the material for which a republication license is sought includes third party materials (such as photographs, illustrations, graphs, inserts and similar materials) which are identified in such material as having been used by permission, User is responsible for identifying, and seeking separate licenses (under this Service or otherwise) for, any of such third party materials; without a separate license, such third party materials may not be used.

3.5. Use of proper copyright notice for a Work is required as a condition of any license granted under the Service. Unless otherwise provided in the Order Confirmation, a proper copyright notice will read substantially as follows: "Republished with permission of [Rightsholder's name], from [Work's title, author, volume, edition number and year of copyright]; permission conveyed through Copyright Clearance Center, Inc. " Such notice must be provided in a reasonably legible font size and must be placed either immediately adjacent to the Work as used (for example, as part of a by-line or footnote but not as a separate electronic link) or in the place where substantially all other credits or notices for the new work containing the republished Work are located. Failure to include the required notice results in loss to the Rightsholder and CCC, and the User shall be liable to pay liquidated damages for each such failure equal to twice the use fee specified in the Order Confirmation, in addition to the use fee itself and any other fees and charges specified.

3.6. User may only make alterations to the Work if and as expressly set forth in the Order Confirmation. No Work may be used in any way that is defamatory, violates the rights of third parties (including such third parties' rights of copyright, privacy, publicity, or other tangible or intangible property), or is otherwise illegal, sexually explicit or obscene. In addition, User may not conjoin a Work with any other material that may result in damage to the reputation of the Rightsholder. User agrees to inform CCC if it becomes aware of any infringement of any rights in a Work and to cooperate with any reasonable request of CCC or the Rightsholder in connection therewith.

4. Indemnity. User hereby indemnifies and agrees to defend the Rightsholder and CCC, and their respective employees and directors, against all claims, liability, damages, costs and expenses, including legal fees and expenses, arising out of any use of a Work beyond the scope of the rights granted herein, or any use of a Work which has been altered in any unauthorized way by User, including claims of defamation or infringement of rights of copyright, publicity, privacy or other tangible or intangible property.

5. Limitation of Liability. UNDER NO CIRCUMSTANCES WILL CCC OR THE RIGHTSHOLDER BE LIABLE FOR ANY DIRECT, INDIRECT, CONSEQUENTIAL OR INCIDENTAL DAMAGES (INCLUDING WITHOUT LIMITATION DAMAGES FOR LOSS OF BUSINESS PROFITS OR INFORMATION, OR FOR BUSINESS INTERRUPTION) ARISING OUT OF THE USE OR INABILITY TO USE A WORK, EVEN IF ONE OF THEM HAS BEEN ADVISED OF THE POSSIBILITY OF SUCH DAMAGES. In any event, the total liability of the Rightsholder and CCC (including their respective employees and directors) shall not exceed the total amount actually paid by User for this license. User assumes full liability for the actions and omissions of its principals, employees, agents, affiliates, successors and assigns.

6. Limited Warranties. THE WORK(S) AND RIGHT(S) ARE PROVIDED "AS IS". CCC HAS THE RIGHT TO GRANT TO USER THE RIGHTS GRANTED IN THE ORDER CONFIRMATION DOCUMENT. CCC AND THE RIGHTSHOLDER DISCLAIM ALL OTHER WARRANTIES RELATING TO THE WORK(S) AND RIGHT(S), EITHER EXPRESS OR IMPLIED, INCLUDING WITHOUT LIMITATION IMPLIED WARRANTIES OF MERCHANTABILITY OR FITNESS FOR A PARTICULAR PURPOSE. ADDITIONAL RIGHTS MAY BE REQUIRED TO USE ILLUSTRATIONS, GRAPHS, PHOTOGRAPHS, ABSTRACTS, INSERTS OR OTHER PORTIONS OF THE WORK (AS OPPOSED TO THE ENTIRE WORK) IN A MANNER CONTEMPLATED BY USER; USER UNDERSTANDS AND AGREES THAT NEITHER CCC NOR THE RIGHTSHOLDER MAY HAVE SUCH ADDITIONAL RIGHTS TO GRANT.

7. Effect of Breach. Any failure by User to pay any amount when due, or any use by User of a Work beyond the scope of the license set forth in the Order Confirmation and/or these terms and conditions, shall be a material breach of the license created by the Order Confirmation and these terms and conditions. Any breach not cured within 30 days of written notice thereof shall result in immediate termination of such license without further notice. Any unauthorized (but licensable) use of a Work that is terminated immediately upon notice thereof may be liquidated by payment of the Rightsholder's ordinary license price therefor; any unauthorized (and unlicensable) use that is not terminated immediately for any reason (including, for example, because materials containing the Work cannot reasonably be recalled) will be subject to all remedies available at law or in equity, but in no event to a payment of less than three times the Rightsholder's ordinary license price for the most closely analogous licensable use plus Rightsholder's and/or CCC's costs and expenses incurred in collecting such payment.

8. Miscellaneous.

    8.1. User acknowledges that CCC may, from time to time, make changes or additions to the Service or to these terms and conditions, and CCC reserves the right to send notice to the User by electronic mail or otherwise for the purposes of notifying User of such changes or additions; provided that any such changes or additions shall not apply to permissions already secured and paid for.

    8.2. Use of User-related information collected through the Service is governed by CCC's privacy policy, available online here:https://marketplace.copyright.com/rs-ui-web/mp/privacy-policy

    8.3. The licensing transaction described in the Order Confirmation is personal to User. Therefore, User may not assign or transfer to any other person (whether a natural person or an organization of any kind) the license created by the Order Confirmation and these terms and conditions or any rights granted hereunder; provided, however, that User may assign such license in its entirety on written notice to CCC in the event of a transfer of all or substantially all of User's rights in the new material which includes the Work(s) licensed under this Service.

    8.4. No amendment or waiver of any terms is binding unless set forth in writing and signed by the parties. The Rightsholder and CCC hereby object to any terms contained in any writing prepared by the User or its principals, employees, agents or affiliates and purporting to govern or otherwise relate to the licensing transaction described in the Order Confirmation, which terms are in any way inconsistent with any terms set forth in the Order Confirmation and/or in these terms and conditions or CCC's standard operating procedures, whether such writing is prepared prior to, simultaneously with or subsequent to the Order Confirmation, and whether such writing appears on a copy of the Order Confirmation or in a separate instrument.

    8.5. The licensing transaction described in the Order Confirmation document shall be governed by and

TH-2661_166122014

construed under the law of the State of New York, USA, without regard to the principles thereof of conflicts of law. Any case, controversy, suit, action, or proceeding arising out of, in connection with, or related to such licensing transaction shall be brought, at CCC's sole discretion, in any federal or state court located in the County of New York, State of New York, USA, or in any federal or state court whose geographical jurisdiction covers the location of the Rightsholder set forth in the Order Confirmation. The parties expressly submit to the personal jurisdiction and venue of each such federal or state court.If you have any comments or questions about the Service or Copyright Clearance Center, please contact us at 978-750-8400 or send an e-mail to support@copyright.com.

v 1.1

TH-2661_166122014

CCC Marketplace™

Order Date	24-Jan-2022	**Type of Use**	Republish in a thesis/dissertation
Order License ID	1181295-1		
ISSN	2046-2069	**Publisher**	RSC Publishing
		Portion	Image/photo/illustration

LICENSED CONTENT

Publication Title	RSC advances	**Publication Type**	e-Journal
Article Title	Detection of phosphate based on phosphorescence of Mn doped ZnS quantum dots combined with cerium(iii)	**Start Page**	46657
		End Page	46664
		Issue	74
		Volume	7
Date	01/01/2011	**URL**	http://pubs.rsc.org/en/Journals/JournalIssues/RA
Language	English		
Country	United Kingdom of Great Britain and Northern Ireland		
Rightsholder	Royal Society of Chemistry		

REQUEST DETAILS

Portion Type	Image/photo/illustration	**Distribution**	Worldwide
Number of images / photos / illustrations	1	**Translation**	Original language of publication
Format (select all that apply)	Print, Electronic	**Copies for the disabled?**	No
		Minor editing privileges?	No
Who will republish the content?	Academic institution	**Incidental promotional use?**	No
Duration of Use	Life of current edition	**Currency**	USD
Lifetime Unit Quantity	Up to 499		
Rights Requested	Main product		

NEW WORK DETAILS

Title	Complexation on the Surface of Quantum Dots for Ion and Molecular Sensing	**Institution name**	IIT Guwahati
		Expected presentation date	2022-01-31
Instructor name	Mihir Manna		

ADDITIONAL DETAILS

TH-2661_166122014

Order reference number	N/A	**The requesting person / organization to appear on the license**	MIHIR MANNA

REUSE CONTENT DETAILS

Title, description or numeric reference of the portion(s)	108	**Title of the article/chapter the portion is from**	Detection of phosphate based on phosphorescence of Mn doped ZnS quantum dots combined with cerium(iii)
Editor of portion(s)	Qin, Jin; Li, Dongxia; Miao, Yanming; Yan, Guiqin	**Author of portion(s)**	Qin, Jin; Li, Dongxia; Miao, Yanming; Yan, Guiqin
Volume of serial or monograph	7	**Issue, if republishing an article from a serial**	74
Page or page range of portion	46657-46664	**Publication date of portion**	2017-10-04

CCC Terms and Conditions

1. Description of Service; Defined Terms. This Republication License enables the User to obtain licenses for republication of one or more copyrighted works as described in detail on the relevant Order Confirmation (the "Work(s)"). Copyright Clearance Center, Inc. ("CCC") grants licenses through the Service on behalf of the rightsholder identified on the Order Confirmation (the "Rightsholder"). "Republication", as used herein, generally means the inclusion of a Work, in whole or in part, in a new work or works, also as described on the Order Confirmation. "User", as used herein, means the person or entity making such republication.

2. The terms set forth in the relevant Order Confirmation, and any terms set by the Rightsholder with respect to a particular Work, govern the terms of use of Works in connection with the Service. By using the Service, the person transacting for a republication license on behalf of the User represents and warrants that he/she/it (a) has been duly authorized by the User to accept, and hereby does accept, all such terms and conditions on behalf of User, and (b) shall inform User of all such terms and conditions. In the event such person is a "freelancer" or other third party independent of User and CCC, such party shall be deemed jointly a "User" for purposes of these terms and conditions. In any event, User shall be deemed to have accepted and agreed to all such terms and conditions if User republishes the Work in any fashion.

3. Scope of License; Limitations and Obligations.

   3.1. All Works and all rights therein, including copyright rights, remain the sole and exclusive property of the Rightsholder. The license created by the exchange of an Order Confirmation (and/or any invoice) and payment by User of the full amount set forth on that document includes only those rights expressly set forth in the Order Confirmation and in these terms and conditions, and conveys no other rights in the Work(s) to User. All rights not expressly granted are hereby reserved.

   3.2. General Payment Terms: You may pay by credit card or through an account with us payable at the end of the month. If you and we agree that you may establish a standing account with CCC, then the following terms apply: Remit Payment to: Copyright Clearance Center, 29118 Network Place, Chicago, IL 60673-1291. Payments Due: Invoices are payable upon their delivery to you (or upon our notice to you that they are available to you for downloading). After 30 days, outstanding amounts will be subject to a service charge of 1-1/2% per month or, if less, the maximum rate allowed by applicable law. Unless otherwise specifically set forth in the Order Confirmation or in a separate written agreement signed by CCC, invoices are due and payable on "net 30" terms. While User may exercise the rights licensed immediately upon issuance of the Order Confirmation, the license is automatically revoked and is null and void, as if it had never been issued, if complete payment for the license is not received on a timely basis either from User directly or through a payment agent, such as a credit card company.

3.3. Unless otherwise provided in the Order Confirmation, any grant of rights to User (i) is "one-time" (including the editions and product family specified in the license), (ii) is non-exclusive and non-transferable and (iii) is subject to any and all limitations and restrictions (such as, but not limited to, limitations on duration of use or circulation) included in the Order Confirmation or invoice and/or in these terms and conditions. Upon completion of the licensed use, User shall either secure a new permission for further use of the Work(s) or immediately cease any new use of the Work(s) and shall render inaccessible (such as by deleting or by removing or severing links or other locators) any further copies of the Work (except for copies printed on paper in accordance with this license and still in User's stock at the end of such period).

3.4. In the event that the material for which a republication license is sought includes third party materials (such as photographs, illustrations, graphs, inserts and similar materials) which are identified in such material as having been used by permission, User is responsible for identifying, and seeking separate licenses (under this Service or otherwise) for, any of such third party materials; without a separate license, such third party materials may not be used.

3.5. Use of proper copyright notice for a Work is required as a condition of any license granted under the Service. Unless otherwise provided in the Order Confirmation, a proper copyright notice will read substantially as follows: "Republished with permission of [Rightsholder's name], from [Work's title, author, volume, edition number and year of copyright]; permission conveyed through Copyright Clearance Center, Inc. " Such notice must be provided in a reasonably legible font size and must be placed either immediately adjacent to the Work as used (for example, as part of a by-line or footnote but not as a separate electronic link) or in the place where substantially all other credits or notices for the new work containing the republished Work are located. Failure to include the required notice results in loss to the Rightsholder and CCC, and the User shall be liable to pay liquidated damages for each such failure equal to twice the use fee specified in the Order Confirmation, in addition to the use fee itself and any other fees and charges specified.

3.6. User may only make alterations to the Work if and as expressly set forth in the Order Confirmation. No Work may be used in any way that is defamatory, violates the rights of third parties (including such third parties' rights of copyright, privacy, publicity, or other tangible or intangible property), or is otherwise illegal, sexually explicit or obscene. In addition, User may not conjoin a Work with any other material that may result in damage to the reputation of the Rightsholder. User agrees to inform CCC if it becomes aware of any infringement of any rights in a Work and to cooperate with any reasonable request of CCC or the Rightsholder in connection therewith.

4. Indemnity. User hereby indemnifies and agrees to defend the Rightsholder and CCC, and their respective employees and directors, against all claims, liability, damages, costs and expenses, including legal fees and expenses, arising out of any use of a Work beyond the scope of the rights granted herein, or any use of a Work which has been altered in any unauthorized way by User, including claims of defamation or infringement of rights of copyright, publicity, privacy or other tangible or intangible property.

5. Limitation of Liability. UNDER NO CIRCUMSTANCES WILL CCC OR THE RIGHTSHOLDER BE LIABLE FOR ANY DIRECT, INDIRECT, CONSEQUENTIAL OR INCIDENTAL DAMAGES (INCLUDING WITHOUT LIMITATION DAMAGES FOR LOSS OF BUSINESS PROFITS OR INFORMATION, OR FOR BUSINESS INTERRUPTION) ARISING OUT OF THE USE OR INABILITY TO USE A WORK, EVEN IF ONE OF THEM HAS BEEN ADVISED OF THE POSSIBILITY OF SUCH DAMAGES. In any event, the total liability of the Rightsholder and CCC (including their respective employees and directors) shall not exceed the total amount actually paid by User for this license. User assumes full liability for the actions and omissions of its principals, employees, agents, affiliates, successors and assigns.

6. Limited Warranties. THE WORK(S) AND RIGHT(S) ARE PROVIDED "AS IS". CCC HAS THE RIGHT TO GRANT TO USER THE RIGHTS GRANTED IN THE ORDER CONFIRMATION DOCUMENT. CCC AND THE RIGHTSHOLDER DISCLAIM ALL OTHER WARRANTIES RELATING TO THE WORK(S) AND RIGHT(S), EITHER EXPRESS OR IMPLIED, INCLUDING WITHOUT LIMITATION IMPLIED WARRANTIES OF MERCHANTABILITY OR FITNESS FOR A PARTICULAR PURPOSE. ADDITIONAL RIGHTS MAY BE REQUIRED TO USE ILLUSTRATIONS, GRAPHS, PHOTOGRAPHS, ABSTRACTS, INSERTS OR OTHER PORTIONS OF THE WORK (AS OPPOSED TO THE ENTIRE WORK) IN A MANNER CONTEMPLATED BY USER;

USER UNDERSTANDS AND AGREES THAT NEITHER CCC NOR THE RIGHTSHOLDER MAY HAVE SUCH ADDITIONAL RIGHTS TO GRANT.

7. Effect of Breach. Any failure by User to pay any amount when due, or any use by User of a Work beyond the scope of the license set forth in the Order Confirmation and/or these terms and conditions, shall be a material breach of the license created by the Order Confirmation and these terms and conditions. Any breach not cured within 30 days of written notice thereof shall result in immediate termination of such license without further notice. Any unauthorized (but licensable) use of a Work that is terminated immediately upon notice thereof may be liquidated by payment of the Rightsholder's ordinary license price therefor; any unauthorized (and unlicensable) use that is not terminated immediately for any reason (including, for example, because materials containing the Work cannot reasonably be recalled) will be subject to all remedies available at law or in equity, but in no event to a payment of less than three times the Rightsholder's ordinary license price for the most closely analogous licensable use plus Rightsholder's and/or CCC's costs and expenses incurred in collecting such payment.

8. Miscellaneous.

    8.1. User acknowledges that CCC may, from time to time, make changes or additions to the Service or to these terms and conditions, and CCC reserves the right to send notice to the User by electronic mail or otherwise for the purposes of notifying User of such changes or additions; provided that any such changes or additions shall not apply to permissions already secured and paid for.

    8.2. Use of User-related information collected through the Service is governed by CCC's privacy policy, available online here:https://marketplace.copyright.com/rs-ui-web/mp/privacy-policy

    8.3. The licensing transaction described in the Order Confirmation is personal to User. Therefore, User may not assign or transfer to any other person (whether a natural person or an organization of any kind) the license created by the Order Confirmation and these terms and conditions or any rights granted hereunder; provided, however, that User may assign such license in its entirety on written notice to CCC in the event of a transfer of all or substantially all of User's rights in the new material which includes the Work(s) licensed under this Service.

    8.4. No amendment or waiver of any terms is binding unless set forth in writing and signed by the parties. The Rightsholder and CCC hereby object to any terms contained in any writing prepared by the User or its principals, employees, agents or affiliates and purporting to govern or otherwise relate to the licensing transaction described in the Order Confirmation, which terms are in any way inconsistent with any terms set forth in the Order Confirmation and/or in these terms and conditions or CCC's standard operating procedures, whether such writing is prepared prior to, simultaneously with or subsequent to the Order Confirmation, and whether such writing appears on a copy of the Order Confirmation or in a separate instrument.

    8.5. The licensing transaction described in the Order Confirmation document shall be governed by and construed under the law of the State of New York, USA, without regard to the principles thereof of conflicts of law. Any case, controversy, suit, action, or proceeding arising out of, in connection with, or related to such licensing transaction shall be brought, at CCC's sole discretion, in any federal or state court located in the County of New York, State of New York, USA, or in any federal or state court whose geographical jurisdiction covers the location of the Rightsholder set forth in the Order Confirmation. The parties expressly submit to the personal jurisdiction and venue of each such federal or state court.If you have any comments or questions about the Service or Copyright Clearance Center, please contact us at 978-750-8400 or send an e-mail to support@copyright.com.

v 1.1

TH-2661_166122014

FRET-Based Biosensor for Oleic Acid in Nanomolar Range with Quantum Dots As an Energy Donor

Author: Sergey V. Dezhurov, Irina Y. Volkova, Maxim S. Wakstein

Publication: Bioconjugate Chemistry

Publisher: American Chemical Society

Date: Mar 1, 2011

PERMISSION/LICENSE IS GRANTED FOR YOUR ORDER AT NO CHARGE

This type of permission/license, instead of the standard Terms and Conditions, is sent to you because no fee is being charged for your order. Please note the following:

- Permission is granted for your request in both print and electronic formats, and translations.
- If figures and/or tables were requested, they may be adapted or used in part.
- Please print this page for your records and send a copy of it to your publisher/graduate school.
- Appropriate credit for the requested material should be given as follows: "Reprinted (adapted) with permission from {COMPLETE REFERENCE CITATION}. Copyright {YEAR} American Chemical Society." Insert appropriate information in place of the capitalized words.
- One-time permission is granted only for the use specified in your RightsLink request. No additional uses are granted (such as derivative works or other editions). For any uses, please submit a new request.

If credit is given to another source for the material you requested from RightsLink, permission must be obtained from that source.

BACK CLOSE WINDOW

ELSEVIER LICENSE TERMS AND CONDITIONS

Jan 26, 2022

This Agreement between Mr. MIHIR MANNA ("You") and Elsevier ("Elsevier") consists of your license details and the terms and conditions provided by Elsevier and Copyright Clearance Center.

License Number	5235410670600
License date	Jan 24, 2022
Licensed Content Publisher	Elsevier
Licensed Content Publication	Talanta
Licensed Content Title	Quantum dots-based ratiometric fluorescence probe for mercuric ions in biological fluids
Licensed Content Author	Qin Mu,Yan Li,Hu Xu,Yunfei Ma,Weihong Zhu,Xinhua Zhong
Licensed Content Date	Feb 15, 2014
Licensed Content Volume	119
Licensed Content Issue	n/a
Licensed Content Pages	8
Start Page	564
End Page	571
Type of Use	reuse in a thesis/dissertation
Portion	figures/tables/illustrations
Number of figures/tables/illustrations	1
Format	both print and electronic
Are you the author of this Elsevier article?	No
Will you be translating?	No
Title	Complexation on the Surface of Quantum Dots for Ion and Molecular Sensing
Institution name	IIT Guwahati
Expected presentation date	Jan 2022
Portions	Graphical abstract
Requestor Location	Mr. MIHIR MANNA Department of Chemistry IIT Guwahati Guwahati, ASSAM 781039 India Attn: Mr. MIHIR MANNA
Publisher Tax ID	GB 494 6272 12
Total	**0.00 USD**
Terms and Conditions	

INTRODUCTION

1. The publisher for this copyrighted material is Elsevier. By clicking "accept" in connection with completing this licensing transaction, you agree that the following terms and conditions apply to this transaction (along with the Billing and Payment terms and conditions established by Copyright Clearance Center, Inc. ("CCC"), at the time that you opened your Rightslink account and that are available at any time at http://myaccount.copyright.com).

GENERAL TERMS

2. Elsevier hereby grants you permission to reproduce the aforementioned material subject to the terms and conditions indicated.

TH-2661_166122014

3. Acknowledgement: If any part of the material to be used (for example, figures) has appeared in our publication with credit or acknowledgement to another source, permission must also be sought from that source. If such permission is not obtained then that material may not be included in your publication/copies. Suitable acknowledgement to the source must be made, either as a footnote or in a reference list at the end of your publication, as follows:
"Reprinted from Publication title, Vol /edition number, Author(s), Title of article / title of chapter, Pages No., Copyright (Year), with permission from Elsevier [OR APPLICABLE SOCIETY COPYRIGHT OWNER]." Also Lancet special credit - "Reprinted from The Lancet, Vol. number, Author(s), Title of article, Pages No., Copyright (Year), with permission from Elsevier."
4. Reproduction of this material is confined to the purpose and/or media for which permission is hereby given.
5. Altering/Modifying Material: Not Permitted. However figures and illustrations may be altered/adapted minimally to serve your work. Any other abbreviations, additions, deletions and/or any other alterations shall be made only with prior written authorization of Elsevier Ltd. (Please contact Elsevier's permissions helpdesk here). No modifications can be made to any Lancet figures/tables and they must be reproduced in full.
6. If the permission fee for the requested use of our material is waived in this instance, please be advised that your future requests for Elsevier materials may attract a fee.
7. Reservation of Rights: Publisher reserves all rights not specifically granted in the combination of (i) the license details provided by you and accepted in the course of this licensing transaction, (ii) these terms and conditions and (iii) CCC's Billing and Payment terms and conditions.
8. License Contingent Upon Payment: While you may exercise the rights licensed immediately upon issuance of the license at the end of the licensing process for the transaction, provided that you have disclosed complete and accurate details of your proposed use, no license is finally effective unless and until full payment is received from you (either by publisher or by CCC) as provided in CCC's Billing and Payment terms and conditions. If full payment is not received on a timely basis, then any license preliminarily granted shall be deemed automatically revoked and shall be void as if never granted. Further, in the event that you breach any of these terms and conditions or any of CCC's Billing and Payment terms and conditions, the license is automatically revoked and shall be void as if never granted. Use of materials as described in a revoked license, as well as any use of the materials beyond the scope of an unrevoked license, may constitute copyright infringement and publisher reserves the right to take any and all action to protect its copyright in the materials.
9. Warranties: Publisher makes no representations or warranties with respect to the licensed material.
10. Indemnity: You hereby indemnify and agree to hold harmless publisher and CCC, and their respective officers, directors, employees and agents, from and against any and all claims arising out of your use of the licensed material other than as specifically authorized pursuant to this license.
11. No Transfer of License: This license is personal to you and may not be sublicensed, assigned, or transferred by you to any other person without publisher's written permission.
12. No Amendment Except in Writing: This license may not be amended except in a writing signed by both parties (or, in the case of publisher, by CCC on publisher's behalf).
13. Objection to Contrary Terms: Publisher hereby objects to any terms contained in any purchase order, acknowledgment, check endorsement or other writing prepared by you, which terms are inconsistent with these terms and conditions or CCC's Billing and Payment terms and conditions. These terms and conditions, together with CCC's Billing and Payment terms and conditions (which are incorporated herein), comprise the entire agreement between you and publisher (and CCC) concerning this licensing transaction. In the event of any conflict between your obligations established by these terms and conditions and those established by CCC's Billing and Payment terms and conditions, these terms and conditions shall control.
14. Revocation: Elsevier or Copyright Clearance Center may deny the permissions described in this License at their sole discretion, for any reason or no reason, with a full refund payable to you. Notice of such denial will be made using the contact information provided by you. Failure to receive such notice will not alter or invalidate the denial. In no event will Elsevier or Copyright Clearance Center be responsible or liable for any costs, expenses or damage incurred by you as a result of a denial of your permission request, other than a refund of the amount(s) paid by you to Elsevier and/or Copyright Clearance Center for denied permissions.

LIMITED LICENSE

The following terms and conditions apply only to specific license types:
15. **Translation**: This permission is granted for non-exclusive world **English** rights only unless your license was granted for translation rights. If you licensed translation rights you may only translate this content into the languages you requested. A professional translator must perform all translations and reproduce the content word for word preserving the integrity of the article.
16. **Posting licensed content on any Website**: The following terms and conditions apply as follows: Licensing material from an Elsevier journal: All content posted to the web site must maintain the copyright information line on the bottom of each image; A hyper-text must be included to the Homepage of the journal from which you are licensing at http://www.sciencedirect.com/science/journal/xxxxx or the Elsevier homepage for books at http://www.elsevier.com; Central Storage: This license does not include permission for a scanned version of the material to be stored in a central repository such as that provided by Heron/XanEdu.
Licensing material from an Elsevier book: A hyper-text link must be included to the Elsevier homepage at http://www.elsevier.com . All content posted to the web site must maintain the copyright information line on the bottom of each image.

Posting licensed content on Electronic reserve: In addition to the above the following clauses are applicable: The web site must

be password-protected and made available only to bona fide students registered on a relevant course. This permission is granted for 1 year only. You may obtain a new license for future website posting.

17. **For journal authors:** the following clauses are applicable in addition to the above:

Preprints:

A preprint is an author's own write-up of research results and analysis, it has not been peer-reviewed, nor has it had any other value added to it by a publisher (such as formatting, copyright, technical enhancement etc.).

Authors can share their preprints anywhere at any time. Preprints should not be added to or enhanced in any way in order to appear more like, or to substitute for, the final versions of articles however authors can update their preprints on arXiv or RePEc with their Accepted Author Manuscript (see below).

If accepted for publication, we encourage authors to link from the preprint to their formal publication via its DOI. Millions of researchers have access to the formal publications on ScienceDirect, and so links will help users to find, access, cite and use the best available version. Please note that Cell Press, The Lancet and some society-owned have different preprint policies. Information on these policies is available on the journal homepage.

Accepted Author Manuscripts: An accepted author manuscript is the manuscript of an article that has been accepted for publication and which typically includes author-incorporated changes suggested during submission, peer review and editor-author communications.

Authors can share their accepted author manuscript:

- immediately
  - via their non-commercial person homepage or blog
  - by updating a preprint in arXiv or RePEc with the accepted manuscript
  - via their research institute or institutional repository for internal institutional uses or as part of an invitation-only research collaboration work-group
  - directly by providing copies to their students or to research collaborators for their personal use
  - for private scholarly sharing as part of an invitation-only work group on commercial sites with which Elsevier has an agreement
- After the embargo period
  - via non-commercial hosting platforms such as their institutional repository
  - via commercial sites with which Elsevier has an agreement

In all cases accepted manuscripts should:

- link to the formal publication via its DOI
- bear a CC-BY-NC-ND license - this is easy to do
- if aggregated with other manuscripts, for example in a repository or other site, be shared in alignment with our hosting policy not be added to or enhanced in any way to appear more like, or to substitute for, the published journal article.

Published journal article (JPA): A published journal article (PJA) is the definitive final record of published research that appears or will appear in the journal and embodies all value-adding publishing activities including peer review co-ordination, copy-editing, formatting, (if relevant) pagination and online enrichment.

Policies for sharing publishing journal articles differ for subscription and gold open access articles:

Subscription Articles: If you are an author, please share a link to your article rather than the full-text. Millions of researchers have access to the formal publications on ScienceDirect, and so links will help your users to find, access, cite, and use the best available version.

Theses and dissertations which contain embedded PJAs as part of the formal submission can be posted publicly by the awarding institution with DOI links back to the formal publications on ScienceDirect.

If you are affiliated with a library that subscribes to ScienceDirect you have additional private sharing rights for others' research accessed under that agreement. This includes use for classroom teaching and internal training at the institution (including use in course packs and courseware programs), and inclusion of the article for grant funding purposes.

Gold Open Access Articles: May be shared according to the author-selected end-user license and should contain a CrossMark logo, the end user license, and a DOI link to the formal publication on ScienceDirect.

Please refer to Elsevier's posting policy for further information.

18. **For book authors** the following clauses are applicable in addition to the above: Authors are permitted to place a brief summary of their work online only. You are not allowed to download and post the published electronic version of your chapter, nor may you scan the printed edition to create an electronic version. **Posting to a repository:** Authors are permitted to post a summary of their chapter only in their institution's repository.

19. **Thesis/Dissertation**: If your license is for use in a thesis/dissertation your thesis may be submitted to your institution in either print or electronic form. Should your thesis be published commercially, please reapply for permission. These requirements include permission for the Library and Archives of Canada to supply single copies, on demand, of the complete thesis and include permission for Proquest/UMI to supply single copies, on demand, of the complete thesis. Should your thesis be published commercially, please reapply for permission. Theses and dissertations which contain embedded PJAs as part of the formal submission can be posted publicly by the awarding institution with DOI links back to the formal publications on ScienceDirect.

Elsevier Open Access Terms and Conditions

You can publish open access with Elsevier in hundreds of open access journals or in nearly 2000 established subscription journals that support open access publishing. Permitted third party re-use of these open access articles is defined by the author's choice of Creative Commons user license. See our open access license policy for more information.

Terms & Conditions applicable to all Open Access articles published with Elsevier:

Any reuse of the article must not represent the author as endorsing the adaptation of the article nor should the article be modified in such a way as to damage the author's honour or reputation. If any changes have been made, such changes must be clearly indicated.

The author(s) must be appropriately credited and we ask that you include the end user license and a DOI link to the formal publication on ScienceDirect.

If any part of the material to be used (for example, figures) has appeared in our publication with credit or acknowledgement to another source it is the responsibility of the user to ensure their reuse complies with the terms and conditions determined by the rights holder.

Additional Terms & Conditions applicable to each Creative Commons user license:

CC BY: The CC-BY license allows users to copy, to create extracts, abstracts and new works from the Article, to alter and revise the Article and to make commercial use of the Article (including reuse and/or resale of the Article by commercial entities), provided the user gives appropriate credit (with a link to the formal publication through the relevant DOI), provides a link to the license, indicates if changes were made and the licensor is not represented as endorsing the use made of the work. The full details of the license are available at http://creativecommons.org/licenses/by/4.0.

CC BY NC SA: The CC BY-NC-SA license allows users to copy, to create extracts, abstracts and new works from the Article, to alter and revise the Article, provided this is not done for commercial purposes, and that the user gives appropriate credit (with a link to the formal publication through the relevant DOI), provides a link to the license, indicates if changes were made and the licensor is not represented as endorsing the use made of the work. Further, any new works must be made available on the same conditions. The full details of the license are available at http://creativecommons.org/licenses/by-nc-sa/4.0.

CC BY NC ND: The CC BY-NC-ND license allows users to copy and distribute the Article, provided this is not done for commercial purposes and further does not permit distribution of the Article if it is changed or edited in any way, and provided the user gives appropriate credit (with a link to the formal publication through the relevant DOI), provides a link to the license, and that the licensor is not represented as endorsing the use made of the work. The full details of the license are available at http://creativecommons.org/licenses/by-nc-nd/4.0. Any commercial reuse of Open Access articles published with a CC BY NC SA or CC BY NC ND license requires permission from Elsevier and will be subject to a fee.

Commercial reuse includes:

- Associating advertising with the full text of the Article
- Charging fees for document delivery or access
- Article aggregation
- Systematic distribution via e-mail lists or share buttons

Posting or linking by commercial companies for use by customers of those companies.

20. **Other Conditions**:

v1.10

Questions? customercare@copyright.com or +1-855-239-3415 (toll free in the US) or +1-978-646-2777.

TH-2661_166122014

CCC Marketplace™

Order Date	24-Jan-2022	**Type of Use**	Republish in a thesis/dissertation
Order License ID	1181492-1		
ISSN	1364-548X	**Publisher**	ROYAL SOCIETY OF CHEMISTRY
		Portion	Image/photo/illustration

LICENSED CONTENT

Publication Title	Chemical communications	**Rightsholder**	Royal Society of Chemistry
Article Title	A two-target responsive reversible ratiometric pH nanoprobe: a white light emitting quantum dot complex.	**Publication Type**	e-Journal
		Start Page	4331
		End Page	4334
		Issue	30
Author/Editor	Royal Society of Chemistry (Great Britain)	**Volume**	55
Date	01/01/1996		
Language	English		
Country	United Kingdom of Great Britain and Northern Ireland		

REQUEST DETAILS

Portion Type	Image/photo/illustration	**Distribution**	Worldwide
Number of images / photos / illustrations	1	**Translation**	Original language of publication
Format (select all that apply)	Print, Electronic	**Copies for the disabled?**	No
		Minor editing privileges?	No
Who will republish the content?	Academic institution	**Incidental promotional use?**	No
Duration of Use	Life of current edition	**Currency**	USD
Lifetime Unit Quantity	Up to 499		
Rights Requested	Main product		

NEW WORK DETAILS

Title	Complexation on the Surface of Quantum Dots for Ion and Molecular Sensing	**Institution name**	IIT Guwahati
		Expected presentation date	2022-01-31
Instructor name	Mihir Manna		

TH-2661_166122014

ADDITIONAL DETAILS

Order reference number	N/A	**The requesting person / organization to appear on the license**	MIHIR MANNA

REUSE CONTENT DETAILS

Title, description or numeric reference of the portion(s)	137	**Title of the article/chapter the portion is from**	A two-target responsive reversible ratiometric pH nanoprobe: a white light emitting quantum dot complex.
Editor of portion(s)	Bhandari, Satyapriya; Mondal, Arup; Pramanik, Sabyasachi; Roy, Shilaj	**Author of portion(s)**	Bhandari, Satyapriya; Mondal, Arup; Pramanik, Sabyasachi; Roy, Shilaj
Volume of serial or monograph	55	**Issue, if republishing an article from a serial**	30
Page or page range of portion	4331-4334	**Publication date of portion**	2019-04-09

CCC Terms and Conditions

1. Description of Service; Defined Terms. This Republication License enables the User to obtain licenses for republication of one or more copyrighted works as described in detail on the relevant Order Confirmation (the "Work(s)"). Copyright Clearance Center, Inc. ("CCC") grants licenses through the Service on behalf of the rightsholder identified on the Order Confirmation (the "Rightsholder"). "Republication", as used herein, generally means the inclusion of a Work, in whole or in part, in a new work or works, also as described on the Order Confirmation. "User", as used herein, means the person or entity making such republication.

2. The terms set forth in the relevant Order Confirmation, and any terms set by the Rightsholder with respect to a particular Work, govern the terms of use of Works in connection with the Service. By using the Service, the person transacting for a republication license on behalf of the User represents and warrants that he/she/it (a) has been duly authorized by the User to accept, and hereby does accept, all such terms and conditions on behalf of User, and (b) shall inform User of all such terms and conditions. In the event such person is a "freelancer" or other third party independent of User and CCC, such party shall be deemed jointly a "User" for purposes of these terms and conditions. In any event, User shall be deemed to have accepted and agreed to all such terms and conditions if User republishes the Work in any fashion.

3. Scope of License; Limitations and Obligations.

    3.1. All Works and all rights therein, including copyright rights, remain the sole and exclusive property of the Rightsholder. The license created by the exchange of an Order Confirmation (and/or any invoice) and payment by User of the full amount set forth on that document includes only those rights expressly set forth in the Order Confirmation and in these terms and conditions, and conveys no other rights in the Work(s) to User. All rights not expressly granted are hereby reserved.

    3.2. General Payment Terms: You may pay by credit card or through an account with us payable at the end of the month. If you and we agree that you may establish a standing account with CCC, then the following terms apply: Remit Payment to: Copyright Clearance Center, 29118 Network Place, Chicago, IL 60673-1291. Payments Due: Invoices are payable upon their delivery to you (or upon our notice to you that they are available to you for downloading). After 30 days, outstanding amounts will be subject to a service charge of 1-1/2% per month or, if less, the maximum rate allowed by applicable law. Unless otherwise specifically set forth in the Order Confirmation or in a separate written agreement signed by CCC, invoices are due and payable on "net 30" terms. While User may exercise the rights licensed immediately upon issuance of the

Order Confirmation, the license is automatically revoked and is null and void, as if it had never been issued, if complete payment for the license is not received on a timely basis either from User directly or through a payment agent, such as a credit card company.

3.3. Unless otherwise provided in the Order Confirmation, any grant of rights to User (i) is "one-time" (including the editions and product family specified in the license), (ii) is non-exclusive and non-transferable and (iii) is subject to any and all limitations and restrictions (such as, but not limited to, limitations on duration of use or circulation) included in the Order Confirmation or invoice and/or in these terms and conditions. Upon completion of the licensed use, User shall either secure a new permission for further use of the Work(s) or immediately cease any new use of the Work(s) and shall render inaccessible (such as by deleting or by removing or severing links or other locators) any further copies of the Work (except for copies printed on paper in accordance with this license and still in User's stock at the end of such period).

3.4. In the event that the material for which a republication license is sought includes third party materials (such as photographs, illustrations, graphs, inserts and similar materials) which are identified in such material as having been used by permission, User is responsible for identifying, and seeking separate licenses (under this Service or otherwise) for, any of such third party materials; without a separate license, such third party materials may not be used.

3.5. Use of proper copyright notice for a Work is required as a condition of any license granted under the Service. Unless otherwise provided in the Order Confirmation, a proper copyright notice will read substantially as follows: "Republished with permission of [Rightsholder's name], from [Work's title, author, volume, edition number and year of copyright]; permission conveyed through Copyright Clearance Center, Inc. " Such notice must be provided in a reasonably legible font size and must be placed either immediately adjacent to the Work as used (for example, as part of a by-line or footnote but not as a separate electronic link) or in the place where substantially all other credits or notices for the new work containing the republished Work are located. Failure to include the required notice results in loss to the Rightsholder and CCC, and the User shall be liable to pay liquidated damages for each such failure equal to twice the use fee specified in the Order Confirmation, in addition to the use fee itself and any other fees and charges specified.

3.6. User may only make alterations to the Work if and as expressly set forth in the Order Confirmation. No Work may be used in any way that is defamatory, violates the rights of third parties (including such third parties' rights of copyright, privacy, publicity, or other tangible or intangible property), or is otherwise illegal, sexually explicit or obscene. In addition, User may not conjoin a Work with any other material that may result in damage to the reputation of the Rightsholder. User agrees to inform CCC if it becomes aware of any infringement of any rights in a Work and to cooperate with any reasonable request of CCC or the Rightsholder in connection therewith.

4. Indemnity. User hereby indemnifies and agrees to defend the Rightsholder and CCC, and their respective employees and directors, against all claims, liability, damages, costs and expenses, including legal fees and expenses, arising out of any use of a Work beyond the scope of the rights granted herein, or any use of a Work which has been altered in any unauthorized way by User, including claims of defamation or infringement of rights of copyright, publicity, privacy or other tangible or intangible property.

5. Limitation of Liability. UNDER NO CIRCUMSTANCES WILL CCC OR THE RIGHTSHOLDER BE LIABLE FOR ANY DIRECT, INDIRECT, CONSEQUENTIAL OR INCIDENTAL DAMAGES (INCLUDING WITHOUT LIMITATION DAMAGES FOR LOSS OF BUSINESS PROFITS OR INFORMATION, OR FOR BUSINESS INTERRUPTION) ARISING OUT OF THE USE OR INABILITY TO USE A WORK, EVEN IF ONE OF THEM HAS BEEN ADVISED OF THE POSSIBILITY OF SUCH DAMAGES. In any event, the total liability of the Rightsholder and CCC (including their respective employees and directors) shall not exceed the total amount actually paid by User for this license. User assumes full liability for the actions and omissions of its principals, employees, agents, affiliates, successors and assigns.

6. Limited Warranties. THE WORK(S) AND RIGHT(S) ARE PROVIDED "AS IS". CCC HAS THE RIGHT TO GRANT TO USER THE RIGHTS GRANTED IN THE ORDER CONFIRMATION DOCUMENT. CCC AND THE RIGHTSHOLDER DISCLAIM ALL

OTHER WARRANTIES RELATING TO THE WORK(S) AND RIGHT(S), EITHER EXPRESS OR IMPLIED, INCLUDING WITHOUT LIMITATION IMPLIED WARRANTIES OF MERCHANTABILITY OR FITNESS FOR A PARTICULAR PURPOSE. ADDITIONAL RIGHTS MAY BE REQUIRED TO USE ILLUSTRATIONS, GRAPHS, PHOTOGRAPHS, ABSTRACTS, INSERTS OR OTHER PORTIONS OF THE WORK (AS OPPOSED TO THE ENTIRE WORK) IN A MANNER CONTEMPLATED BY USER; USER UNDERSTANDS AND AGREES THAT NEITHER CCC NOR THE RIGHTSHOLDER MAY HAVE SUCH ADDITIONAL RIGHTS TO GRANT.

7. Effect of Breach. Any failure by User to pay any amount when due, or any use by User of a Work beyond the scope of the license set forth in the Order Confirmation and/or these terms and conditions, shall be a material breach of the license created by the Order Confirmation and these terms and conditions. Any breach not cured within 30 days of written notice thereof shall result in immediate termination of such license without further notice. Any unauthorized (but licensable) use of a Work that is terminated immediately upon notice thereof may be liquidated by payment of the Rightsholder's ordinary license price therefor; any unauthorized (and unlicensable) use that is not terminated immediately for any reason (including, for example, because materials containing the Work cannot reasonably be recalled) will be subject to all remedies available at law or in equity, but in no event to a payment of less than three times the Rightsholder's ordinary license price for the most closely analogous licensable use plus Rightsholder's and/or CCC's costs and expenses incurred in collecting such payment.

8. Miscellaneous.

    8.1. User acknowledges that CCC may, from time to time, make changes or additions to the Service or to these terms and conditions, and CCC reserves the right to send notice to the User by electronic mail or otherwise for the purposes of notifying User of such changes or additions; provided that any such changes or additions shall not apply to permissions already secured and paid for.

    8.2. Use of User-related information collected through the Service is governed by CCC's privacy policy, available online here:https://marketplace.copyright.com/rs-ui-web/mp/privacy-policy

    8.3. The licensing transaction described in the Order Confirmation is personal to User. Therefore, User may not assign or transfer to any other person (whether a natural person or an organization of any kind) the license created by the Order Confirmation and these terms and conditions or any rights granted hereunder; provided, however, that User may assign such license in its entirety on written notice to CCC in the event of a transfer of all or substantially all of User's rights in the new material which includes the Work(s) licensed under this Service.

    8.4. No amendment or waiver of any terms is binding unless set forth in writing and signed by the parties. The Rightsholder and CCC hereby object to any terms contained in any writing prepared by the User or its principals, employees, agents or affiliates and purporting to govern or otherwise relate to the licensing transaction described in the Order Confirmation, which terms are in any way inconsistent with any terms set forth in the Order Confirmation and/or in these terms and conditions or CCC's standard operating procedures, whether such writing is prepared prior to, simultaneously with or subsequent to the Order Confirmation, and whether such writing appears on a copy of the Order Confirmation or in a separate instrument.

    8.5. The licensing transaction described in the Order Confirmation document shall be governed by and construed under the law of the State of New York, USA, without regard to the principles thereof of conflicts of law. Any case, controversy, suit, action, or proceeding arising out of, in connection with, or related to such licensing transaction shall be brought, at CCC's sole discretion, in any federal or state court located in the County of New York, State of New York, USA, or in any federal or state court whose geographical jurisdiction covers the location of the Rightsholder set forth in the Order Confirmation. The parties expressly submit to the personal jurisdiction and venue of each such federal or state court.If you have any comments or questions about the Service or Copyright Clearance Center, please contact us at 978-750-8400 or send an e-mail to support@copyright.com.

v1.1

TH-2661_166122014

JOHN WILEY AND SONS LICENSE TERMS AND CONDITIONS

Jan 26, 2022

This Agreement between Mr. MIHIR MANNA ("You") and John Wiley and Sons ("John Wiley and Sons") consists of your license details and the terms and conditions provided by John Wiley and Sons and Copyright Clearance Center.

License Number	5235420229589
License date	Jan 24, 2022
Licensed Content Publisher	John Wiley and Sons
Licensed Content Publication	Small
Licensed Content Title	A White Light-Emitting Quantum Dot Complex for Single Particle Level Interaction with Dopamine Leading to Changes in Color and Blinking Profile
Licensed Content Author	Sabyasachi Pramanik, Satyapriya Bhandari, Uday Narayan Pan, et al
Licensed Content Date	Apr 17, 2018
Licensed Content Volume	14
Licensed Content Issue	20
Licensed Content Pages	7
Type of Use	Dissertation/Thesis
Requestor type	University/Academic
Format	Print and electronic
Portion	Figure/table
Number of figures/tables	1
Will you be translating?	No
Title	Complexation on the Surface of Quantum Dots for Ion and Molecular Sensing
Institution name	IIT Guwahati
Expected presentation date	Jan 2022
Portions	Scheme 1
Requestor Location	Mr. MIHIR MANNA Department of Chemistry IIT Guwahati Guwahati, ASSAM 781039 India Attn: Mr. MIHIR MANNA
Publisher Tax ID	EU826007151
Total	**0.00 USD**
Terms and Conditions	

TERMS AND CONDITIONS

This copyrighted material is owned by or exclusively licensed to John Wiley & Sons, Inc. or one of its group companies (each a"Wiley Company") or handled on behalf of a society with which a Wiley Company has exclusive publishing rights in relation to a particular work (collectively "WILEY"). By clicking "accept" in connection with completing this licensing transaction, you agree that the following terms and conditions apply to this transaction (along with the billing and payment terms and conditions established by the Copyright Clearance Center Inc., ("CCC's Billing and Payment terms and conditions"), at the time that you opened your RightsLink account (these are available at any time at http://myaccount.copyright.com).

Terms and Conditions

TH-2661_166122014

- The materials you have requested permission to reproduce or reuse (the "Wiley Materials") are protected by copyright.

- You are hereby granted a personal, non-exclusive, non-sub licensable (on a stand-alone basis), non-transferable, worldwide, limited license to reproduce the Wiley Materials for the purpose specified in the licensing process. This license, **and any CONTENT (PDF or image file) purchased as part of your order,** is for a one-time use only and limited to any maximum distribution number specified in the license. The first instance of republication or reuse granted by this license must be completed within two years of the date of the grant of this license (although copies prepared before the end date may be distributed thereafter). The Wiley Materials shall not be used in any other manner or for any other purpose, beyond what is granted in the license. Permission is granted subject to an appropriate acknowledgement given to the author, title of the material/book/journal and the publisher. You shall also duplicate the copyright notice that appears in the Wiley publication in your use of the Wiley Material. Permission is also granted on the understanding that nowhere in the text is a previously published source acknowledged for all or part of this Wiley Material. Any third party content is expressly excluded from this permission.

- With respect to the Wiley Materials, all rights are reserved. Except as expressly granted by the terms of the license, no part of the Wiley Materials may be copied, modified, adapted (except for minor reformatting required by the new Publication), translated, reproduced, transferred or distributed, in any form or by any means, and no derivative works may be made based on the Wiley Materials without the prior permission of the respective copyright owner.**For STM Signatory Publishers clearing permission under the terms of the STM Permissions Guidelines only, the terms of the license are extended to include subsequent editions and for editions in other languages, provided such editions are for the work as a whole in situ and does not involve the separate exploitation of the permitted figures or extracts,** You may not alter, remove or suppress in any manner any copyright, trademark or other notices displayed by the Wiley Materials. You may not license, rent, sell, loan, lease, pledge, offer as security, transfer or assign the Wiley Materials on a stand-alone basis, or any of the rights granted to you hereunder to any other person.

- The Wiley Materials and all of the intellectual property rights therein shall at all times remain the exclusive property of John Wiley & Sons Inc, the Wiley Companies, or their respective licensors, and your interest therein is only that of having possession of and the right to reproduce the Wiley Materials pursuant to Section 2 herein during the continuance of this Agreement. You agree that you own no right, title or interest in or to the Wiley Materials or any of the intellectual property rights therein. You shall have no rights hereunder other than the license as provided for above in Section 2. No right, license or interest to any trademark, trade name, service mark or other branding ("Marks") of WILEY or its licensors is granted hereunder, and you agree that you shall not assert any such right, license or interest with respect thereto

- NEITHER WILEY NOR ITS LICENSORS MAKES ANY WARRANTY OR REPRESENTATION OF ANY KIND TO YOU OR ANY THIRD PARTY, EXPRESS, IMPLIED OR STATUTORY, WITH RESPECT TO THE MATERIALS OR THE ACCURACY OF ANY INFORMATION CONTAINED IN THE MATERIALS, INCLUDING, WITHOUT LIMITATION, ANY IMPLIED WARRANTY OF MERCHANTABILITY, ACCURACY, SATISFACTORY QUALITY, FITNESS FOR A PARTICULAR PURPOSE, USABILITY, INTEGRATION OR NON-INFRINGEMENT AND ALL SUCH WARRANTIES ARE HEREBY EXCLUDED BY WILEY AND ITS LICENSORS AND WAIVED BY YOU.

- WILEY shall have the right to terminate this Agreement immediately upon breach of this Agreement by you.

- You shall indemnify, defend and hold harmless WILEY, its Licensors and their respective directors, officers, agents and employees, from and against any actual or threatened claims, demands, causes of action or proceedings arising from any breach of this Agreement by you.

- IN NO EVENT SHALL WILEY OR ITS LICENSORS BE LIABLE TO YOU OR ANY OTHER PARTY OR ANY OTHER PERSON OR ENTITY FOR ANY SPECIAL, CONSEQUENTIAL, INCIDENTAL, INDIRECT, EXEMPLARY OR PUNITIVE DAMAGES, HOWEVER CAUSED, ARISING OUT OF OR IN CONNECTION WITH THE DOWNLOADING, PROVISIONING, VIEWING OR USE OF THE MATERIALS REGARDLESS OF THE FORM OF ACTION, WHETHER FOR BREACH OF CONTRACT, BREACH OF WARRANTY, TORT, NEGLIGENCE, INFRINGEMENT OR OTHERWISE (INCLUDING, WITHOUT LIMITATION, DAMAGES BASED ON LOSS OF PROFITS, DATA, FILES, USE, BUSINESS OPPORTUNITY OR CLAIMS OF THIRD PARTIES), AND WHETHER OR NOT THE PARTY HAS BEEN ADVISED OF THE POSSIBILITY OF SUCH DAMAGES. THIS LIMITATION SHALL APPLY NOTWITHSTANDING ANY FAILURE OF ESSENTIAL PURPOSE OF ANY LIMITED REMEDY PROVIDED HEREIN.

- Should any provision of this Agreement be held by a court of competent jurisdiction to be illegal, invalid, or unenforceable, that provision shall be deemed amended to achieve as nearly as possible the same economic effect as the original provision, and the legality, validity and enforceability of the remaining provisions of this Agreement shall not be affected or impaired thereby.

TH-2661_166122014

- The failure of either party to enforce any term or condition of this Agreement shall not constitute a waiver of either party's right to enforce each and every term and condition of this Agreement. No breach under this agreement shall be deemed waived or excused by either party unless such waiver or consent is in writing signed by the party granting such waiver or consent. The waiver by or consent of a party to a breach of any provision of this Agreement shall not operate or be construed as a waiver of or consent to any other or subsequent breach by such other party.

- This Agreement may not be assigned (including by operation of law or otherwise) by you without WILEY's prior written consent.

- Any fee required for this permission shall be non-refundable after thirty (30) days from receipt by the CCC.

- These terms and conditions together with CCC's Billing and Payment terms and conditions (which are incorporated herein) form the entire agreement between you and WILEY concerning this licensing transaction and (in the absence of fraud) supersedes all prior agreements and representations of the parties, oral or written. This Agreement may not be amended except in writing signed by both parties. This Agreement shall be binding upon and inure to the benefit of the parties' successors, legal representatives, and authorized assigns.

- In the event of any conflict between your obligations established by these terms and conditions and those established by CCC's Billing and Payment terms and conditions, these terms and conditions shall prevail.

- WILEY expressly reserves all rights not specifically granted in the combination of (i) the license details provided by you and accepted in the course of this licensing transaction, (ii) these terms and conditions and (iii) CCC's Billing and Payment terms and conditions.

- This Agreement will be void if the Type of Use, Format, Circulation, or Requestor Type was misrepresented during the licensing process.

- This Agreement shall be governed by and construed in accordance with the laws of the State of New York, USA, without regards to such state's conflict of law rules. Any legal action, suit or proceeding arising out of or relating to these Terms and Conditions or the breach thereof shall be instituted in a court of competent jurisdiction in New York County in the State of New York in the United States of America and each party hereby consents and submits to the personal jurisdiction of such court, waives any objection to venue in such court and consents to service of process by registered or certified mail, return receipt requested, at the last known address of such party.

WILEY OPEN ACCESS TERMS AND CONDITIONS

Wiley Publishes Open Access Articles in fully Open Access Journals and in Subscription journals offering Online Open. Although most of the fully Open Access journals publish open access articles under the terms of the Creative Commons Attribution (CC BY) License only, the subscription journals and a few of the Open Access Journals offer a choice of Creative Commons Licenses. The license type is clearly identified on the article.

The Creative Commons Attribution License

The Creative Commons Attribution License (CC-BY) allows users to copy, distribute and transmit an article, adapt the article and make commercial use of the article. The CC-BY license permits commercial and non-

Creative Commons Attribution Non-Commercial License

The Creative Commons Attribution Non-Commercial (CC-BY-NC)License permits use, distribution and reproduction in any medium, provided the original work is properly cited and is not used for commercial purposes.(see below)

Creative Commons Attribution-Non-Commercial-NoDerivs License

The Creative Commons Attribution Non-Commercial-NoDerivs License (CC-BY-NC-ND) permits use, distribution and reproduction in any medium, provided the original work is properly cited, is not used for commercial purposes and no modifications or adaptations are made. (see below)

Use by commercial "for-profit" organizations

Use of Wiley Open Access articles for commercial, promotional, or marketing purposes requires further explicit permission from Wiley and will be subject to a fee.

Further details can be found on Wiley Online Library http://olabout.wiley.com/WileyCDA/Section/id-410895.html

Other Terms and Conditions:

TH-2661_166122014

v1.10 Last updated September 2015

Questions? customercare@copyright.com or +1-855-239-3415 (toll free in the US) or +1-978-646-2777.

TH-2661_166122014

A dual-emitting quantum dot complex nanoprobe for ratiometric and visual detection of Hg^{2+} and Cu^{2+} ions

M. Manna, S. Roy, S. Bhandari and A. Chattopadhyay, *J. Mater. Chem. C*, 2020, **8**, 6972 **DOI:** 10.1039/D0TC01788D

TH-2661_166122014

A Ratiometric and Visual Sensing of Phosphate by White Light Emitting Quantum Dot Complex

Author: Mihir Manna, Shilaj Roy, Satyapriya Bhandari, et al
Publication: Langmuir
Publisher: American Chemical Society
Date: May 1, 2021

PERMISSION/LICENSE IS GRANTED FOR YOUR ORDER AT NO CHARGE

This type of permission/license, instead of the standard Terms and Conditions, is sent to you because no fee is being charged for your order. Please note the following:

- Permission is granted for your request in both print and electronic formats, and translations.
- If figures and/or tables were requested, they may be adapted or used in part.
- Please print this page for your records and send a copy of it to your publisher/graduate school.
- Appropriate credit for the requested material should be given as follows: "Reprinted (adapted) with permission from {COMPLETE REFERENCE CITATION}. Copyright {YEAR} American Chemical Society." Insert appropriate information in place of the capitalized words.
- One-time permission is granted only for the use specified in your RightsLink request. No additional uses are granted (such as derivative works or other editions). For any uses, please submit a new request.

If credit is given to another source for the material you requested from RightsLink, permission must be obtained from that source.

Recognition and ratiometric visual sensing of long-chain unsaturated fatty acids by a white-light-emitting quantum-dot complex

M. Manna, S. Bhandari and A. Chattopadhyay, *J. Mater. Chem. C*, 2021, **9**, 13810 **DOI:** 10.1039/D1TC03167H

TH-2661_166122014